Investigation of N-terminus MLL Complexes on the Reversion of Taxane Resistance in Castration-Resistant Prostate Cancer

By

İpek Bulut

A Dissertation Submitted to the
Graduate School of Health Sciences in Partial
Fulfillment of the Requirements for the Degree
of

Doctor of Philosophy

in

Cellular and Molecular Medicine

KOÇ ÜNİVERSİTESİ

Aug 5, 2024

Investigation of N-terminus MLL Complexes on the Reversion of Taxane Resistance in Castration-Resistant Prostate Cancer

Koc University

Graduate School of Health Sciences

This is to certify that I have examined this copy of a doctoral dissertation by

İpek Bulut

and have found that it is complete and satisfactory in all respects,
and that all revisions required by the final
examining committee has been made.

Committee Members:

Prof. Ceyda Açılan AYHAN (Advisor)

Prof. T. Tamer ÖNDER

Assoc. Prof N.C Tolga EMRE

Assist. Prof. Gözde Korkmaz

Assoc. Prof. Hilal Yazıcı Malkoçoğlu

Date: 05.08.2024

To those who have lost loved ones to cancer…

ABSTRACT

Investigation of N-terminus MLL Complexes on the Reversion of Taxane Resistance in Castration-Resistant Prostate Cancer

İpek Bulut

Doctor of Philosophy in Cellular and Molecular Medicine, Aug 5, 2024

Prostate cancer (PC) typically relies on androgen for abnormal growth, and androgen deprivation therapy (ADT) is preferred as the primary treatment. However, patients frequently progress to a castration-resistant (CR) stage, where tumor growth becomes unresponsive to ADT. Despite the common use of conventional chemotherapeutics like Taxanes (Docetaxel-Dtx, Cabazitaxel-Cbz), either alone or in conjunction with hormone therapies, certain tumors may experience recurrence. This work focuses on the epigenetic regulations conferring Dtx resistance in CRPC.

Firstly, the generation of Dtx-resistant cells was conducted using the dose increment method, and subsequently, our model was confirmed via *in vitro* and *in vivo* models. Epigenetic drug screening identified MLL-Menin and MLL-WDR5 inhibitors as hit molecules that effectively reverse drug resistance through G2/M arrest and apoptosis induction. N- and C-terminal binding partners of MLL were individually knocked out via CRISPR-cas9. Our analysis led to the discovery of sensitivity on DtxR cells upon Menin depletion, while no effect was observed on parental counterparts. On the other hand, parental cells lacking Menin expression showed reduced capacity to develop drug resistance, suggesting an indispensable role of Menin for the drug refractory phenotype. Restoring several Menin mutants led to the identification of another effective factor, LEDGF, which specifically diminishes colony growth on the DtxR model. RNA-seq analysis was conducted on parental and DtxR cells, upon Menin and LEDGF ablation. GSEA analysis revealed positively enriched mTOR signaling, E2F targets, and G2M checkpoints gene sets in DtxR cells. Interestingly, Menin and LEDGF depletion significantly reversed the enrichment profile of the interested gene sets. Initially, we revealed the essentiality of the mTOR pathway in DtxR maintenance and cell growth. Furthermore, mTOR expression was significantly reduced in Menin knockout cells.

On the other hand, Menin depletion triggered a significant synergy with Torin (mTOR inhibitor) and Dtx in our resistant model. Recovering Menin also induced mTOR expression in our DtxR model and abolished the observed synergy. Menin and mTOR correlation was also increased in metastatic CRPC in patient-derived clinical data. Furthermore, our ChIP-qPCR experiments demonstrated Menin enrichment on mTOR promoter region in DtxR CRPC cells. Competition experiments exhibited significant domination by control cells; indicating Menin depletion results in a slower rate of cell division. A higher proportion of Menin knockout cells accumulated in the G1 cell cycle state. Furthermore, two important factors promoting G1-S transition, Cyclin D1 and CDK20 were significantly lower in Menin-depleted cells. Restoring Menin also rescued expression patterns of these targets; furthermore, Menin occupied the promoter region of Cyclin D1 and CDK20. This slow growth rate observed in Menin ablated cells also provided a slight resistance against CDK4/6 inhibitors.

Overall, Menin appears as a key regulator that confers drug resistance through mTOR upregulation and controls G1-S progression via Cyclin D1 and CDK20 in our DtxR model. Menin and LEDGF both contribute to essentiality in DtxR cells, while Menin shows enrichment on the promoter regions of specific targets. Our study provides a detailed analysis of Dtx resistance in CRPC, through epigenetic regulation.

OZETCE

N-terminal MLL Komplekslerinin Kastrasyona Dirençli Prostat Kanserinde Taksan Direncini Geri Döndürmedeki Rollerinin Araştırılması

İpek Bulut

Hücresel ve Moleküler Tıp, Doktora, 5 Ağustos 2024

Prostat kanseri (PK) tipik olarak androjen hormonuna bağlı olarak anormal büyüme gösterir ve birincil tedavi olarak kastrasyon tedavisi (androjen yoksunluğu, KT) tercih edilmektedir. Bununla birlikte, hastalar sıklıkla tümör büyümesinin KT'ye yanıt vermediği kastrasyona dirençli (KD) aşamaya ilerler. Taksan (Dosetaksel-Dtx, kabazitaksel-Cbz) gibi geleneksel kemoterapötikler tek başına veya hormon tedavileriyle birlikte yaygın olarak kullanılmasına rağmen, bazı tümörler nüks edebilir. Bu çalışma KDPK'lerde Dtx direncine olanak sağlayan epigenetik düzenlemelere odaklanmaktadır.

İlk olarak doz artırım yöntemi uygulanarak Dtx dirençli Du145 hücrelerimiz oluşturulmuş ve modelimiz doğrulanmıştır. Epigenetik ilaç taraması sonucunda MLL-Menin ve MLL-WDR5 inhibitörleri, G2/M tutulması ve apoptoz indüksiyonu yoluyla ilaç direncini etkili bir şekilde tersine çeviren isabetli moleküller olarak tanımlanmıştır. MLL proteinin farklı bağlanma ortakları (hem N, hem de C terminalinde) ayrı ayrı hedeflenmiş ve DtxR hücrelerinin Menin deplesyonuna karşı duyarlı olduğu, parental muadillerinde ise hiçbir etki gözlemlenmediği keşfedilmiştir. Öte yandan, Menin ekspresyonu olmayan parental hücrelerin, ilaca direnç geliştirme kapasitesinin azaldığı gözlemlenmiştir, bu durum Menin'in ilaca dirençli fenotip için vazgeçilmez rolünü ortaya koymaktadır. Farklı Menin mutantlarının geri kazandırılması, DtxR modelinde koloni büyümesini özellikle azaltan başka bir etkili faktör olan LEDGF'nin tanımlanmasına olanak sağlamıştır. Menin veya LEDGF nakavt ve kontrol parental ve DtxR hücreleri üzerinde RNA sekans analizi gerçekleştirilmiştir. GSEA analizi, edinilen ilaç direncinin ardından pozitif olarak zenginleşmiş mTOR sinyali, E2F hedefleri, ve G2/M kontrol noktaları gen setlerini göstermiştir. İlginç bir şekilde Menin ve LEDGF deplesyonu, bu bahsedilen gen setlerindeki zenginleşme profilini önemli ölçüde tersine çevirmiştir. Ayrıca, mTOR'un DtxR hücre büyümesindeki hayati rolü

ortaya çıkarılmıştır. Öte yandan, Menin nakavt hücrelerinde mTOR ekspresyonu önemli ölçüde azalmış; ayrıca Menin deplesyonu, dirençli modelimizde Torin (mTOR inhibitörü) ve Dtx ile önemli bir sinerjiyi tetiklemiştir. Menin'in geri kazandırılması ayrıca DtxR modelimizde mTOR ifadesini uyarmış ve gözlemlenen sinerjiyi ortadan kaldırmıştır. Menin ve mTOR korelasyonu klinik verilere göre metastatik KDPK'de artmıştır, ayrıca ChIP-qPCR deneylerimiz DtxR KDPK hücrelerimizdeki mTOR promotör bölgesinde Menin zenginleşmesini göstermiştir. Rekabet deneylerinde, popülasyonda kontrol hücreleri önemli bir hakimiyet sağlamıştır; bu da Menin deplesyonunun yavaş hücre bölünmesi fenotipine neden olduğunu göstermektedir. Menin nakavt DtxR hücreleri yüksek oranda G1 hücre döngüsü fazında birikmiş, ayrıca G1-S geçişini teşvik eden iki önemli faktör olan Siklin D1 ve CDK20, Menin nakavt hücrelerde önemli ölçüde azalmıştır. Menin'in geri kazandırılması aynı zamanda bu hedeflerin ifade seviyelerini de kurtarmıştır; ayrıca Menin'in Siklin D1 ve CDK20'nin promotör bölgesine bağlanabildiği gösterilmiştir. Menin ablasyonlu hücrelerde gözlenen bu yavaş büyüme fenotipi, CDK4/6 inhibitörlerine karşı da bir direnç sağlamıştır.

Özetle Menin, mTOR artışı üzerinden ilaç direnci sağlayan ve Siklin D1 ve CDK20 üzerinden G1-S geçişini kontrol eden önemli bir düzenleyici protein olarak karşımıza çıkmaktadır. Menin ve LEDGF'nin her ikisi de DtxR hücrelerinde hücre büyümesi için gerekli olduğu görülürken, Menin bahsi geçen hedeflerin promotör bölgelerinde zenginleşme göstermiştir. Çalışmamız KDPK'deki Dtx direncinin epigenetik açıdan ayrıntılı bir analizini sunmaktadır.

ACKNOWLEDGMENTS

Firstly, I would like to express my gratitude to my thesis advisor Prof. Dr. Ceyda Açılan Ayhan for her guidance, support, and encouragement throughout my doctoral thesis. I am sincerely grateful for her the advices she gave for my studies and my future as a scientist. I would like to thank Prof. Dr. Tamer Onder and Assoc. Prof. NC. Tolga Emre, Assist. Prof. Gözde Korkmaz and Assoc. Prof. Hilal Yazıcı Malkoçoğlu for being on my thesis committee.

Secondly, I owe special thanks to Dr. Buse Cevatemre for her constructive comments and warm friendship over the last six years. I would like to thank the Koç University Research Center for Translational Medicine (KUTTAM) for the research environment they provided. I also would like to express my warm thanks to Barış Sergi, Büşra Yıldırım, Evrim Göksel, and Deniz Özen for their close friendship, for making me laugh all the time and for improving my journey.

I would like to extend my gratitude and love to my parents and my sister Merve, I am thankful for their unconditional love and support. My parents welcomed me into their house and accommodated me while I was having financial difficulties, without their assistance, I could not have completed my education. I would also like to express my special thanks to my significant other, Burak, for his endless affection for me for a decade. I can not thank him enough for encouraging me throughout this experience and always being patient with my hectic schedule.

I would like to dedicate this thesis to all the beautiful souls I have met in my life, who lost their battles with cancer.

TABLE OF CONTENTS

LIST OF TABLES

LIST OF FIGURES

ABBREVIATIONS

ABCB1	ATP-binding cassette subfamily B member 1
ADT	Androgen Deprivation Therapy
AML	Acute Myeloid Leukemia
ASH2L	Absent, small or homeotic 2-like protein
AR	Androgen Receptor
ARE	Androgen Responsive Elements
ATP	Adenosine Triphosphate
BRD	Bromodomain-containing Proteins
BET	Bromodomain and Extra-Terminal motif (BET) proteins
CAK	CDK-activating Kinase
CBP	CREB-binding protein
CBZ	Cabazitaxel
CCND1	Cyclin D1
CDK4/6	Cyclin Dependent Kinase 4/6
CDK20	Cyclin Dependent Kinase 20
CEND1	Cell Cycle Exit and Neuronal Differentiation
ChIP	Chromatin Immunoprecipitation
ChIP-seq	Chromatin Immunoprecipitation sequencing
CRPC	Castration-Resistant Prostate Cancer
CYP17A1	Cytochrome P450 17A1
DBD	DNA Binding Domain
DHT	Dihydrotestosterone
DNA	Deoxyribonucleic Acid
DNMT	DNA Methyltransferase

DPY30	Histone Methyltransferase Complex Regulatory Subunit
DTX	Docetaxel
EGFR	Epithelial Growth Factor Receptor
GR	Glucocorticoid Receptor
GSEA	Gene Set Enrichment Analysis
HDAC	Histone Deacetylase
HIF	Hypoxia Inducible Factor
HMT	Histone Methyltransferase
HSP	Heat Shock Proteins
KDM5B	Lysine-specific demethylase 5B
LBD	Ligand Binding Domain
LEDGF	Lens Epithelium Derived Growth Factor
LHRH	Luteinizing Hormone
MDR1	Multi-Drug Resistance Protein 1
MEF	Mouse Embryonic Fibroblasts
MEN1	Multiple Endocrine Neoplasia 1
MLL1	Mixed Lineage Leukemia 1
MTOR	Mammalian Target of Rapamycin
NDRG1	N-Myc Downstream Regulated 1
NSAA	Nonsteroidal antiandrogen
NSCLC	Non-small Cell Lung Cancer
P300	Histone Acetyltransferase P300
PC	Prostate Cancer
PDAC	Pancreatic Ductal Adenocarcinoma
PI3K	Phosphoinositide 3-kinase
PL-D1	Phospholipase D1

PLKi	Polo-like Kinase inhibitor
PRAD	Prostate Adenocarcinoma
PSA	Prostate Spesific Antigen
PWWP	Pro-Trp-Trp-Pro
RBBP5	Retinoblastoma-Binding Protein 5
RNA	Ribonucleic Acid
RNA-seq	RNA-sequencing
SET1	Set1/Ash2 Histone Methyltransferase Complex Subunit SET1
SET8	Set1/Ash2 Histone Methyltransferase Complex Subunit SET8
TNBC	Triple Negative Breast Cancer
TRxGS	Trithorax-group proteins
TSS	Transcription Start Site
WDR5	WD Repeat Domain 5

Chapter 1

INTRODUCTION

1.1. Prostate Cancer

1.1.1. Prostate Cancer Progression and Therapy Options

Prostate cancer (PC) affects men of various racial and ethnic backgrounds, leading to higher mortality rates primarily due to the disease's often late detection [Sekhoacha et al., 2022]. Prostate cancer can present as either a localized tumor or an advanced metastatic form [Keyes et al., 2013]. The histological examination of specimens, including Gleason scores, prostate-specific antigen (PSA) levels, and clinical staging (T1, T2, T3, and T4), closely correlates with the pathological extent of the disease [Walsh et al., 2007]. For localized tumors, clinical treatments include radical prostatectomy, prostate brachytherapy, external beam radiation, and active surveillance [Keyes et al., 2013]. Given that most prostate cancer cases are hormone-dependent at diagnosis, androgen signaling plays a crucial role. Notably, the androgen receptor (AR) continues to be vital for the survival of many castration-resistant prostate cancer (CRPC) subtypes [Claessens et al., 2014]. Consequently, AR-targeting therapies are beneficial for many patients with metastatic CRPC [Merseburger et al., 2015]. For decades, continuous androgen deprivation therapy (ADT) with medications such as enzalutamide and bicalutamide was the standard care for metastatic prostate cancer, from 1941 to 2015. However, recent studies demonstrated that combining ADT with six courses of taxane chemotherapy significantly improved survival outcomes [Sweeney et al., 2015; James et al., 2016; Pagliarulo, 2018]. The AR is crucial not only for the normal development and function of the prostate gland but also for the progression of prostate cancer to an androgen-independent state [Lonergan and Tindall, 2011]. As a ligand-dependent transcription factor, AR is expressed in many normal tissues and all primary prostate cancers. In the absence of a ligand (such as androgens, 5α-dihydrotestosterone (DHT), or testosterone), AR remains in the cytoplasm bound to heat shock proteins (HSPs) [Crumbaker et al., 2017]. Upon ligand binding to the AR's ligand-binding domain (LBD), AR dimerizes, undergoes phosphorylation by various kinases, and changes conformation, exposing its

nuclear localization signal (NLS). In the nucleus, the AR DNA-binding domain (DBD) binds to androgen-responsive elements (AREs), inducing the transcription of AR-sensitive genes and recruiting transcriptional co-activators and co-suppressors [Eder et al., 2011; Obinata et al., 2017]. In addition to its role as a transcription factor, ligand-bound AR can activate secondary messengers, leading to the stimulation of MAPK/ERK and AKT pathways, which promote excessive cell growth, division, and survival [Liao et al., 2013]. Cytokines released by macrophages in the tumor microenvironment also interact with AR [Izumi and Chang, 2013]. AR is essential for cell survival, proliferation, and invasion in both early and advanced stages of prostate cancer [Haag et al., 2005; Snoek et al., 2009]. Several AR target genes contribute to tumor progression by regulating cell growth, metabolism, or biosynthesis [Massie et al., 2011; Levina et al., 2015]. While ADT is typically the standard treatment for prostate cancer, castration therapy aims to create an androgen-deprived state in the tumor by using hormone-releasing hormone (LHRH) agonists that disrupt the hypothalamic-pituitary-testicular axis. Common LHRH agonists include leuprolide, goserelin, triptorelin, and histrelin [Helsen et al., 2014].

Ketoconazole and abiraterone inhibit the synthesis of adrenal and intracellular androgens by targeting CYP17A1, thereby preventing the activation of the androgen receptor (AR) [Peer et al., 2014]. AR antagonists, or antiandrogens, inhibit AR activity by binding directly to the receptor, blocking androgens from exerting their biological effects. First-generation non-steroidal antiandrogens (NSAAs) such as bicalutamide (Bic) and second-generation antiandrogens like enzalutamide (Enz) compete with dihydrotestosterone (DHT), blocking both AR's nuclear translocation and its DNA binding, which impedes tumor growth [Bohl et al., 2005; Bianchini et al., 2014]. ODM-201 is a novel AR antagonist that binds to AR and exhibits antiproliferative effects in subcutaneous VCaP xenograft models [Helsen et al., 2014]. EPI-001 is another compound that inhibits AR function irrespective of ligand presence, affecting androgen-induced gene expression and proliferation both in vitro and in LNCaP xenograft mouse models. Conversely, ASC-J9 destabilizes full-length AR and its splice variants by binding to the receptor [Helsen et al., 2014].

Patient-derived prostate cancer (PC) cell lines and clinical castration-resistant prostate cancer (CRPC) samples often exhibit various androgen receptor (AR) splice variants (AR-Vs). These AR-Vs typically lack the C-terminus of the ligand-binding domain (LBD) and can mediate AR signaling independently of ligand binding. AR splice variant-7 (AR-V7) is a frequently observed mutant and is associated with a poor response to hormonal therapies such as abiraterone and enzalutamide [Zhu and Luo, 2020]. Besides androgens produced in the testicles and adrenal glands, tumors themselves can generate androgens, which further enhance AR activity [Montgomery et al., 2008]. This self-sustaining AR activity within the tumor contributes to its resistance to castration therapy.

1.1.2 Castration-Resistant Prostate Cancer

Although androgen deprivation therapy (ADT) initially provides some benefits, it typically leads to a castration-resistant state within two to three years [Harris et al., 2009]. Research indicates that castration-resistant prostate cancer (CRPC) is not entirely hormone-refractory; rather, the androgen axis continues to play a crucial role in the disease's function and progression. The androgen receptor (AR) remains a primary driver in CRPC maintenance, though other pathways can also contribute to castration resistance [Chandrasekar et al., 2015]. Despite ADT-induced androgen blockade, residual low levels of androgens may persist, allowing certain cells to adapt by either amplifying AR expression (hypersensitivity pathway) or acquiring mutations in the AR that enable activation by non-androgenic substances [Visakorpi et al., 1995; Brooke and Bevan, 2009]. AR amplification has also been observed in hormone-naïve cases [Merson et al., 2014], with approximately 20% of metastatic CRPC cases showing AR amplification. This phenotype renders CRPC hypersensitive to even minimal androgen levels, thus accelerating disease progression [Chandrasekar et al., 2015; Coutinho et al., 2016]. Additionally, point mutations in the AR gene have been identified that enhance AR activity in the presence of non-androgenic hormones [McDonald et al., 2000; Chen et al., 2015; Azad et al., 2015] and low androgen levels [Scariano et al., 2008; Jernberg et al., 2017]. Beyond AR amplification or mutation, over 150 distinct enzymes have been identified as co-repressors and activators of AR. AR recruits various coregulators that can either activate or inhibit transcriptional activity, potentially contributing to CRPC

development [Ueda et al., 2002; Debes et al., 2002; Wissmann et al., 2007; Agoulnik and Weigel, 2008; Ni et al., 2010].

The discovery of constitutively active AR-Vs is often linked to the deletion of the C-terminal ligand-binding domain (LBD) [Sun et al., 2010]. While most castration-resistant prostate cancer (CRPC) cell lines exhibit low AR-V expression, AR-V7, which lacks the LBD and is constitutively active, is detectable using antibody-based methods in CRPC cases [Guo et al., 2009]. AR-Vs play a significant role in resistance to contemporary CRPC therapies. Even in the absence of androgens, AR-V7 can activate the PSA promoter. Reformulated niclosamide has been reported to inhibit AR-V7 and enhance the effectiveness of abiraterone in CRPC treatment [Parikh et al., 2021]. Another key enzyme, cytochrome P450, family 17 (CYP17A1), is involved in the conversion of dihydrotestosterone (DHT). A loss of CYP17A1 activity leads to a significant reduction in androgen production. Abiraterone is an irreversible CYP17A1 inhibitor; however, overexpression or mutations in CYP17A1 can confer resistance in CRPC [Cai et al., 2011]. Additionally, various growth factors (e.g., IGF, KGF), cytokines, and receptor tyrosine kinases (e.g., Src, Her-2) can enhance CRPC maintenance through ligand-independent activation of AR signaling [Wen et al., 2000; Wu et al., 2006; Wang et al., 2009; Gao et al., 2022]. Moreover, several oncogenic signaling pathways, such as NF-κB, PI3K/AKT, and mTOR, have been implicated in the development of CRPC [Zhang et al., 2009; Lee et al., 2015; Bitting and Armstrong, 2013].

1.1.3 Taxane Therapy in CRPC

Taxanes function by binding to beta-tubulins on microtubules, inhibiting their depolymerization. This action stalls the cell cycle, induces mitotic block, and promotes cell death [Abal et al., 2003]. Paclitaxel, the first taxane developed, was approved by the FDA in 1992 for the treatment of refractory ovarian cancer [Kudo and Sagae, 1992; Kampan et al., 2015]. Docetaxel, a semi-synthetic derivative of paclitaxel, is used to treat breast and ovarian cancers that have not responded to other therapies [Katsumata et al., 2003]. Cabazitaxel, a modified derivative of docetaxel, has been suggested as a treatment option to overcome taxane resistance [Abidi, 2013].

Before the introduction of docetaxel therapy, patients were treated with mitoxantrone, an antineoplastic agent, and prednisone, a corticosteroid. Both of these treatments alleviated pain and improved survival to some extent [Osoba et al., 1999; Berry et al., 2002]. Docetaxel, which received FDA approval in 2004 for its ability to extend survival in CRPC patients with metastatic disease, showed significant benefits [Petrylak et al., 2004; Tannock et al., 2004; Abidi, 2013]. Despite this, approximately 50% of patients initially responded to docetaxel, but resistance developed in the remaining patients within 6–8 months. Furthermore, within a year of initiating treatment, many men receiving docetaxel exhibited a trend toward poor prognosis [Lohiya et al., 2016].

Resistance to taxane medications, primarily due to increased expression of the multidrug resistance (MDR) 1 gene, which produces P-glycoprotein—a drug efflux pump that reduces intracellular taxane concentrations—is a major challenge. Cabazitaxel, which includes additional methyl groups compared to paclitaxel and docetaxel, has shown some efficacy in overcoming P-glycoprotein-mediated resistance [Kartner et al., 1983; Mellado et al., 2016]. Nonetheless, taxane resistance continues to impede clinical success, highlighting the need for a deeper understanding of its mechanisms to improve survival outcomes in castration-resistant prostate cancer (CRPC) patients [Sekino and Teishima, 2020]. Although initial responses to taxane therapy in CRPC can be positive, drug resistance often develops over time [Bumbaca and Li, 2018]. Various mechanisms have been identified concerning taxane resistance, including androgen receptor (AR) variants, tubulin mutations, activation of cancer stem cells, centrosome amplification and aggregation, drug pumps, multidrug resistance, and PI3K/AKT signaling pathways [Kuroda et al., 2009; Sanchez et al., 2009; Hara et al., 2010; Kosaka et al., 2011; Castillo et al., 2014; Wiltshire et al., 2010]. Detailed understanding of these mechanisms is crucial for developing novel therapeutic strategies to address taxane resistance in CRPC patients.

1.1.4 Taxane Resistance in CRPC

Several mechanisms have been identified that promote drug resistance either directly or indirectly. These include epithelial-mesenchymal transition, DNA damage repair, evasion of apoptosis, mutations that alter drug-target interactions, drug efflux, and epigenetic modifications [Bradshaw and Arceci, 1998; Spoelstra et al., 1991; Duesberg et al., 2000; Choy et al., 2005; Ji, 2010; Salehan and Morse, 2013; Krishna Vadlapatla et al., 2013; Mitra et al., 2015; Bacolod, 2021; Ketkar and Dutt, 2022]. Resistance can also develop through reduced drug activation, as many anticancer agents require metabolic activation. The activation of detoxification systems, such as the GST superfamily, can lead to drug inactivation [Housman et al., 2014]. Additionally, inactivation of p53 and related regulators promotes drug resistance by enabling cells to bypass apoptosis [Hientz et al., 2017]. Targeting signaling kinases such as Ras, Src, Raf, and MEK is effective in combating uncontrolled cell growth. However, mutations in receptor tyrosine kinases within the EGFR family, such as HER2, which is overexpressed in 30% of breast cancer patients, can lead to resistance to EGFR inhibitors like gefitinib and erlotinib [Bose and Ma, 2021]. Some therapeutics, such as temozolomide and platinum-based drugs, induce guanine O6 alkylation, which is repaired by MGMT, converting it back to guanine and thus protecting DNA from permanent damage. Overexpression of MGMT has been shown to protect both stem cells and tumors from alkylating agents [Blanc et al., 2004; Passagne et al., 2006; Maier et al., 2010].

Metastatic cancer cells often exhibit significant heterogeneity, with individual cells undergoing various differentiation pathways. This diversity results in different responses to treatments. Epithelial-to-mesenchymal transition (EMT) promotes the formation of additional metastatic cancer cells, thereby inducing signals that contribute to survival and drug resistance. Heterogeneous tumors exhibiting stem cell characteristics often show resistance to drugs [Turner and Reis-Filho, 2012; Housman et al., 2014]. Two widely researched strategies to combat drug resistance are reducing efflux and increasing drug accumulation within cells. Proteins from the ATP-binding cassette (ABC) transporter family facilitate this efflux and are well-studied regulators at the plasma membrane. ATP hydrolysis at the nucleotide-binding site induces a conformational change when a specific substrate binds to the transmembrane domain, driving the substrate outside the cell and

thus preventing toxin accumulation [Sauna and Ambudkar, 2001]. The first discovered ABC transporter, Multi-drug Resistance (MDR1), produces P-glycoproteins (P-gp), which have broad substrate specificity and can pump out various xenobiotics, including vinca alkaloids, anthracyclines, taxanes, and kinase inhibitors [Szakács et al., 2004; Yang et al., 2008]. Although overexpression of ABC transporters is strongly correlated with poor clinical outcomes, direct inhibitors of these pumps (such as verapamil, elacridar, and zosuquidar) are not recommended for clinical use due to their side effects [Ween et al., 2015].

1.2. Epigenetics in Cancer

1.2.1 Epigenetic Regulations in Prostate Cancer

Epigenetic dysregulation can influence cancer progression, including in prostate cancer [Egger et al., 2004]. Factors such as DNA methylation, histone modifications, cell-free DNA, and non-coding RNAs have been reported to affect the regulation of prostate cancer [Conteduca et al., 2021]. Multiple methylation-related genes have been associated with prostate cancer to date. The most commonly hypermethylated tumor suppressor genes in prostate cancer are involved in processes such as DNA damage repair, cell cycle regulation, and apoptosis [Mahapatra et al., 2012]. DNA methylation is catalyzed by a family of conserved enzymes known as DNA methyltransferases (DNMTs), with CpG dinucleotides serving as the primary targets for methylation in DNA chains [Moore et al., 2013].

Investigating CpG hypermethylation in both normal and tumor tissues is a common approach to identifying accurate diagnostic markers for various diseases. Methylation profiling offers high accuracy and minimally invasive potential for diagnosing rare types of prostate cancer, surpassing existing methods in sensitivity and specificity. DNA methylation analysis is preferred for prognostic and diagnostic purposes due to its applicability with peripheral blood or urine samples, making it convenient and accessible. For instance, Kobayashi et al. demonstrated that activation of DNMT3B1 and DNMT3B2 leads to higher methylation levels, which provide advantages to tumor cells. Another study found that increased methylation of CD24 in tumor samples correlated with poorer

survival in prostate cancer patients [Tolkach et al., 2021]. Several other biomarkers have been identified with hypermethylation patterns in prostate cancer, including GSTP1, RASSF1, APC, CDH1, MGMT, and NKX3.1 [Konishi et al., 2002; Woodson et al., 2003; Asatiani et al., 2005; Chen et al., 2013].

There are significant differences in the patterns between normal and cancer samples for several types of alterations, including histone methylation and acetylation [Chiam et al., 2014]. Ngollo et al., provided intensive data on the enrichment of H3K27me3 marker around promoter regions in PC samples with higher Gleason scores. H3K9 methylation is usually known for its role in silencing activity [Jih et al., 2017], in lineage-specific gene expression, another study identified a dominant H3K9 methylation pattern in advanced prostate tissue [Ellinger et al., 2010]. In a study including immunohistochemistry stainings with different PC samples, H4K20me1 staining was increased in patients with lymph node metastases, and patients with high Gleason scores showed higher expression of H4K20me2 [Behbahani et al., 2012]. In samples with increased serum PSA levels, high expression in different HDACs (1, 2, and 3) was also observed [Weichert et al., 2008], and treatment with HDAC inhibitors showed promising results regarding, increased cell cycle arrest and apoptosis [Biersack et al., 2022]. Some studies also showed testosterone induction enhances H3 acetylation in PSA promoters [Kang et al., 2004]. Main histone acetyltransferase complex proteins CBP and p300 are crucial in conferring the growth of CRPC [Welti et al., 2021]. Besides acetylation, super-enhancers also confer H3K27ac, and recruit transcription factors in PC inducing gene sets [Chen et al., 2020]. Targeting acetylation reader complex BRD4, with JQ1 abolishing AR target genes activity, JQ1 also diminished CRPC growth *in vivo* [Asangani et al., 2014].

KDM1A (also known as LSD1) has attracted attention due to its role in H3K4 demethylation and activation of the Myc oncogene in prostate cancer [Amente et al., 2010]. Elevated expression of KDM1A in initial prostate cancer has been linked to a higher likelihood of relapse following prostatectomy [Kahl et al., 2006]. Extensive research has highlighted EZH2 as a major player in prostate cancer. EZH2 expression is significantly upregulated from normal tissues to prostate cancer and further to castration-resistant prostate cancer (CRPC) [Varambally et al., 2002; Bryant et al., 2007]. Reducing

EZH2 expression decreases prostate cancer invasiveness [Varambally et al., 2002], and subsequent studies by Shin and Kim demonstrated that EZH2 facilitates extracellular matrix (ECM) degradation via matrix metalloproteinases (MMPs) and promotes invasion. In addition to histone modifications, miRNA expression is also altered in prostate cancer, with changes that either activate oncogenes or silence tumor suppressors [Peng and Croce, 2016]. Several miRNAs have been reported to regulate androgen receptor (AR) activity [Sikand et al., 2010].

1.2.2 Epigenetic Regulations in Drug Resistance

Cancer stem cells (CSCs) are often considered major contributors to therapy resistance due to their shared properties with resistant cells, such as epithelial-to-mesenchymal transition (EMT), increased efflux potential, quiescence, and evasion of apoptosis [Adhikari et al., 2022]. After therapy, selection pressure may favor inherently drug-resistant cells, or tumor cells may activate specific signaling pathways to acquire chemoresistance [Easwaran et al., 2014; Jin et al., 2017]. Several studies have highlighted the role of epigenetic modulation in the survival and maintenance of CSCs or drug-tolerant cells. Resistant cells can reprogram their epigenome through DNA methylation and modifications of histone and non-histone proteins to adapt to increased drug pressure [Liau et al., 2017]. High expression of ABC transporters in CSCs is linked to promoter hypomethylation [Zappe and Cichna-Markl, 2020], while afatinib has been shown to increase DNMT activity, resulting in hypermethylation of the ABCG2 promoter in breast cancer cells [Wang et al., 2014]. Additionally, treatment with 5-aza-2'-deoxycytidine or trichostatin A has been reported to increase ABCB1 mRNA expression in drug-sensitive cell lines. Furthermore, the epigenetic regulation of ABCB1 and Breast Cancer Resistance Protein (BCRP) through HDAC inhibition has been documented [Tomiyasu et al., 2014; You et al., 2020].

Drug-metabolizing enzymes (DMEs) are essential for the biotransformation and detoxification of therapeutics. In prostate cancer, CYP24A1, a member of the DME family, is repressed by promoter methylation and the histone repressor mark H3K9me2 [Luo et al., 2010]. The methylation status of DMEs' promoters can predict the treatment efficacy of hormone-responsive breast cancers. Specifically, the P450 family has been

reported to be a predictor of treatment response in tamoxifen-treated patients [Widschwendter et al., 2004]. As previously discussed, DNA repair systems are another mechanism by which cells can develop resistance. Drug-resistant cells may avoid increased DNA damage by enhancing their repair capacity. For example, hMLH1, a key enzyme involved in mismatch repair, has been reported to be hypomethylated around its promoter region in colorectal cancers [Hermann et al., 1998].

Hypermethylation of several genes can inhibit cell death pathways, thereby providing tumor cells with a resistant phenotype. For instance, hypermethylation of the promoters of Bcl-2 and Bik has been observed in prostate cancer [Murphy et al., 2011]. Additionally, in bladder carcinoma cells, the cell cycle regulator p21 is repressed due to increased HDAC activity around its promoter [Richon et al., 2000]. Similarly, hypermethylation of the promoters of Bad, Bax, Bak, and Puma in multiple myeloma has been linked to stalled apoptosis and enhanced cell survival [Pompeia et al., 2004]. Furthermore, the repressed activity of apoptotic pathway regulators Caspase 8 and 10, due to promoter methylation, has been reported in various cancers [Shivapurkar, 2002; Malekzadeh et al., 2009; Cho et al., 2010].

Numerous studies have demonstrated that in addition to genetic abnormalities, epigenetic changes are crucial for cancer cell maintenance and, importantly, for acquiring chemoresistance [Kongkham et al., 2008; Dunwell et al., 2010; De Carvalho et al., 2012; Brown et al., 2014; Baylin and Jones, 2016; Guo et al., 2019; Shah and Rawal, 2019; Li et al., 2020]. These epigenetic alterations are reversible by various groups of epigenetic modifiers, making them attractive targets for therapeutic intervention. Recently, our group discovered that ABCB1 is regulated epigenetically via the BRPF1 bromodomain reader protein. Taxane resistance can be reversed with BRPF inhibitors, and BRPF is enriched at the MDR1 promoter, supporting its role in transcriptional regulation [Cevatemre et al., 2024]. Drugs that modify the epigenome represent a promising alternative for use in conjunction with conventional or combinatorial therapies. To develop more effective treatment options, it is crucial to continue exploring the complex epigenetic regulatory systems that drive drug resistance. Identifying epigenetic regulators

that contribute to the progression or reversal of taxane-resistant metastatic prostate cancer is the primary focus of the proposed study.

1.3. MLL-Complexes in Cancer Progression

1.3.1 MLL Complexes in Cancer

The MLL (KMT2) family is a major epigenetic regulator that controls H3K4 methylation through core partners such as WDR5, RbbP5, DPY30, and ASH2L, which collectively enhance genomic accessibility and active gene expression [Milne et al., 2005]. MLL family proteins are highly conserved, even in unicellular eukaryotes [Schuettengruber et al., 2011]. Studies highlight the critical role of ASH2L and Rbbp5 in facilitating SET histone methyltransferase activity [Cao et al., 2010]. The loss of WDR5 or MLL results in reduced catalytic activity of MLL, underscoring the scaffolding role of WDR5 within MLL complexes [Karatas et al., 2010]. KMT2A and KMT2B are reported to exhibit higher activity in methylating H3 at me1 and me2 levels, but have limited me3 activity [Dou et al., 2006]. The functional role of H3K4 methylation has been extensively studied in the context of transcription, with reader proteins playing a key role in dictating transcriptional activation [Taverna et al., 2007; Ruthenburg et al., 2007]. Beyond their primary role in transcription and epigenetic remodeling, mutations in MLL are of significant interest due to their association with various cancers, including leukemia and some solid tumors [Krivtsov and Armstrong, 2007; Ding et al., 2008; Liedtke and Cleary, 2009]. Kandoth et al. utilized next-generation sequencing to analyze over three thousand samples across twelve tumor types and identified the MLL family as one of the most frequently mutated gene families in human cancers. KMT2A rearrangements, including translocations, tandem duplications, and amplifications, account for approximately 10% of human leukemias and are associated with poor prognosis [Ayton and Cleary, 2001]. To date, more than 70 fusion proteins involving KMT2A have been identified, indicating a heterogeneous pathogenesis. KMT2A fusion proteins may initiate leukemic transformation from hematopoietic stem cells, promoting stem cell characteristics such as self-renewal and increased expression of oncogenic genes [Liedtke and Cleary, 2009]. Inhibitors targeting MLL have shown potential in halting leukemia transformation [Grembecka et al., 2012; Borkin et al., 2015; Lei et al., 2021].

In solid tumors, MLL was found to bind AR and activate AR-target genes, furthermore, MLL-Menin inhibition, diminished CRPC tumor size in mice [Malik et al., 2015]. In breast cancer, the MLL and FOXQ1 axis was upregulated to initiate the EMT phenotype [Mitchell et al., 2022]. In glioblastoma, MLL contributed to CSC characteristics through HOXA10 [Gallo et al., 2013]. Through H3K4 methylation MLL was inducing PD-L1 transcription in pancreatic tumors, resulting in evasion of immune response. Indeed, MLL inhibition with PD-L1 antibody treatment decreased pancreatic tumor growth [Lu et al., 2017].

1.3.2 The Role of MLL Complexes Menin and LEDGF in Cancer

While MLL has multiple binding proteins, Menin (Multiple Endocrine Neoplasia 1) and LEDGF (Lens Epithelium Derived Growth Factor) are distinct partners of the complex due to their affinity to bind the N-terminus of the methyltransferase. Structural studies showed that Menin has a DNA binding domain in COOH-edge [La et al., 2004]. Menin also binds with MLL, and composes a complex with WDR5 and ASH2L, resulting in H3K4 methylation on the promoter of relative genes. On the other hand, so far, in all MLL-fused conditions menin interaction was preserved, highlighting the requirement of Menin to initiate oncogenic activation [Hughes et al., 2004, Milne et al., 2005, Yokoyama et al., 2005]. Several studies provided data on Menin's role in engaging MLL methyltransferase to promoters of relevant genes [Milne et al., 2005, Chen et al., 2006, Dreijerink et al., 2006]. MLL1 and Menin control the expression of multiplexed genes, however, they do not always join forces together [Scacheri et al., 2006]. On the other hand, Dreijerink et al. revealed that nearly 83% of Menin binding sites were covering the TSS region in ER-positive breast cancer. Multiple ChIP-seq data support the high incidence of Menin enrichment in the TSS, usually in leukemic, breast, and colon cancer cell lines [ChIP Atlas: Target Genes, 2024].

Last year, an interesting finding was reported by Lin et al.; the group assigned a remarkable role for Menin and suggested that Menin is the reader protein for H3K79me2. H3K79 methylation is the gene body histone mark, the responsible eraser still unknown in higher eukaryotes, and Dot1L is known to be the writer protein of the relative

epigenetic target [Hyun et al., 2017]. H3K79me has been reported to confer leukemogenesis via HOXA9 expression by Dot1L-based methylation in MLL-fused samples [Okada et al., 2005]. We anticipate a rise in the number of studies focusing on the advanced roles of menin in circumstances where H3K79me is investigated. Menin also contributes histone arginine methylation regulation via PRMT5 and induces H4R3me2 to suppress target gene expression [Gurung et al., 2013]. Another silencing-related histone regulation by Menin was reported via suppressor of variegation 3–9homolog protein 1 (SUV39H1). This interaction increases H3K9me3 in the promoter of relative genes [Yang et al., 2013].

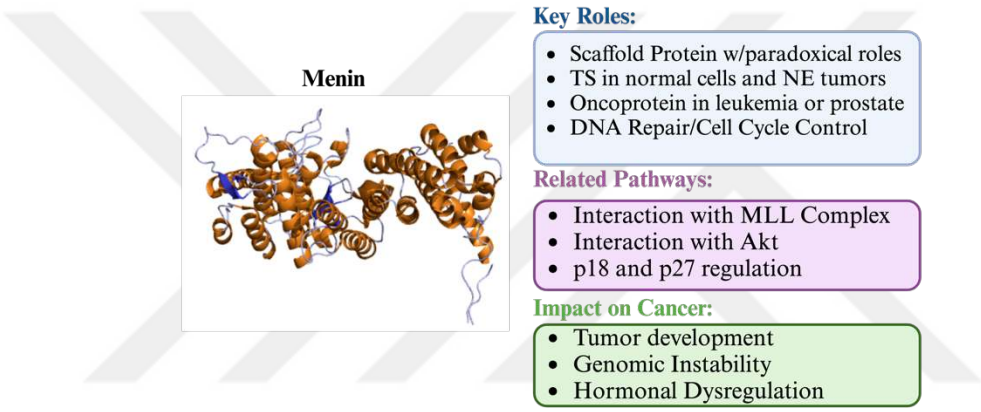

Figure 1. 1: Predicted 3D structure of Menin and its important roles in cancer
Adapted from Matkar et al., 2013.

In addition to its role in histone methylation, Menin has been implicated in interactions with various transcription factors. For instance, JUND1, a member of the AP1 protein family that regulates cell proliferation, exhibits reduced activity upon binding with Menin [Agarwal et al., 1999]. Additionally, Menin has been shown to decrease Akt activity by altering its subcellular localization in pancreatic adenomas [Wang et al., 2011]. These findings initially led to the perception of Menin primarily as a tumor suppressor. However, more recent studies have uncovered additional functions of Menin. Notably, through its transactivating domain (TAD), Menin can bind to and activate Myc, acting as an enhancer for Myc target genes. This interaction suggests that Menin can promote Myc-dependent proliferation and oncogenic activity in various cancers [Wu et al., 2017].

NF-κB is another crucial regulator of the transcriptome known to interact with Menin. In hepatocellular carcinoma studies, Menin was found to influence Sirt1 occupancy on specific transcription factors, leading to the deacetylation of p65 [Gang et al., 2013]. Recent research by Dreijerink et al. has further elucidated Menin's role, highlighting its enhancer-like function within the MLL-Menin complex in ER-positive breast cancer. The study demonstrated that Menin associates with the GATA3/FOXA1 complex to form loop-like structures between the enhancer region and the H3K4me3 mark at the transcription start site (TSS). Menin-positive patients exhibited poorer outcomes with tamoxifen treatment, and pulldown experiments confirmed the physical interaction between Menin and ER [Imachi et al., 2010]. Menin's interactions extend beyond ER. Malik et al. demonstrated that in VCaP and LNCaP cell lines, Menin directly associates with MLL complexes to promote AR target gene expression. Silencing ASH2L, MLL, and Menin completely abolished VCaP-derived xenografts. Their pull-down assays revealed direct binding of AR and Menin on the promoters of genes known to regulate AR-mediated progression.

Menin-associated proteins (MAPs) have gained attention for their roles in cancer from various perspectives. For instance, Menin helps cancer cells evade metabolic stress, facilitating adaptation. Downregulation of Menin or MAPs has been shown to alter the glycolysis-to-oxidative phosphorylation ratio in breast cancer [Chou et al., 2020]. In advanced breast cancer, Menin’s interaction with LINC00355 results in abnormal proliferation by reducing p27 expression, thereby promoting an aggressive phenotype [Eteleeb et al., 2022]. In colorectal malignancies, Menin contributes to oncogenic activation through the upregulation of SPK2, and both Menin inhibitors and EGFR inhibitors have demonstrated promising results [Katona et al., 2019]. Additionally, another study revealed that MLL-Menin inhibitors can induce ferroptosis in breast, ovarian, and pancreatic cancers [Kato et al., 2020].

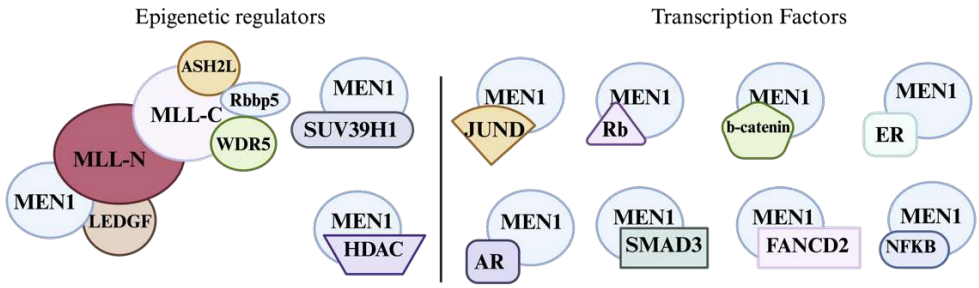

Figure 1. 2: Different epigenetic regulators or transcription factors which reported to interact with the Menin protein.

Menin also plays a role in CRPC cell growth and resistance through HSP27-mediated regulation. Using the anti-sense oligo silencing (ASO) method to target Menin has been shown to enhance sensitivity in CRPC cells [Cherif et al., 2022]. Similarly, in triple-negative breast cancer (TNBC), ASO-mediated silencing of Menin was reported to halt tumor progression in Hs 578T cells [Nguyen et al., 2021]. Menin has been linked to a migration phenotype in Du145 prostate cancer cells through the suppression of TIMP2 [Kim et al., 2022]. Additionally, a clinical study found that elevated Menin expression is observed in 44.4% of adult gliomas and is associated with poor prognosis, including larger tumor size and shorter survival time [Wang et al., 2020].

Depending on the type of cancer, Menin has been identified as either a tumor suppressor or an oncogenic regulator in numerous studies. Menin is a multifaced protein that performs a wide range of functions in different types of cancer cells. Its involvement in a myriad of pathways including, metabolism, transcription, histone regulation, metastasis, regulation of major signaling pathways, or drug resistance ensures that Menin will undoubtedly continue to captivate the interest of cancer researchers. A major critical role of Menin is its function as an adaptor, connecting MLL and its oncogenic counterparts to LEDGF [Yokoyama and Cleary, 2008]. LEDGF protein is an indispensable factor for MLL-Menin-dependent gene regulation in MLL-mutated leukemias also LEDGF ablation remediates the disease phenotype in mouse models [Méreau et al., 2013, El Ashkar et al., 2018]. LEDGF, a member of the epi-enzyme family, bears PWWP domain, known for its interaction with H3K36me3, alongside several other enzymes [Pradeepa et al., 2012; Sundarraj et al., 2017]. Ablation of LEDGF in mouse models leads to

developmental abnormalities due to its role in regulating Hox genes via MLL [Yu et al., 1995; Sutherland et al., 2006]. Additionally, LEDGF contributes to DNA repair pathways and splicing mechanisms [Daugaard et al., 2012; Singh et al., 2015; Pradeepa et al., 2017; Liedtke et al., 2021].

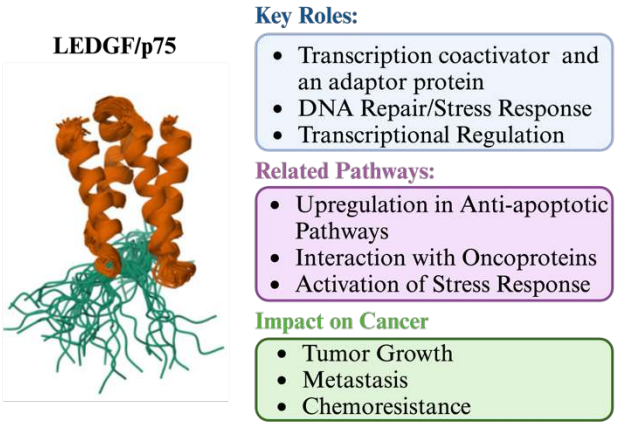

Figure 1. 3: Predicted 3D structure of LEDGF and its important roles in cancer. Adapted from Blokken et al., 2017.

LEDGF has been reported to induce a refractory phenotype to chemotherapy in MLL and prostate cancer [Ríos-Colón et al., 2017; Ortiz-Hernandez et al., 2021; Canella et al., 2022]. In ovarian cancers, LEDGF is enriched at the VEGF-C promoter, contributing to angiogenesis [Sapoznik et al., 2009]. Additionally, LEDGF oncoprotein activates oxidative stress-dependent resistance in prostate cancer [Basu et al., 2012]. In some cases, human papillomavirus induces both LEDGF mRNA and protein levels in virus-positive cervical lesions [Leitz et al., 2014]. Overexpression of LEDGF has been associated with poor prognosis in clinical cases of cervical cancer [Yin et al., 2017].

A broad expression analysis of LEDGF across various tissue microarrays showed that LEDGF was significantly upregulated in 15 out of 17 tumor types, including breast, prostate, and colon cancers, compared to non-tumor samples [Basu et al., 2012]. The ability of LEDGF/p75 to bind specific transcription factors and promote the transactivation of genes related to stress, inflammation, antioxidants, and cancer contributes to its stress survival properties [Singh et al., 2001]. LEDGF (p75) has an alternative splice variant, p52, which contains the first 352 amino acids of the N-terminus.

The p75 variant is more highly expressed in cancer cells, likely due to its pro-survival properties [Ge et al., 1998; Daniels et al., 2005]. Similar to MLL, LEDGF can induce fusion proteins via chromosomal dysregulation in leukemias and promote resistance to daunorubicin treatment in AML [Huang et al., 2007].

Emerging evidence suggests that LEDGF has oncoprotein-like features, making it a critical player in cancer biology. This versatile protein is implicated in various cellular processes that contribute to the initiation, progression, and maintenance of cancer.

1.4. mTOR Pathway

1.4.1 mTOR Pathway in Cancer

The mammalian target of rapamycin (mTOR) is involved in numerous signaling pathways throughout the body, overseeing cell growth and regulating cell death. The mTOR pathway is often hyperactive in tumors, likely due to its crucial roles in controlling transcription and translation, thus playing a key role in tumor metabolism [Sarbassov et al., 2005]. The mTOR forms two distinct complexes: mTOR complex 1 (mTORC1) and mTOR complex 2 (mTORC2), which are both physically and functionally different [Szwed et al., 2021]. mTORC1 typically comprises four components (mTOR, GβL, deptor, raptor), while mTORC2 includes six components (mTOR, GβL, PRR5, Rictor, SIN1, and deptor). Depending on the cell's energy status, mTORC1 has dual functions; it promotes cell growth when energy sources are ample and initiates catabolic reactions when energy is scarce. Conversely, mTORC2 supports cell division and survival [Jhanwar-Uniyal et al., 2017].

Under normal conditions, cells rely on mTOR activation to maintain growth and division. However, in tumor cells, aberrant mTOR activation can lead to abnormal cell division and metastasis [Hsieh et al., 2012]. Tumor cells can activate the PI3K/(PTEN)/AKT/TSC pathways to stimulate mTORC1 [Nathan et al., 2017]. Approximately 40-50% of primary prostate tumors and an even higher percentage of cases of castration-resistant prostate cancer (CRPC) exhibit PTEN loss, resulting in a hyperactive PI3K/Akt pathway [Wise et al., 2017]. Similarly, activation of the PI3K/Akt/mTOR pathway has been implicated in

tumorigenesis in the breast, liver, colon, and other tissues [Johnson et al., 2010; Guerrero-Zotano et al., 2016; Golob-Schwarzl et al., 2017].

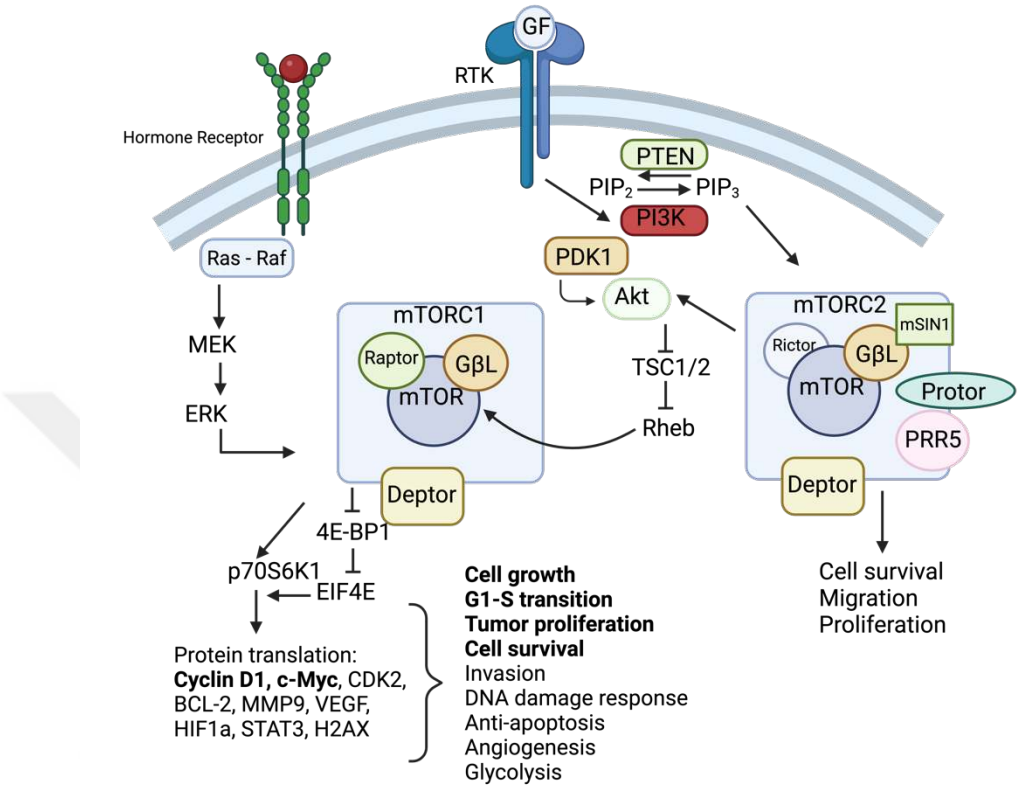

Figure 1. 4: mTOR pathways and downstream targets

Adapted from, Jhanwar-Uniyal et al., 2017, Tian et al, 2019, Murugan et al., 2019, and Zou et al., 2020.

mTORC1 typically binds to lysosomal membranes, whereas mTORC2 associates with plasma and ribosomal membranes. These complexes are influenced by a variety of endogenous and exogenous stimuli, such as hormones, growth factors, nutrients, energy levels, and hypoxia [Tian et al., 2019]. Several signaling pathways, including Ras-MAPK and PI3K/Akt, along with other intracellular factors, regulate mTORC1 (Figure 4). The PI3K/Akt pathway predominantly activates mTORC1 in response to oncogenic growth factors [Stefani et al., 2021]. Once activated, mTORC1 signals downstream targets like S6K1 and 4E-BP1, which play crucial roles in translation [Ma and Blenis, 2009]. In the downstream cascade, eukaryotic initiation factor 4E (eIF-4E) induces protein translation to facilitate the G1-S transition [Montanaro and Pandolfi, 2004]. Thus, mTORC1 regulates cell cycle progression, and when its activity is low, 4E-BP1 is

dephosphorylated, stalling protein translation [Rad et al., 2018]. Additionally, mTORC1 enhances HIF1α, PP2A, and STAT3, promoting invasion and the synthesis of nucleotides and lipids [Marhold et al., 2015; Tian et al., 2019]. Consequently, cancer cells rely on mTORC1 activity to grow rapidly and secure necessary nutrients.

mTORC2 is regulated by the PI3K/Akt pathway, similar to mTORC1, and its downstream effectors include SGK, PKC, and Akt [Szwed et al., 2021]. The PI3K/Akt axis is frequently activated in cancer, promoting mTORC2-dependent cell proliferation in various tumors [Willems et al., 2012; Khan et al., 2015]. mTORC1 and mTORC2 negatively regulate each other through complex feedback mechanisms [Jhanwar-Uniyal et al., 2017]. mTORC2 can activate SGK, which in turn induces myc-dependent targets like NDRG1, leading to oncogenic cell proliferation [Chekmarev et al., 2021]. Additionally, mTORC2-mediated PKC phosphorylation may facilitate cell migration, providing a competitive advantage to cancer cells [Gan et al., 2012].

mTOR is one of the most mutated/altered pathways in human cancers, indeed mTOR inhibitors have shown promising results in different studies with different tumor types [Yuan et al., 2009, Pópulo et al., 2012, Zaytseva et al., 2012, Xie et al., 2016]. Rapamycin is the first inhibitor of mTOR, and is reported to promote G1 cell cycle arrest [Fingar et al., 2004, Foster et al., 2010]. It also reduces VEGF and HIF1α, therefore reducing dissemination [Xue et al., 2009]. 10 mTOR inhibitors made it to the clinical trials in different tumors [Xie et al., 2016]. Due to kinase domain similarity, some inhibitors effectively inhibited both PI3K and mTOR, therefore named as dual inhibitors of PI3K/mTOR. For example, NVP-BEZ235 exhibits anti-tumor properties in animal studies [Maira et al., 2008]. Later on, Torin 1, a second generation mTOR inhibitor was developed as an ATP-competitive target by AstraZeneca [Thoreen et al., 2009]. Several studies identified the potential effects of Torin 1 in different cancers [Liu et al., 2010, Francipane and Lagasse, 2013, Amin et al., 2021].

1.4.2 mTOR Pathway in Drug Resistance

Multiple mechanisms contribute to the development of chemotherapy resistance, ultimately resulting in treatment failures. Factors such as the upregulation of drug efflux, immunosuppression, metabolic changes, pro-survival signaling, and enhanced DNA repair are key drivers of drug-refractory phenotypes [Zahan et al., 2020]. Over the past few decades, the role of mTOR activation in drug resistance systems has become increasingly evident [Stephan et al., 2004; Beuvink et al., 2005; Guerrero-Zotano, 2016; Dong et al., 2021]. The relationship between mTOR and microtubule-targeting drugs was first identified in vincristine resistance [VanderWeele et al., 2005]. Subsequent studies revealed that increased mTOR activity is associated with paclitaxel resistance in ovarian cancer [Foster et al., 2010]. Additionally, PI3K has been reported to regulate the expression of MDR1, a transmembrane drug transporter, leading to drug resistance in leukemia and prostate cancer [Lee et al., 2004; Tazzari et al., 2007]. Activation of Akt, an upstream signaling partner of mTOR, has been implicated in conferring drug insensitivity to various chemotherapy agents in leukemia, breast, prostate, and gastric cancers [Chen et al., 2001; Clark et al., 2002; Bortul et al., 2003; Lee et al., 2005; Berns et al., 2007; Yu et al., 2008]. The modulation of mTOR pathways has been consistently linked to chemotherapy resistance, as documented by Jiang and Liu in their comprehensive review of mTOR-related drug resistance cases up to 2008. Since then, further studies have continued to expand our understanding of this topic [Foster et al., 2010; Murugan et al., 2019; Gremke et al., 2020; Dong et al., 2021].

Inhibiting mTOR may enhance chemotherapy responses, as indicated by various studies [Strömberg et al., 2004; Dengler et al., 2005; Beeram et al., 2007; Squillace et al., 2012; Reita et al., 2019]. Given that mTOR-related pathways are intricately connected with major cellular signaling pathways, mTORC1 is hyperactivated in the majority of human malignancies. This pervasive activation has led to a growing interest in incorporating mTOR-based chemotherapy regimens. Clinical studies have examined the effectiveness of several mTOR inhibitors, such as temsirolimus and everolimus, in treating castration-resistant prostate cancer (CRPC). Although some studies have shown promising results, the overall efficacy of mTOR inhibitors as single-agent therapies remains limited [Armstrong et al., 2013; Kruczek et al., 2013; Barata et al., 2019; George et al., 2020].

This has prompted researchers to explore combination therapies to enhance therapeutic efficacy and overcome resistance mechanisms. mTOR inhibitors may be combined with other chemotherapeutics, androgen receptor (AR) inhibitors, or targeted therapies such as epigenetic drugs [Ellis et al., 2013; Thomas et al., 2013; Wei et al., 2017; Raith et al., 2023].

In this thesis, we generated taxane-resistant CPRC cell lines and revealed epigenetic targets capable of reversing taxol resistance. Our screen highlighted the role of MLL-Menin inhibitors in improving drug response in combination treatment. Our CRISPR-cas9-based analysis indicated Menin and LEDGF proteins are essential to Docetaxel-resistant cells, and their depletion significantly remitted the growth of resistant cells while showing no significant effect on parental cells. Our RNA-seq analysis revealed upregulation in the mTOR pathway during the acquisition of drug resistance. Depleting Menin and LEDGF significantly reversed mTOR-related gene sets, furthermore, mTOR inhibition in Menin-null cells significantly improved the chemotherapy response of taxol-resistant cells. Menin-null cells showed reduced mTOR expression and Menin was found to be enriched in mTOR promoter. Menin silencing also resulted in reduced cycling phenotype in resistant cells, suggesting mTOR-dependent growth is maintained by Menin presence in our taxol-resistant model. Additionally, Cyclin D1 levels were significantly reduced following mTOR silencing, furthermore, Menin was also enriched in Cyclin D1 and CDK20 promoter.

.

Chapter 2

MATERIALS and METHODS

2.1 Generation of Drug-Resistant Cell Lines

Du145 cell lines were purchased from ATCC (HTB-81), all cell lines were routinely grown at 37℃ in a 5% CO_2 humidified atmosphere in RPMI- 1640 (Sigma Aldrich #R8758) supplemented with heat-inactivated 10% fetal bovine serum (FBS; Biowest #1810), 100 U/ml of penicillin, and 100 µg/ml of streptomycin (Life Technologies #15140122). To develop drug resistance, Du145 cells were subjected to the IC_{50} level of 1 nM as the initial Docetaxel (Sigma #01885) dose or vehicle (DMSO) for 72 h. Subsequently, the drug-survived population was allowed to grow in the drug-free environment to recover. Later on, the remaining cells were subjected to a double dose of docetaxel, and this cycle was repeated until the cells reached an IC_{50} of 250 nM. Docetaxel was prepared in DMSO with 500 mM of main stock. In parallel, parental cells were grown in a medium containing the corresponding dose of DMSO, synchronized with similar passaged conjugates.

Du145 Drug Sensitive Parental Cells: “P”

Du145 Drug Resistant Cells: “DtxR”

2.2 Sulforhodamine B (SRB) Viability Assay

P and DtxR cells (4×10^3) were seeded on 96-well plates a day before relative drug treatment. Drugs or chemicals used in all experiments are given in **Table 2.1.** Following drug treatment (72 h), cells were fixed with 50% (w/v) Trichloroacetic acid (TCA, Sigma, T6399) at 4°C for 1 h. To remove TCA, wells were washed off with distilled water or dH_2O, and the plates were air-dried. Later on, wells were stained with 50 µL of 0.4% (w/v in 1% acetic acid) SRB dye (Santa Cruz, sc-253615) for 30 min, followed by washing with 1% acetic acid solution. The SRB-stained wells were air-dried, and the

dye was dissolved using 150 µL of 10 mM Trizma base solution (Sigma, T1503), with mild shaking at RT for 10 min. Absorbance measurements were obtained at 564 nm using a microplate reader (Synergy H1 Hybrid reader, BioTek).

Table 2. 1: Chemicals used in drug treatments.

Chemical Name	Catalog number
Docetaxel	Sigma #01885
EpiDrug Library	Cayman Chemicals, 11076
MI-2	Cayman Chemicals, 29218
MI-3	Cayman Chemicals, 27214
MI-136	Cayman Chemicals, 19245
MI-463	Cayman Chemicals, 33525
WDR5-0103	Selleckchem, S2184
Verapamil	Cayman Chemicals, 14288
Puromycin	Sigma Aldrich, P8833
Hygromycin	GoldBio, H-270-1
Blasticidin	Thermo Fisher Scientific, R210001
Amphicilin	GoldBio, A-301-5
Kanamycin	GoldBio, K-120-5
Calcein-AM	Invitrogen™, C1430
Torin1	Cayman Chemicals, 10997
CINK4	Cayman Chemicals, 17974

Abemaciclib	Cayman Chemicals, 17740
Palbociclib	Cayman Chemicals, 16273
Ribociclib	Cayman Chemicals, 17666
Ryuvidine	Cayman Chemicals, 16614

2.3 Colony Formation Experiments

P and DtxR (1×10^3) cells were seeded on 12-well plates a day before relative treatment. Following treatment (72 h), cells were grown for an additional 10-12 days in a fresh drug-free medium. At the end of the treatment, formed colonies were fixed with methanol (Merck, 1.06009) for 10 min at -20°C, and washed with distilled water twice. The wells were stained with 0.5% (w/v) crystal violet solution (Merck, 1.09218) for 20 min, and the dye was washed five to six times with distilled water. The quantification of colonies was performed using CellCounter software by Nghia Ho.

2.4 Cell Cycle Analysis

Following the treatment, (1×10^5) cells were washed with PBS (EcoTech, PBS500), and fixed with 70% ethanol (Merck, 100983) at -20°C for at least 3 h or overnight. Residual ethanol was removed with PBS wash twice and the cell pellet was stained with 200 µL of Cell Cycle Reagent (Luminex Corporation, MCH100106) for 20 min at RT in the dark, and the cell cycle stage was evaluated depending on the DNA content, which analyzed by using flow cytometry (Muse™ Cell Analyzer) with 5000 events.

2.5 Apoptosis analysis

1×10^5 cells were seeded on 6-well plates 16 h before drug treatment. Following treatment (48 – 72 h), cells were washed with 100 µL of PBS (EcoTech, PBS500), and stained with Muse™ Caspase-3/7 kit (CYTEK, MCH100108). Muse™ Caspase 3/7 Reagent was diluted in PBS with a ratio of 1:8 to prepare a working solution. The cell

(50 µL) and working solution (5 µL) mixture was incubated for 30 min at 37°C. Subsequently, cells were stained with 150 µL Muse™ Caspase 7-AAD working solution (containing Muse™ Caspase 7-AAD was diluted in 1 × Assay Buffer with a ratio of 1:75) and the tubes were incubated at RT for 5 min in the dark. Caspase 3/7 and 7-AAD positive cells were counted by using by using flow cytometry (Muse™ Cell Analyzer) with 5000 events.

2.6 siRNA-mediated silencing

siControl, siABCB1, siMLL, siMEN1, and siWDR5 were obtained from (Thermo Fisher Scientific, #4390843 and Ambion, #AM107890, #AM143227, #AM136959). P and DtxR (1×10^5) cells were seeded on 6-well plates 16 h before transfection. 75-100 pmol of each siRNA was transfected into the cells using Lipofectamine (Invitrogen, L3000001) following the manufacturer's protocols. Briefly, 200 µL of OptiMEM (Gibco, 31985) and 5 µL of Lipofectamine 3000 reagent were mixed. In another tube, 200 µL of OptiMEM and 75-100 pmol of siRNA were mixed. Diluted siRNA was added to a diluted Lipofectamine 3000-containing tube, and incubated for 15 min at RT. The RNA-lipid complex was given to the cells by the drop-wise method. The next day, Lipofectamine was removed by the addition of a fresh medium. At the end of the incubation time (48 – 72 h), cells were trypsinized and seeded for relative experiment, remaining cells were separated for RNA isolation.

2.7 PCR for Genomic DNA amplification

Genomic DNA was isolated in Du145-P, -DtxR, and another resistant cell line -CbzR, using a Nucleospin Tissue kit (Macherey Nagel, 740952.50) according to the manufacturer's protocol. For PCR reaction, 10 ng of genomic DNA was used, and the relative quantification of ABCB1 copy number was validated by using LightCycler 480 SYBR Green I Master mix (Roche Diagnostics, 04707516001) and 150 nM of F-R primers. The primer sequence was received from Yabuki et al., 2007, and designed to target the intersection of intron 11 and exon 12 and amplify 71 base pairs of product. The PCR reaction was incubated at 95°C for 5 min, followed by 40 cycles of 95°C for

10 s, 55°C for 30 s, and 72°C for 30 s. Normalizations were calculated with the $2^{(-\Delta\Delta CT)}$ method.

2.8 RT-qPCR

RNA samples were extracted using Quick-RNA™ Microprep Kit (Zymo Research, R1050) and reverse transcribed into cDNA with M-MLV Reverse Transcriptase (Thermo Fisher Scientific, 28025013). RT-qPCR amplification was performed with 10 ng material of cDNA and 150 nM of gene-specific primers (given in **Table 2.2**) using LightCycler 480 SYBR Green I Master mix (Roche Diagnostics, 04707516001). The experiment was run on LightCycler 480 (Roche Diagnostics), and incubated at 95°C for 5 min, followed by 40 cycles of 95°C for 10 s, 58°C for 30 s, and 72°C for 30 s. The relative amounts of gene expressions were calculated with the $2^{(-\Delta\Delta CT)}$ method.

Table 2. 2: 5'-3' sequence information of primers used for RT-qPCR, cloning, or ChIP-qPCR.

MLL-F	TTGCCCTTGGCCGAAAAC
MLL-R	TTTGATGGGTGGAGCAAGAGG
MEN1-F	TGGCCGACCTGTCTATCATC
MEN1-R	TCGGAGACCTTCTTCACCAG
WDR5-F	CAAAGCAGTGTCCTCCGTGA
WDR5-R	AATTTCCCATCATACGCGCC
ABCB1-F	ACAGAGGGGATGGTCAGTGT
ABCB1-R	TCACGGCCATAGCGAATGTT
CDK20-F	TAGTTGCCCTCAAGAAGGTGGC
CDK20-R	GTGTGGGAACACAGCCTTCAGT
CEND1-F	ACAACCACAGCAACCTGAAGCC
CEND1-R	ACTGGCAGCCTCATCTTCCTCC
CCND1-F	TCTACACCGACAACTCCATCCG
CCND1-R	TCTGGCATTTTGGAGAGGAAGTG

mTOR-F	AACCTCCTCCCCTCCAATGA
mTOR-R	TCAGCGGTAAAAGTGTCCCC
CBP-F	CAGTTTGCCCACCTTCCCTA
CBP-R	GCTGCTGTATCAGTTTGCGT
GAPDH-F	CTGACTTCAACAGCGACACC
GAPDH-R	GTTGTCATACCAGGAAATGAGC
ACTB-F	TCACCATGGATGATGATATCGC
ACTB-R	ATAGGAATCCTTCTGACCCATGC
MYC-F	CCTGGTGCTCCATGAGGAGAC
MYC-R	CAGACTCTGACCTTTTGCCAGG
pro-CCND1-1-F	GGCTTGGATATGGGGTGTCG
pro-CCND1-1-R	GGGATTTAGGGGGTGAGGTG
pro-CCND1-2-F	TCGTGGCGTTCTTGGAAATG
pro-CCND1-2-R	ACCACGAGAAGGGGTGACT
pro-CCND1-3-F	TCAGGGATGGCTTTTGGGC
pro-CCND1-3-R	CAAAGATCAAAGCCCGGCAG
pro-mTOR-1-F	CATAAAGAGCGCTAGCCCGA
pro-mTOR-1-R	ACTCAAGGAGTCCGGTGTCT
pro-mTOR-2-F	GAATTACACCGGGAGGGGTC
pro-mTOR-2-R	GGAGAACCAATCGGTCGTGA
pro-mTOR-3-F	CTCAGAATTACACCGGGAGGG
pro-mTOR-3-R	CCACTCACACATCCGGTACG
proNGP-F	TACACCACTCAAGGGAAACTGGAA
proNGP-R	TGGAACTTCTGGAAGACACTGGAA
gMEN1-1-F	AAACCGTTGCCCTTGCCGTGCCAGC
gMEN1-1-R	CACCGCTGGCACGGCAAGGGCAACG

gMEN1-2-F	CACCGCCAGGCATGATCCTCAGACA
gMEN1-2-R	AAACTGTCTGAGGATCATGCCTGGC
gMEN1-3-F	CACCGGAAGACGAGGAGATCTACA
gMEN1-3-R	AAACTGTAGATCTCCTCGTCTTCC
gLEDGF-1-F	CACCGCTACTCCAAAAGCTGCCAGA
gLEDGF-1-R	AAACTCTGGCAGCTTTTGGAGTAG
gLEDGF-2-F	CACCGTCTAAAAGTGAGTCCTAAAAG
gLEDGF-2-R	AAACCTTTTAGGACTCACTTTTAGA
MEN1-PAM-F	TGTCCACCTCGCACTGTCTGAGG
MEN1-PAM-R	TCCCGGAGACCCAGGGCC
MEN1-P12L-F	ACGCTGTTCCTGCTGCGCTCC
MEN1-P12L-R	CTTCTGGGCGGCCTTCAG
MEN1-H139D-F	GGATCGGGCCGACATCCAGTC
MEN1-H139D-R	TTGAAGTAGGAGCGGCTG
MEN1-A242V-F	ATGGTGTGTGTCATCAACCCT
MEN1-A242V-R	GAACGCCACCTCCATCTT
MEN1-E255K-F	CGACTCGCTGAAGCTTCTGCA
MEN1-E255K-R	GTGTGCAGGTCAATGGAAG
gMLL-F	AAACCTCCGTCGTACAATTTGTAC
gMLL-R	CACCGTACAAATTGTACGACGGAG
gCBP-F	AAACGGGTTGATACTAGAGCCGCTC
gCBP-R	CACCGAGCGGCTCTAGTATCAACCC
gP300-F	AAACGATCGCAGCAATTCTGACAGC
gP300-R	CACCGCTGTCAGAATTGCTGCGATC
gSET1A-F	CACCGCCCCCGTACGCGCAAGCACC
gSET1A-R	AAACGGTGCTTGCGCGTACGGGGG

gRBBP5-F	CACCGCTTTGACTTGCACCTTTAAC
gRBBP5-R	AAACGTTAAAGGTGCAAGTCAAAG
gNT-F	GTATTACTGATATTGGTGGG
gNT-R	CCCACCAATATCAGTAATAC
MEN1-3xFLAG-NheI-F	ATATATGCTAGCATGGGGCTGAAGGCCGCCCA
MEN1-3xFLAG-NotI-R	ATATATGCGGCCGCGAGGCCTTTGCGCTGCCGCT
LEDGF-3xFLAG-NheI-F	TATATGCTAGCATGACTCGCGATTTCAAACC
LEDGF-3xFLAG-NotI-R	ATATATGCGGCCGCGTTATCTAGTGTAGAATCCT
shMEN1-F	TGCTGTTGACAGTGAGCGACCGAGTACAGTCTGTATCAAATAGTGAAGCCAC AGATGTATTTGATACAGACTGTACTCGGGTGCCTACTGCCTCGGA
shMEN1-R	TGCTGTTGACAGTGAGCGACCGGGAAGACGAGGAGATCTATAGTGAAGCCAC AGATGTATAGATCTCCTCGTCTTCCCGGCTGCCTACTGCCTCGGA
shGFP-F	CCGGTGAATTAGATGGCGATGTTAACTCGA GTTAACATCGCCATCTAATTCATTTTTG
shGFP-R	AATTCAAAAATGAATTAGATGGCGATGTTAAC TCGAGTTAACATCGCCATCTAATTCA
shmTOR-F	CCGGTCGCCACTGTGCGGATCATTTCTCGAGA AATGATCCGCACAGTGGCGATTTTTG
shmTOR-R	AATTCAAAAATCGCCACTGTGCGGATCATTTC TCGAGAAATGATCCGCACAGTGGCGA
ABCB1genoDNA-F	AGATCTACCAGGACGAGTGAGAAAA
ABCB1genoDNA-R	AACAGTCAGTTCCTATATCCTGTGTCT
GAPDHgenoDNA-F	AAGAAGATGCGGCTGACTGT
GAPDHgenoDNA-R	CGGCTACTAGCGGTTTTACG

2.9 Protein Extraction and Western Blotting

Proteins were extracted by cell lysis method with RIPA Lysis Buffer (EcoTech-RIPA-100) containing 1x Protease Inhibitor Cocktail (Cell Signaling Technology, #5871) on

ice for 15 min. The suspension was centrifuged at 17.000×*g*, 20 min at 4°C. Protein-containing supernatant was collected and kept on ice. Concentration analysis was performed with the Pierce™ BCA Protein Assay Kit (Thermo Scientific™, 23225). 20 µg of protein samples were loaded on 4–15% SDS-PAGE gel (Mini-PROTEAN TGX™ Precast Gels, Bio-rad, 161-0317). Separation of different-sized proteins was obtained via electrophoresis at 100 V for 60 min. The separated proteins were transferred onto the PVDF membrane (Bio-Rad, 1620177) at 200 mA for 120 min (for high kDa) or 1 A for 30 min (for low kDa) and immunoblotted with primary antibodies overnight at 4°C. The antibody list is given in **Table 2.3**. The following day, the membrane was incubated with HRP-conjugated secondary antibodies for 1 h at RT. The chemiluminescence signal was stimulated by Immobilon Forte Western HRP substrate (Millipore, WBLUF0100) and detected with the BIORAD Chemi-Doc XRS+ System. Band intensities were quantified using ImageJ software.

Table 2. 3: Antibody list used in western blot analysis

Antibody	**Catalog number**	**Dilution Factor**
Anti-beta Actin Antibody (Rb)	Abcam, ab227387	1:5000 NFDM
Anti-GAPDH Antibody (Rb)	Abcam, ab9485	1:5000 NFDM
Anti-ABCB1 Antibody (Rb)	CST, 13978S	1:2000 BSA
Anti-Menin Antibody (Rb)	Abcam, ab31902	1:2000 NFDM
Anti-LEDGF Antibody (Rb)	Invitrogen, MA514821	1:2000 BSA
Anti-FLAG M2 Antibody (Ms)	Sigma Aldrich, F3165	1:2000 NFDM
Anti-ASH2L Antibody (Rb)	CST, 5019	1:2000 BSA
Anti-SET1A Antibody (Rb)	Abclonal, a18231	1:1000 NFDM
Anti-RBBP5 Antibody (Rb)	Abclonal, a6965	1:1000 NFDM
Anti-CyclinD1 Antibody (Rb)	CST, 55506S	1:2000 BSA
Anti-CyclinB1 Antibody (Rb)	CST, D5C10	1:2000 BSA
Anti-pCyclinB1 Antibody, (Rb)	CST, 4131S	1:2000 BSA
Anti-CyclinE1 Antibody (Ms)	CST, 419S	1:1000 NFDM
Goat Anti-Rabbit IgG H&L (HRP)	Abcam, ab205718	1:2500 NFDM
Goat Anti-Mouse IgG H&L (HRP)	Abcam, ab205719	1:2500 NFDM

2.10 Calcein-AM Experiment

P or DtxR (4×10^3) cells were seeded on black 96-well plates the day before drug treatment (5 µM, 3h). Cells were then incubated with 125 nM calcein-AM (Invitrogen™, C1430), was dissolved in PBS (EcoTech, PBS500), for 30 min at 37°C in the dark. At the end of incubation, calcein was removed gently with the fresh medium. Images were acquired by an inverted fluorescence microscope (Leica DMI8).

2.11 Analysis of Clinical Data

Clinical data depicting Menin and LEDGF expression from Prostate Adenocarcinoma, TCGA Firehose Legacy, and RNA-seq analysis study based on patient samples were obtained from cBioPortal (Cerami et al, 2012; Gao et al., 2013). https://www.cbioportal.org/

2.12 Generation of Menin or LEDGF Knockout Cell Lines

The gRNA sequences were designed using Benching software (https://www.benchling.com) as listed in **Table 2.2**. Initially, RNA-based oligos were phosphorylated with the T4 PNK enzyme (New England Biolabs, M0201S), and annealed according to Feng Zheng protocol [Ran et al., 2013]. Subsequently, LentiCRISPR v2 plasmid (Addgene, 52961) was digested with BsmBI-v2 (NEB, R0739), dephosphorylated via Antarctic Phosphatase (NEB, M0289) and purified using the NucleoSpin Gel and PCR Cleanup kit (Macherey-Nagel, 740609). Phosphorylated gRNA oligos and LentiCRISPR v2 plasmid were ligated (100 ng of vector and relative insert ratio with 7:1) with T4 DNA ligase (NEB, M0202S) at 25°C for 2 h, and 16°C for overnight. The transformation was performed with Stbl3 competent bacteria (prepared with the calcium-chloride method) with heat shock protocol (4°C for 30 min, 42°C for 45 sec, and 4°C for 5 min). Following transfection, competent bacteria were grown in SOC medium for recovery for 1 h, at 37°C, 225 rpm. Later on, bacteria were transferred to LB agar with the relative antibiotic for overnight incubation at 37°C. The next day, single colonies were picked and grown in liquid culture in LB broth with the relative antibiotic for overnight incubation at 37°C. Lastly, bacteria were subjected to the plasmid isolation method as described in the Macherey-

Nagel MidiPlus Plasmid Isolation Kit (740410). Hek293T cells were co-transfected with psPAX2 (Addgene, 12260), pVSVg (Addgene, 14888), and guide-cloned lentiCRISPRv2 (Addgene #98290) carrying puromycin resistance with PEI (ABP Bioscience, P017-1), according to the manufacturer's protocol. Lentiviral particles were collected and filtered (0.45 μm) on the 2nd and 3rd days of the transfection, aliquoted, and snap-frozen with liquid nitrogen. Protamine sulfate (8 μg/ml) (Thermo Fisher Scientific, A11559IK) was used to improve transduction efficiency; 2-10 μg/ml of puromycin (Thermo Fisher Scientific, J61278.MB) was used for selection, and validation of the protein expression was performed via western blotting using anti-MEN1, and -LEDGF antibodies.

2. 13 Generating MEN1 Rescue Cells with Point Mutations

Menin rescue plasmids were kindly gifted by Tamer Onder Lab, Koc University. I cloned the plasmids into a lentiviral system to improve transduction efficiency.

Initially, to circumvent Cas9 activity, pBABE Hygro WT MEN1 (Addgene plasmid, #11024) was mutated from the NGG (PAM) recognition site using specific primers. Subsequently, specific primers to generate P12L, H139D, A242V, and E255K mutations were used to generate using the (PAM) mutated plasmid. For that, Q5 Site-Directed Mutagenesis Kit (NEB, E0554) protocols were followed. Primer sequences are given in **Table 2.2.** To improve viral transduction efficiency, mutated MEN1 sequences were cloned into a lentiviral overexpression plasmid (Addgene, 163447). Sequences were amplified using Phusion High Fidelity DNA Polymerase (NEB, M0530), mixed with 20 ng of plasmid DNA and 150 nM specific primers (addition with NheI and NotI cut sites) and incubated at 98°C for 30 min, followed by 40 cycles of 98°C for 10 s, 72°C for 30 s, and 72°C for 120 s. PCR products were run on the agarose gel for base pair validation and isolated with Gel and PCR Clean-up Kit (Macherey-Nagel, 740609.50). Cleaned PCR products and Backbone plasmid were digested with NheI (NEB, R3131) and NotI (NEB, R3189) enzymes, at 37°C for 6 h. Digested products were cleaned with the aforementioned purification method and ligated with T4 DNA ligase (NEB, M0202S) at 25°C for 2 h, and 16°C overnight. Transformation, plasmid isolation, transfection, and virus production were performed as described in section

2.11. All mutations were confirmed by whole plasmid sequencing. Validation of MEN1 rescue was obtained via western blotting using anti-MEN1 antibody.

2. 14 RNA-seq and GSEA Analysis

Identification of differentially expressed genes belongs to the hard work of Dr. Hamza Syed from the School of Medicine, Koç University.

Poly-A capturing, library construction, and next-generation sequencing were performed by BGI Group (Hong Kong, China). Sequencing was produced with 20 million readings/samples and 150 bp no-stranded PE150 pair-ended readings. First, the quality of the reads is evaluated by FastQC software (http:/www.bioinformatics.Babraham.ac.uk/projects/fastqc/). Sequencing data were paired using the current reference genome (NCBI GRCh38), using HiSAT2 (http://daehwankimlab.github.io/hisat2/) software. Following the alignment, the read counts were quantified using featureCounts (http://bioinf.wehi.edu.au/featureCounts/). Additionally, to obtain differentially expressed genes, the results were analyzed using the R package DESeq2 (https://bioconductor.org/packages/release/bioc/html/DESeq2.html). Genes showing different expression patterns were further identified using Ensembl (https://m.ensembl.org/info/data/biomart/index.html).

To identify gene set enrichment analysis, preranked DEG file.rnk (FDR <0.05) was uploaded to GSEA_4.3.2.app. The comparisons were performed with;

-h.all.v2023.1.Hs.symbols.GMT,

-c5.go.bp.v2023.2.Hs.symbols.GMT,

-c5.go.cc.v2023.2.Hs.symbols.GMT,

-c5.go.mf.v2023.2.Hs.symbols.GMT,

-c6.all.v2023.2.Hs.symbols.GMT datasets in the MsigDB database.

Enrichment bubbles were generated by using https://www.bioinformatics.com.cn/en.

2.15 Generation of FLAG-tagged MEN1 and LEDGF Overexpressing Cells

MEN1 and LEDGF cDNA sequences were amplified using Du145-DtxR cDNA pool with the forward and reverse primers covering the beginning and ending of cDNA sequences with NheI and NotI cut site additions, respectively. The stop codon was excluded for 3xFLAG addition. pLJC2-GPT2-3xFLAG (Addgene, 163447) plasmid was cut with NheI (NEB, R3131) and NotI (NEB, R3189) enzymes and the backbone was dephosphorylated with Antarctic Phosphatase (NEB, M0289) and purified. The remaining procedures including PCR reaction, ligation, transformation, plasmid isolation, and lentivirus production were performed as described in sections 2.11 and 2.12. Validation of the overexpression was confirmed via western blotting using FLAG, MEN1, and LEDGF antibodies.

2.16 Constitutive Silencing via shRNA

shFF and shMEN1 plasmids were kindly gifted from Tamer Onder Lab, Koc University. The shRNA sequences were designed using Benching software (https://www.benchling.com) as listed in **Table 2.2**. Initially, RNA-based oligos were phosphorylated with the T4 PNK enzyme (New England Biolabs, M0201S), and annealed. Subsequently, PLKO.1puro plasmid (Addgene, 8453) was digested with AgeI and EcoRI, dephosphorylated via Antarctic Phosphatase (NEB, M0289) and purified using the NucleoSpin Gel and PCR Cleanup kit (Macherey-Nagel, 740609). Phosphorylated oligos and backbone plasmid were ligated (200 ng of vector and relative insert ratio with 7:1) with T4 DNA ligase (NEB, M0202S) at 25°C for 2 h, and 16°C for overnight. Transformation, isolation, and lentiviral particle production were performed as described in 2.12. Validation of the expression was performed via western blotting using anti-MEN1 antibody, or RTqPCR with mTOR primers.

2.17 ChIP-qPCR

EV-3xFLAG, MEN1-3xFLAG, LEDGF-3xFLAG (9×10^6 number of cells- each condition) overexpressing DtxR cells was crosslinked with 1% formaldehyde (Sigma Aldrich, 818708) at RT for 5-10 min. The addition of glycine (Sigma Aldrich, G7126)

(125 mM, 5 min) was performed to terminate the cross-linking procedure. Cell suspension and pellet were separated using cold centrifugation at 1000 g for 5 min. Following two PBS (EcoTech, PBS500) wash, pellet was resuspended in ChIP Lysis Buffer (50 mM HEPES; 1 mM EDTA; 140 mM NaCl; 1% Triton X-100; 0.1% Na-deoxycholate; 1% SDS; 1 mM PMSF; Protease Inhibitor Cocktail), vortexed, and incubated on ice for 15 min. Obtained chromatin was sheared with Bioruptor Plus sonicator (Diagenode) with 5 cycles (30 s on/ 30 s off) until DNA size reached 250-500 base pairs. Sheared DNA was centrifuged at 10.000 g for 10 min at 4°C, and supernatant was collected. For the pre-clearing step, DNA was incubated with Dynabeads® (Thermo Fisher protein A magnetic beads, 10001D) (15 µL for each condition) at 4°C for 30 min. Magnetic beads and antibodies (FLAG antibody - Sigma Aldrich, F3165 and a non-specific IgG antibody - Thermo Fisher Scientific, 10400C) were rotated in PBS-T for 1 h at RT. PBS-T was separated using a magnetic rack and pre-cleared chromatin was transferred into a tube containing a magnetic bead and antibody complex. This mixture was incubated overnight at 4°C with slow rotation. The next day, magnetic beads were washed with each buffer twice for 5 min. Respectively, beads were washed with ChIP lysis buffer (no SDS), low-salt buffer (0.1% SDS, 1% Triton-X 100, 2 mM EDTA, 20 mM Tris-HCl, 140 mM NaCl, pH 8.1), high salt buffer (0.1% SDS, 1% Triton-X 100, 2 mM EDTA, 20 mM Tris-HCl, 500 mM NaCl, pH 8.1), LiCl-containing buffer (0.25 M LiCl, 1% IGEPAL-CA 630, 1% deoxycholic acid, 1 mM EDTA, 10 mM Tris, pH 8.1), Tris-EDTA solution. For elution, beads were incubated with elution buffer containing 1% SDS (Bio-Rad, 1610418) and 0.1 M NaHCO3 (Merck, S6014) for 30 min at RT with slow rotation. ChIP'ed DNA-protein complex was treated with RNase A (0.3 mg/ml) (Thermo Fisher Scientific, 12091039) and 5M of NaCl (Merck, S9888) for 30 min at 37°C. Later on, tubes were incubated with proteinase K (0.3 mg/ml) (Thermo Fisher Scientific, EO0492) at 65°C for 1 h, to separate DNA and protein cross-links. Eluted DNA was enriched by using the ChIP DNA Clean & Concentrator kit (Zymo Research, D5205). Eukaryotic Promoter DataBase EPD was used to retrieve promoter regions for designing target primers (https://epd.expasy.org/epd/). Primers were designed using the NCBI primer designing tool (https://www.ncbi.nlm.nih.gov/tools/primer-blast/) and primer sequences are given

in **Table 2.2**. ChIP-qPCR was performed on Thermo Scientific PikoReal Real-Time PCR System. For the enrichment calculation, % input method was exerted.

2.18 Competition Assay

Menin knockout resistant cells were transduced with mCherry fluorescent protein containing lentiviral plasmid and cells showing positivity for the mCherry fluorescence were sorted with Sony SH800 Cell Sorter. Equal numbers (5×10^3) of non-targeting (non-labeled) and Menin knockout resistant cells (mCherry labeled) were mixed in a 1:1 ratio, seeded, and co-cultured for 10 days. At the beginning and the end of the co-culturing period, the percentage of mCherry signal in the mixed population was measured by Beckman Coulter Cytoflex flow cytometry.

2.19 Statistical Analysis

Significant tests were performed between control and treatment groups using GraphPad Prism version 10 or Microsoft Excel 2024. Depending on the analysis, student's t-test, one or two-way ANOVA was used.

Annotations:

nd: not determined / ns $p > 0.05$ / * $p \leq 0.05$ / ** $p \leq 0.01$ / *** $p \leq 0.001$

Chapter 3

RESULTS

3.1 Generation and Validation of Resistant Model

To generate our resistant model, we implemented a dose increment approach, a widely utilized strategy used in resistance studies (**Figure 3.1**). Du145 cells were treated with the initial IC_{50} dose of Docetaxel (1 nM), for 72 h. The survival population was allowed to recover until cells were replenished. In the next cycle, a doubled dose was administered until cells reached a 250-fold increase in IC_{50} response. To have proper control, drug-naive (parental) cells were simultaneously subcultured for the passage-equivalent counterparts.

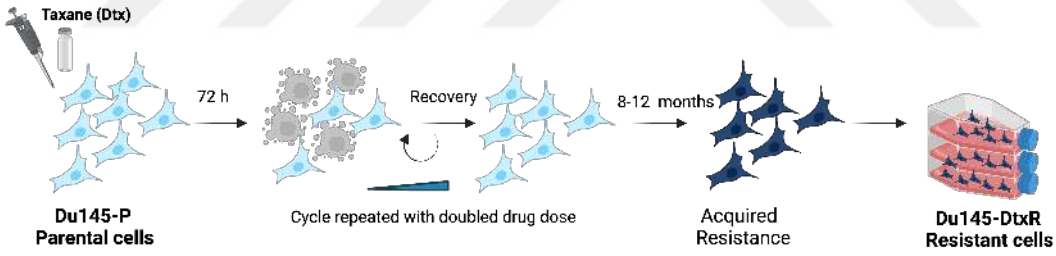

Figure 3. 1: Generation of Docetaxel-resistant CRPC cells

The schematic showing the process of Dtx resistance development in Du145 cells using the dose increment method over a one-year period. Parental cells are represented with light blue and drug-refractory DtxR cells are represented with dark blue. Figure created with Biorender.com.

The refractory phenotype of resistant cells is shown in (**Figure 3.2**). P and DtxR cells were treated with an increased dose of Docetaxel (Dtx) for three days for cell viability experiments as an evaluation of acute response. As depicted in (**Figure 3.2A**), parental cells could not survive even at the lowest dosages, but resistant cells did not exhibit any significant cell death even at the maximum dose. For a longer response, we employed a

colony formation assay. As shown in (**Figure 3.2.B-C**), parental cells can not grow any colonies higher than 1 nM, however, resistant clones grow consistently even in 125 nM of Dtx treatment.

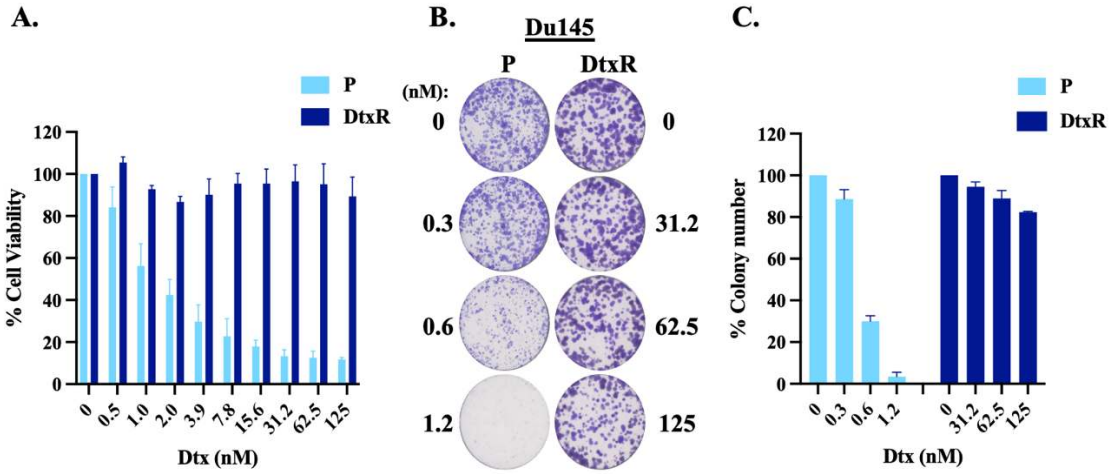

Figure 3. 2: Validation of Dtx resistant Du145 cells

A. SRB cell viability results of parental and resistant cells in different doses of Dtx. **B.** Crystal violet stainings of colony formation assay with parental and resistant cells comparison to a 10-fold high dose of Dtx response. **C.** Normalized (%) colony numbers of parental and resistant cells. Graphs represent the average of ± standard deviation of 3 biological repeats. Colony numbers counted with CellCounter software by Nghia Ho.

3.2 Epigenetic Targeting of Drug Resistance

To identify epigenetic modifiers that confer drug resistance, we screened our cells with an epi-drug library containing 145 chemicals. These drugs were defined as activators or inhibitors of different epigenetic enzymes, which promote writing, erasing, or reading activity. We employed a combination treatment with 5 µM of epidrug, and 125 nM of Dtx for 72 h. As shown in **Figure 3.3**, Dtx alone did not trigger any significant cell death, on the other hand, some epidrugs alone (to the right) induced cell death. Interestingly, five different chemicals induced a significant sensitization of resistant cells against Dtx. While each target has been allocated for other theses and projects, MI-2, an MLL-Menin inhibitor significantly reverted resistance phenotype upon the combination with Dtx.

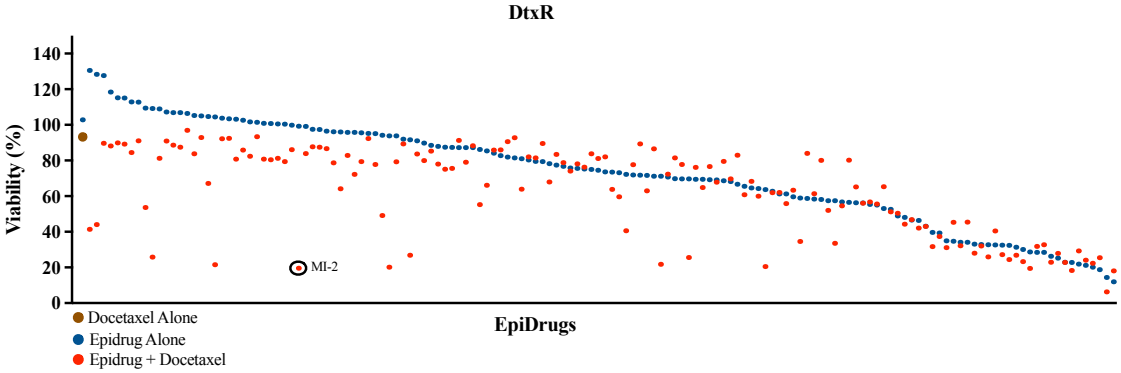

Figure 3. 3: Cell viability results of epigenetic drug screen with 145 compounds and Dtx combination

Cayman Epigenetic Screening Library (11076), was implemented as co-treatment with Dtx, the graph showing cumulative data of SRB cell viability results with screening different compounds (5 µM) and a single dose of Dtx (125 nM) for 72 hours. The s*creening experiment was conducted in collaboration with Dr. Buse Cevatemre, Koc University.*

To validate that targeting MLL-Menin interaction reverses Dtx resistance, we tested other MLL-Menin inhibitors (MI-2, MI-3, MI-136, MI-463), and MLL-WDR5 inhibitor (WDR5-0103), with increased Dtx dose (**Figure 3.4A**). As shown in the figure, the acute response was significantly detrimental, and upon combination viability percentages precipitously dropped. Similarly, MLL-Menin or MLL-WDR5 inhibitors in combination with Dtx significantly harmed the colony-forming ability of Dtx-resistant cells (**Figure 3.4B**). Up to our recent knowledge, we are the first group to report such synergy, a valuable indication in resistance studies with drug-based aspects.

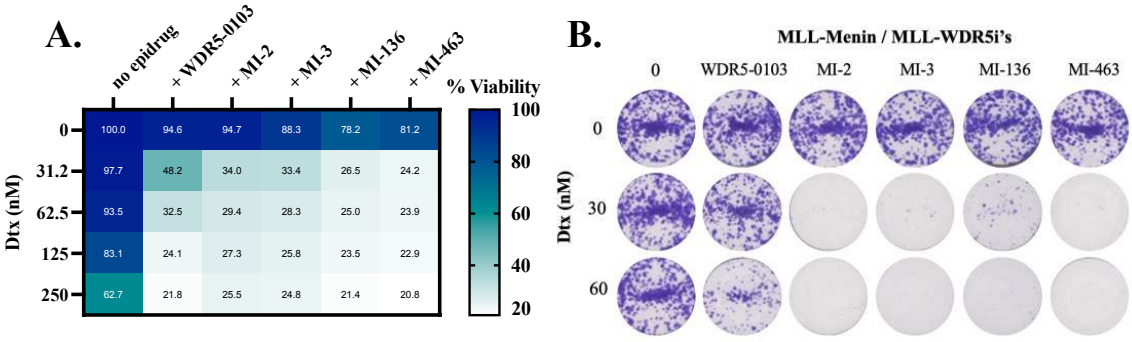

Figure 3. 4: MLL-Menin and MLL-WDR5 targeting compounds reverse Dtx resistance in CRPC model

A. SRB cell viability results of combination treatment on Dtx-resistant cells with MLL-inhibitors (5 μM of WDR5-0103, MI-2, MI-463 and 2.5 μM of MI-3, MI-136) with Dtx (125 nM) for 72 h. **B.** Crystal violet stainings on Dtx-resistant cells following the combination with the MLL-inhibitors (2.5 μM) with Dtx (0-60 nM). Heat maps and colony images represent the two biological repeats.

MLL inhibition in CRPC has been reported to regulate AR expression [Malik et al., 2015], and slowed down tumor growth *in vivo*. Without a taxane administration, the group identified MLL-Menin targeting compound MI-503, as a valuable hit to decrease CRPC growth in VCap cells. Interestingly, in our study, AR-negative Du145 cells, regardless of their taxane resistance, did not induce cell death in MLL-target inhibition alone (**Figure 3.5**). In a cell viability screen (**Figure 3.5 A-B**) or colony formation experiments (**Figure 3.5 C-D**) MLL-Menin or MLL-WDR5 inhibitors alone did not induce anti-tumor activity.

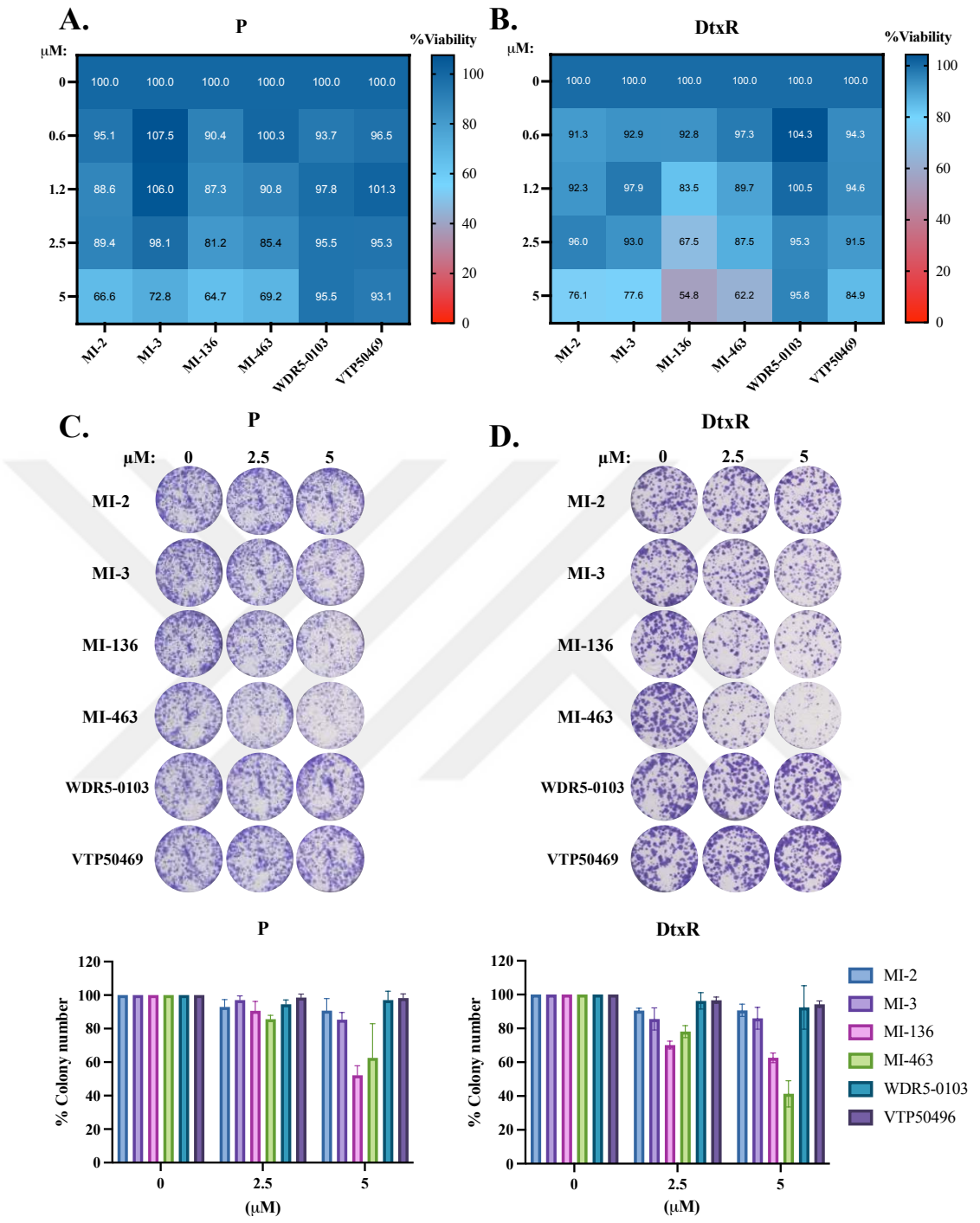

Figure 3. 5: MLL-Menin and MLL-WDR5 targeting compounds do not show an anti-tumor effect on their own in Du145 cells

A-B. SRB cell viability results of single-agent treatment on P or DtxR cells with increased doses of MLL inhibitors (0-5 µM) for 72 h. **C-D.** Crystal violet stainings on P or DtxR cells following the single agent treatment with the MLL inhibitors (0-5 µM). Heat maps and graphs represent the average of ± standard deviation of two biological repeats. Colony numbers counted with CellCounter software by Nghia Ho.

The working principle of taxane is the failure of microtubule function during cell division and induced G2/M arrest for stalling uncontrolled proliferation [Suffnes, 1993]. Since our resistant cells showed drug refractory phenotype and MLL-Menin combination re-sensitized taxane-induced cell death, we investigated cell cycle patterns in combination treatment. Normally, a drug-naive cell shows increased G2/M arrest upon taxane treatment, however, our drug-resistant cells showed no significant arrest. Interestingly, only upon the combination with MI-2 and Dtx, the majority of the population was arrested in the G2/M cycle (**Figure 3.6 A-B**). This phenotype indicates that MI-2 increases the absorption of taxane and induces the re-activation of the anti-tumor effects of Dtx. Inevitably, the accumulation of G2/M arrest results in programmed cell death, as represented in induced Caspase 3/7 positivity (**Figure 3.6 C-D**).

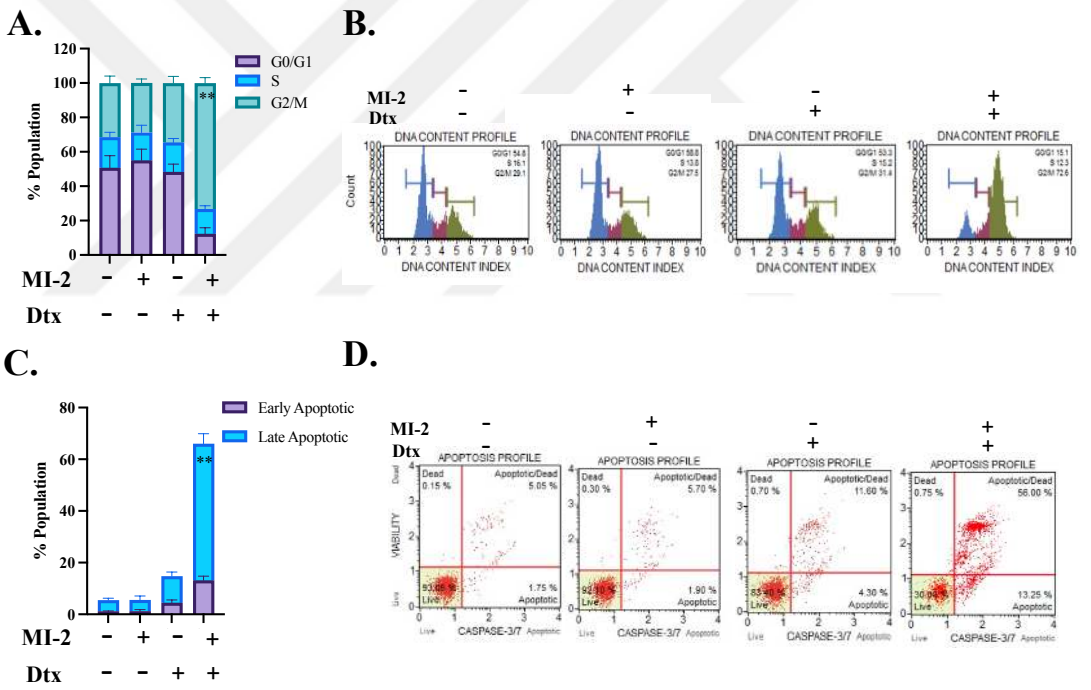

Figure 3. 6: MI-2 and Dtx combination results in G2/M arrest and programmed cell death in DtxR cells.

A. Graph showing cell cycle distribution in MI-2 or/and Dtx treated DtxR cells. **B.** Flow cytometric charts representing induced G2/M arrest (green) populations in each treatment group. **C.** Graph showing early or late apoptotic cell distribution in MI-2 or/and Dtx-treated DtxR cells. **D.** Flow cytometric charts showing Caspase 3/7 and PI positivity. Live cells accumulate in the lower left (negative for each staining), early apoptotic cells accumulate in the lower right (positive for Caspase 3/7), late apoptotic cells accumulate in the higher right (positive for Caspase 3/7 and PI), and dead cells

accumulate in the higher left (positive for PI). Graphs represent the average of ± standard deviation of three biological repeats. (One-way ANOVA, ** $p \leq 0.01$).

3.3 ABCB1 is One of the Major Regulator of Drug Refractory Mechanism

The Multidrug resistance gene (MDR1 or ABCB1), is one of the major factors contributing the drug resistance [Goldstein, 1996]. To evaluate the contribution of ABCB1 activity in our resistance models, we looked into the ABCB1 protein levels in DtxR and CbzR (Cabazitaxel Resistant Du145 cells- another model generated in our lab) via western blotting. As shown in **Figure 3.7A**, in both resistant cells, the ABCB1 drug pump was tremendously overexpressed compared to parental cells. To test whether this overexpression was triggered due to gene amplification, or an epigeneticly regulated mechanism, we used a primer set specifically designed to amplify intron-exon junctions in the ABCB1 genomic region [Yabuki et al., 2007]. As seen in **Figure 3.7B**, CbzR-resistant cells, showed 5 fold increase of ABCB1 gene copy, compared to parental and DtxR. Suggesting, that induced ABCB1 in DtxR, was conferred by epigenetic regulation, however, CbzR cells altered gene copy amplification during the acquisition of drug resistance. Later on, we silenced ABCB1 in DtxR cells via siRNA (**Figure 3.7C**), and the Dtx response was significantly enhanced (**Figure 3.7D**). This data indicated that ABCB1 appears as a master regulator mechanism that controls drug uptake in our resistance model. As the MLL-Menin inhibitor and Dtx combination reversed this phenotype, we investigated ABCB1 activity following MI-2 treatment. To do this, we used the Calcein-AM protocol. Calcein-AM is a non-fluorescent dye, diffused into the cell, but expelled with an ABCB1 pump. In cells with no ABCB1 activity, Calcein-AM is uptaken, and esterases break down the molecule, to its fluorescence conjugate (Calcein), yielding green fluorescent protein. However, if the cells have higher ABCB1 activity, Calcein-AM is expelled immediately by ABCB1 pumps, therefore no fluorescent activity is observed (**Figure 3.7E**). As expected, parental cells showed high green fluorescence activity, and resistant cells holding high ABCB1 expression, showed no significant green fluorescence (**Figure 3.7F**). Interestingly, MI-2 treatment on DtxR cells significantly stalled ABCB1 activity, and cells were not successful in repelling Calcein-AM dye. Verapamil (ABCB1 inhibitor)

was used as a positive control. This data indicates that MI-2 treatment detained ABCB1 activity and increased drug uptake in resistant cells.

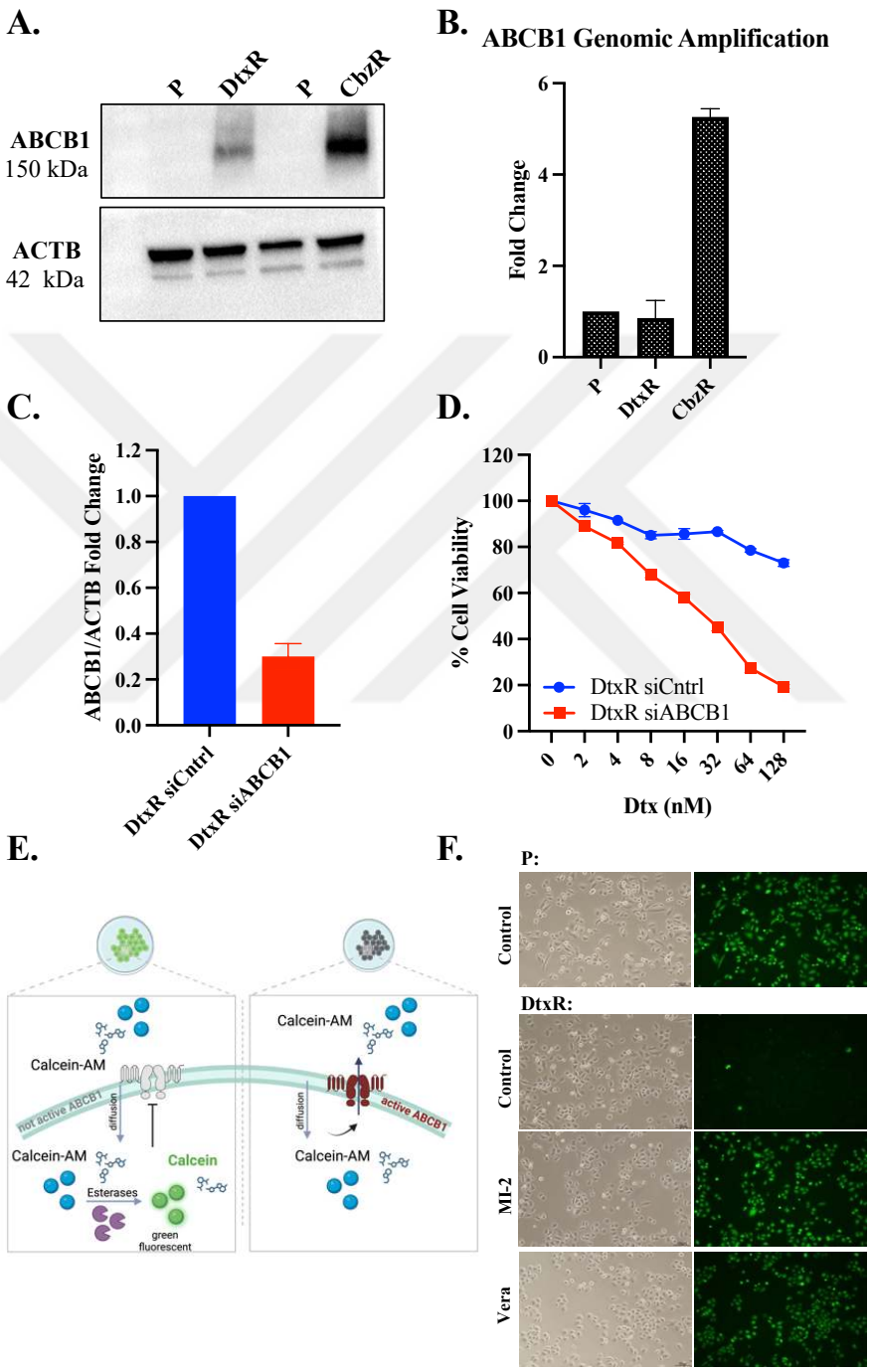

Figure 3. 7: ABCB1 is significantly activated in DtxR cells

A. Western blot showing ABCB1 protein expression in P, DtxR, and CbzR cells. **B.** Graph showing ABCB1 copy number normalizations in P, Dtx, and CbzR cells. **C.** RT-

qPCR results showing ABCB1 mRNA expression, 48 h later following siRNA treatment. **D.** Cell viability results of DtxR cells, upon ABCB1 silencing and taxane treatment. **E.** Schematic showing the working principle of Calcein-AM in ABCB1 active or inactive cells. Figure created with Biorender.com. **F**. Bright-field or fluorescent images of P and DtxR cells following Calcein treatment. Images were acquired by Leica DMI8 at a 10 x magnification, scale bar is 100 µm in all images.

3.4 MLL Partner Proteins and Importance of Menin in DtxR Cells

Our combination experiments revealed four MLL-Menin and one MLL-WDR5 inhibitor as hits to revert taxane resistance. MI-2, MI-3, MI-136, and MI-463 block the interaction with MLL and Menin binding site, while WDR5-0103 breaks interaction with MLL and WDR5 [Borkin et al., 2015, Senisterra et al., 2013]. First, we assessed clinical data showing, MLL, MEN1, and WDR5 expression levels in PRAD, using the Wanderer tool. According to this data, between tumor and normal tissues, MLL was significantly downregulated. On the other hand, Menin and WDR5 were upregulated (**Figure 3.8B**). While MLL has multiple binding partners, we evaluated which partner inhibition is essential for drug-resistant phenotype. Therefore, we silenced common protein partners of hit inhibitors, via siRNA in both parental and resistant cells (**Figure 3.8C**). Interestingly, MLL and WDR5 seemed to be essential targets for both parental and resistant cells, probably due to their essential roles in histone methylation [Lu et al., 2018]. However, Menin (MEN1) silencing only diminished colony forming capacity of resistant cells, hinting Menin could be a potential target for the observed phenotype (**Figure 3.8D**).

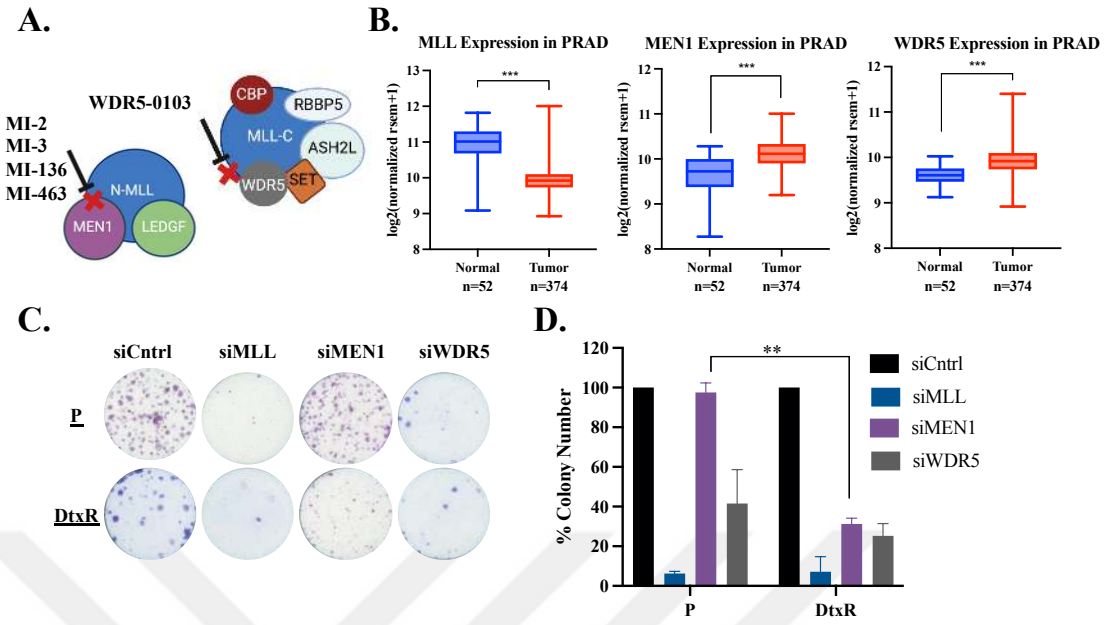

Figure 3. 8: Silencing Menin specifically diminishes resistant colonies

A. Schematic showing different binding partners of N-terminus of MLL, and C-terminus of MLL, figure was generated with Biorender.com. **B.** Clinical data, represented as box plots of relative target (MLL, Menin, and WDR5) mRNA levels from TCGA Wanderer. The x-axis represents samples normal or tumor, the y-axis represents *RNAseq V2* values (normalized *RSEM)* (t-test, ***p≤ 0.001). **C.** Colony formation experiments of P and DtxR cells upon silenced MLL, Menin, and WDR5 conditions. **D.** Normalized colony numbers counted with CellCounter software by Nghia Ho. Graphs represent the average of ± standard deviation of two biological repeats (One-way ANOVA, ** p≤ 0.01)

As Menin silencing, only affected DtxR cell growth, we further analyzed Menin's effect on our resistant model via CRISPR-cas9 targeting. We isolated two knockout clones for P and three knockout clones for DtxR cells. These clones showed complete deletion of Menin protein levels successfully (**Figure 3.9A**). As shown in **Figure 3.9B**, menin ablation did not induce a significant difference in colony forming ability of parental cells. However, two resistant Menin-null clones (KO1, KO2) displayed few colonies, and KO3 yielded half as many colonies as control (**Figure 3.9C**). These results indicated the essentiality of Menin for DtxR cells, and for the convenience of further experiments, we continued with DtxR-KO3.

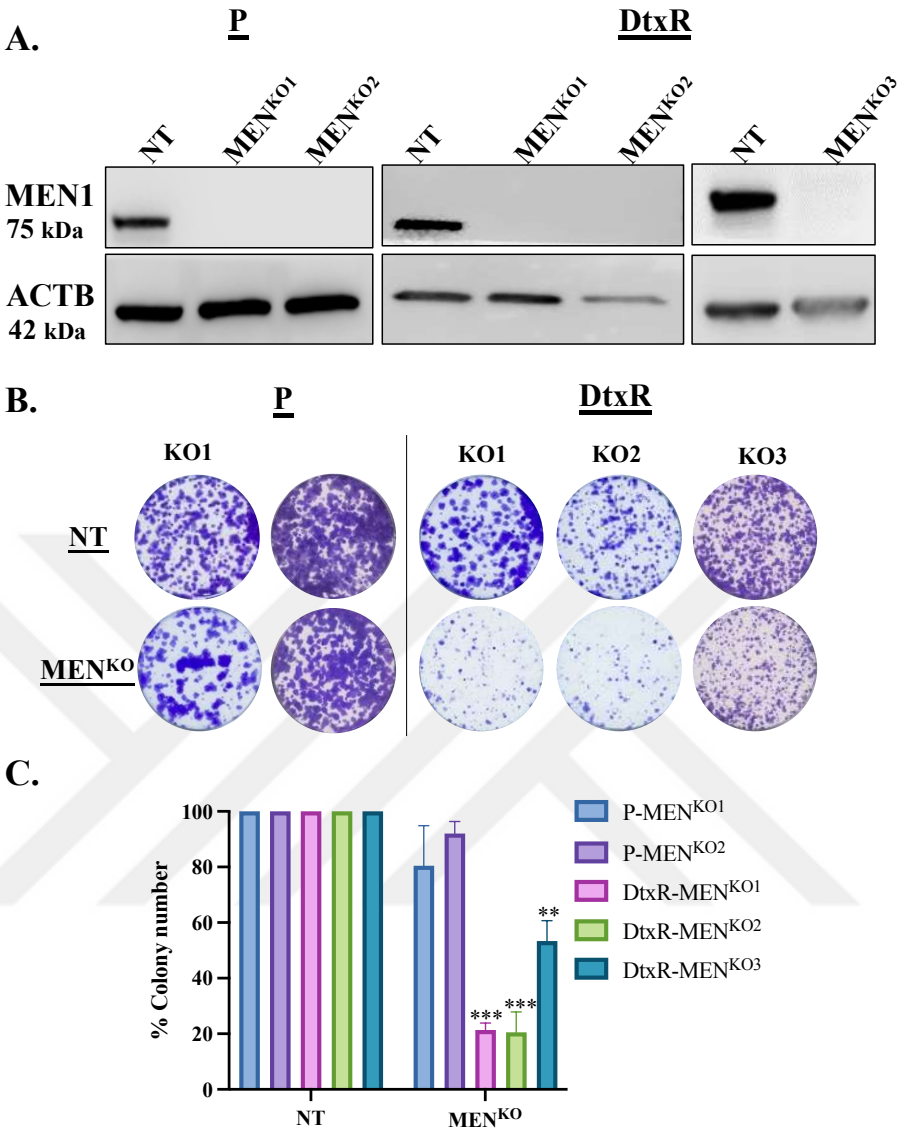

Figure 3. 9: Menin Knockout Significantly Reduces DtxR Colony Forming Ability

A. Western blot showing MEN1 protein levels in control (non-targeting) and Menin knockout P and DtxR cells. **B.** Crystal violet staining showing colony numbers following Menin depletion. **C.** Graphs showing normalized % colony numbers counted with CellCounter software by Nghia Ho. The graph represents the average of ± standard deviation of three biological repeats (One-way ANOVA, ** $p \leq 0.01$, *** $p \leq 0.001$).

We then performed a rescue experiment with wild-type and different mutants of Menin. Initially, we generated a PAM mutant to avoid active cas9 activity, then used specific primers to generate different mutants of Menin protein unable to bind with MLL and LEDGF. Menin protein bearing P12L mutation was reported to have lower binding activity for LEDGF, and other mutants (H139D, A242V, and E255K) have been reported to yield lower H3K4 methylation due to their disrupted connection with MLL

histone methyltransferase [Agarwal et al., 1999, Carling et al., 1998, Huang et al., 2012, Hughes et al., 2004, Stratakis et al., 2000].

As seen in **Figure 3.10A**, the Menin guide completely abolished Menin expression and MEN^{WT} provided significant rescue for protein expression. On the other hand, P12L, and H139D yielded Menin protein with lower stability, compared to A242V and E255K mutants. Expected phenotypes regarding each mutant are given in **Figure 3.10B**. We assessed the effect of Menin recapitulation concerning colony-forming ability on DtxR cells. As depicted in **Figure 3.10C-D, the** Menin guide (polyclonal) reduced the colony-forming capacity of DtxR cells by 40%, and reintroducing Menin restored this effect. On the other hand, rescuing Menin expression with P12L mutant, yielded the lowest numbers of colonies. P12L mutant was generating a Menin protein with lower binding to its known partner LEDGF, we therefore tested the impact of LEDGF ablation on colony growth for our model. We knocked out LEDGF expression in our P and DtxR cells with CRISPR-cas9, and validated abolished protein expression with western blot (**Figure 3.10E**). Interestingly, similar to Menin, LEDGF ablation only showed anti-tumor effects on Dtx-resistant models (**Figure 3.10F-G**). Cumulatively, these data showed N-terminus MLL complexes Menin and LEDGF are essential factors for the resistant CRPC model.

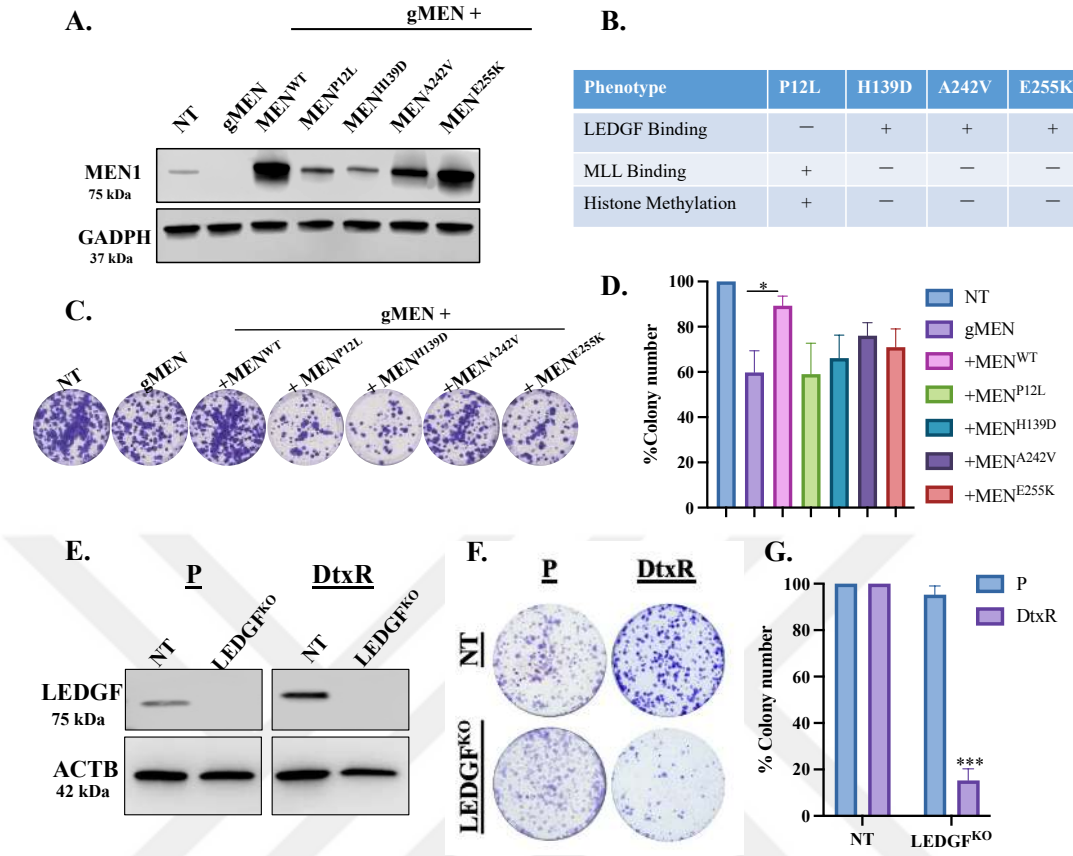

Phenotype	P12L	H139D	A242V	E255K
LEDGF Binding	–	+	+	+
MLL Binding	+	–	–	–
Histone Methylation	+	–	–	–

Figure 3. 10: Rescuing wild-type and mutated Menin expression reveals other targets for resistance.

A. Western blot showing Menin protein levels, in different conditions regarding control, guided, overexpressed with wild-type or mutated Menin. **B.** Table showing expected phenotypes of each Menin mutation. **C.** Colony formation results showing relative colony-forming ability of DtxR cells, following knock-out and rescue cases. **D.** Graph showing % normalized colony numbers, regarding different Menin expressions including knock out, and relative rescues. Data represent the average of ± standard deviation of five biological repeats. **E.** Western blot showing LEDGF protein levels, in P and DtxR cells, following treatment with NT or LEDGF guide RNA. **F.** Colony formation results show the impact of LEDGF concerning colony growth on P and DtxR cells. **G.** Graph showing % normalized colony numbers, counted with CellCounter software by Nghia Ho. Data represent the average of ± standard deviation of three biological repeats (One-way ANOVA, *p≤ 0.05, *** p≤0.001).

Subsequently, we assessed MEN1 and LEDGF expression in clinical data using cBioPortal. This study performed RNA-sequencing within a patient group with 501 samples (Firohose Legacy), which underwent radical prostatectomy. According to this, MEN1 expression was significantly enhanced in patients with Gleason scores of 6 vs 8,

and 6 vs 9 (**Figure 3.11A**). Similarly, LEDGF expression was increased in patients with Gleason score 6 vs 10 (limited sample size, but significant increase) (**Figure 3.11 B**).

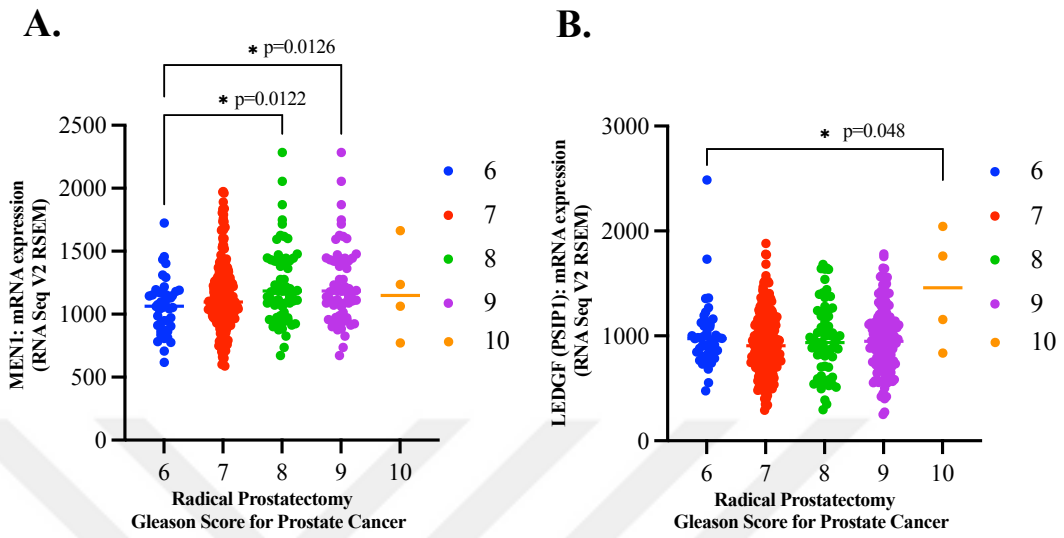

Figure 3. 11: Clinical relevance of Menin and LEDGF in patient samples with Advanced Prostate Cancer

A-B. Clinical data, represented as scatter dot plots of relative target (Menin and LEDGF) mRNA levels from TCGA, Prostate Adenocarcinoma Firehose Legacy study (GDAC-PRAD-20160128), data obtained by cbioportal.org. The x-axis represents Gleason scores of samples, the y-axis represents *RNAseq V2* values (normalized transcript per million, TPM values) by *RSEM* (One-way ANOVA, *p≤ 0.05).

As we have demonstrated the importance of the N-terminal MLL binding partners Menin and LEDGF, we were also interested in assessing the effect of C-terminal MLL complexes for P and DtxR cells. Histone methyltransferase activity of the C-terminus MLL requires SET domain binding activity [Milne et al., 2002]. Additionally, other proteins such as ASH2L, RBBP5, and WDR5 are known to interact with MLL through the SET domain. [Dou et al., 2006; Patel et al., 2009; Cao et al., 2010], even histone acetyltransferases CBP and p300 [Ernst et al., 2002]. We knocked out known protein partners of MLL and evaluated the impact on colony formation on P and DtxR cells. MLL, CBP, and p300 depletion exhibited major essentiality on both cells, likely due to their major role in regulating histone methylation and acetylation. ASH2L knockout-resistant cells displayed no colonies, while parental cells merely exhibited limited colonies. RBBP5 ablation did not induce a phenotypic change in any condition, and

SET1A silencing specifically impeded colony growth in resistant cells (**Figure 3.12E**). Indeed, further studies are warranted to test the essential targets in these resistant clones.

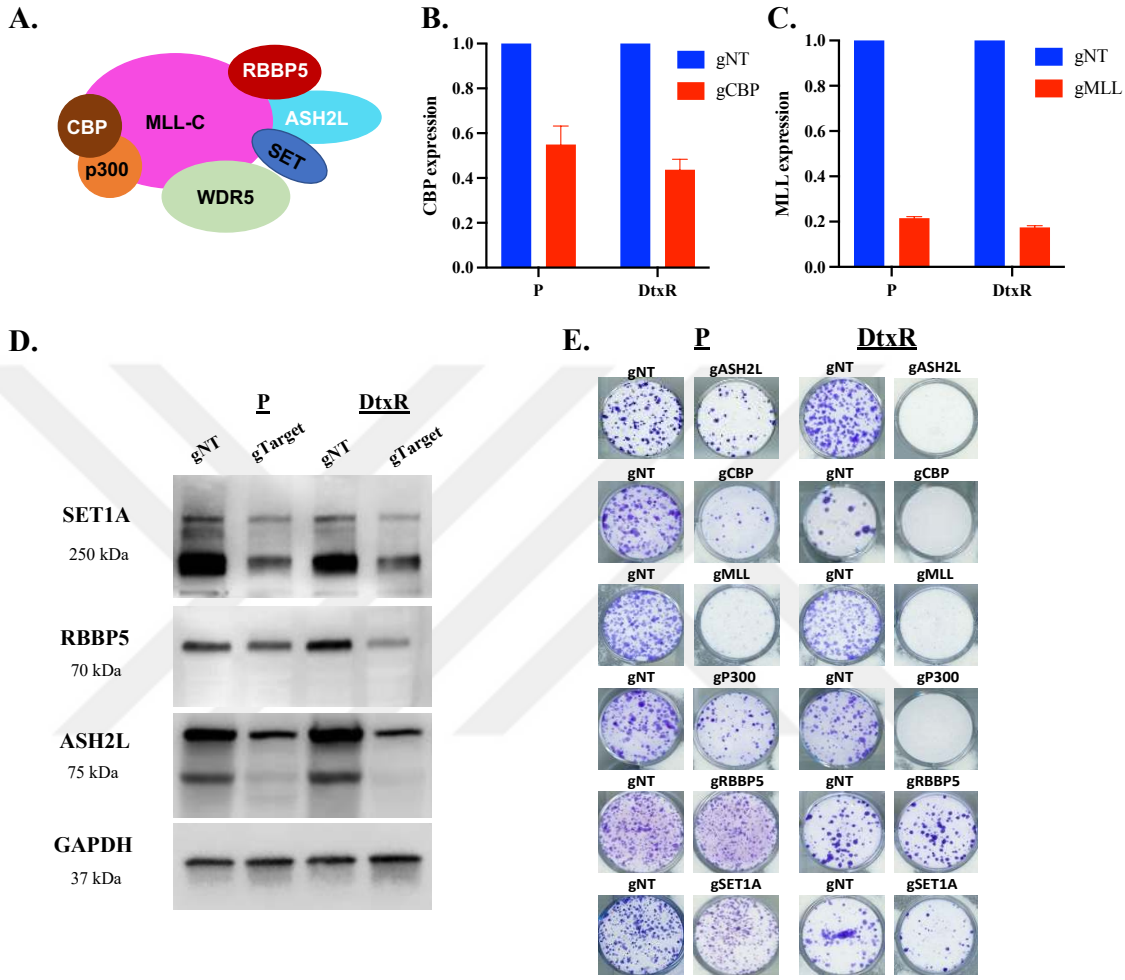

Figure 3. 12: C-terminus MLL complexes and their depletion in CRPC

A. Cartoon showing the C-terminus MLL partners, the figure was generated in Biorender.com. **B-C.** mRNA expression of CBP and P300 via RT-qPCR in P and DtxR cells following with target guide treatment. **D.** Protein levels of SET1A, RBBP5, and ASH2L in P and DtxR cells following with target guide treatment. **E.** Colony formation of P and DtxR cells treated with gASHL2, gCBP, gMLL, gP300, gRBBP5, and gSET1A.

3.5 RNA-sequencing

To reveal differentially expressed genes (DEGs) and pathways in our divergent cell models, we performed RNA-sequencing with 8 cell lines (P, DtxR, P^{NT}, $PMEN^{KO}$, $PLEDGF^{KO}$, $DtxR^{NT}$, $DtxRMEN^{KO}$, $DtxRLEDGF^{KO}$). As shown in **Figure 3.2**, **Figure 3.9,** and **Figure 3.10**, resistant phenotype and knockout phenotypes were repeatedly confirmed. We have performed these comparisons, following RNA sequencing:

i) DtxR vs P

ii) DtxR MEN^{KO} vs $DtxR^{NT}$

iii) P MEN^{KO} vs P^{NT}

iv) DtxR $LEDGF^{KO}$ vs $DtxR^{NT}$

V) P $LEDGF^{KO}$ vs P^{NT}

Initially, we compared our DtxR and P cells, to eliminate non-significant differentially expressed genes (DEGs), by using FDR<0.05 and $|Log_2FC|>0.5$ cutoff. This exclusion revealed 2830 up and 3642 downregulated genes in DtxR cells (**Figure 3.13A**). Each differentially expressed gene was depicted via volcano plot with their relative -logFDR and Log_2FC values. We have highlighted one of the most significantly upregulated genes ABCB1 (**Figure 3.13B)**, validating our earlier results on multi-drug resistant phenotype (**Figure 3.7**). Although it is important to examine the critically changed genes, we aimed to approach the data from a broader and more comprehensive perspective. To do this, we ran our DEGs file in GSEA analyzer software to identify enriched gene pathways regarding the acquisition of the drug resistance process. Despite this analysis provided major data, we highlighted the interesting enriched (positively or negatively) pathways in Hallmarks, Gene ontology (Biological Processes-BP, Molecular Function-MF, Cellular Compartments-CC), and Oncogenic Factors (**Figure 3. 13C**). Particularly, Myc Targets, E2F Targets, Unfolded Protein Response, G2M Checkpoints, mTOR signaling, and Mitotic spindle gene sets were positively enriched in Hallmarks gene set in DtxR resistant cells (NES>0, p<0.05). Ribosomal biogenesis and mitochondrial gene expression were also positively enriched in Biological Processes. In correlation, spliceosomal or proteasomal complexes, and mitochondrial subunits were positively enriched in CC, also ribosome and RNP complex were positively enriched in MF gene sets. On the other hand, mTOR, KRAS, and VEGF

oncogenic pathways were positively enriched (**Figure 3.13C**). Specifically, we highlighted three pathways that were significantly enriched given in **Figure 3.13D**. E2F Targets, G2M Checkpoints, and mTOR were representing high NES scores (2.09, 1.78, 2.78) with significant p-values.

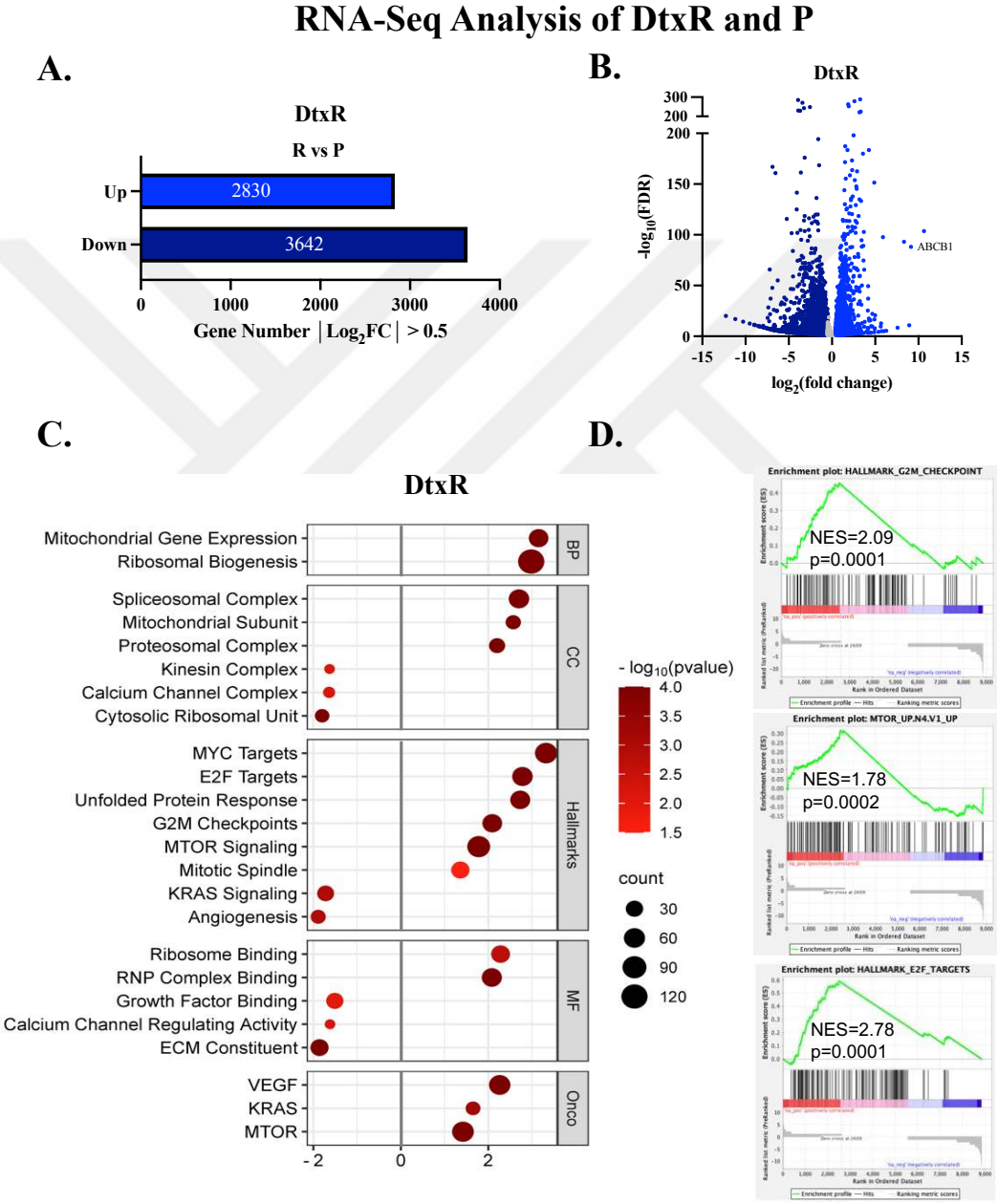

Figure 3. 13: RNA-seq analysis of DtxR-resistant cells

A. The graph shows the number of up or downregulated genes in DtxR-resistant cells. **B.** Volcano plot representing each DEG, positioned depending on Log_2FC (x-axis) and -logFDR (y-axis) values. **C.** The bubble plot shows enriched pathways in different gene sets including, Hallmarks, BP, MF, CC, and Oncogenic pathways. Circle depicting the count of DEG in the relevant gene set, and color depicting, the significance of p-value. The bubble plot was visualized with the SRplot web server (https://www.bioinformatics.com.cn/en). **D.** Graphs showing Enrichment plots of chosen gene sets which significantly enhanced in DtxR cells.

Secondly, we analyzed transcriptomic differences in Menin WT and KO cells. We have used two different Menin knockout clones that overlapped the common differentially expressed genes in both clones and carried out further analysis. As shown in the Principal Component Analysis (PCA) plot, (**Figure 3.15A**), KO clones (KO2 and KO3), exactly overlapped on the same spot in PCA, suggesting the clone-specific differences were negligible. Menin ablation in both cell lines (P and DtxR), caused significant transcriptomic variances as depicted in **Figure 3.15A.** Indeed, Menin KO led to 2077 up and 2120 downregulated genes in DtxR cells (**Figure 3.14.C**). Similarly, a volcano plot was utilized to represent DEGs, and Menin was highlighted as one of the most depleted genes in the knockout cells (**Figure 3.14B**). However, many genes were also observed to have lower LogFC values than Menin, indicating downstream targets of Menin were highly affected by its ablation. To reveal differentiated gene sets, we again employed GSEA analysis and represented our data with an enrichment bubble plot (**Figure 3.14C**). As expected, MLL complex, H3 Methyl Transferase Activity, and Histone Lysine N-Methyl transferase activity were negatively enriched in Menin-null DtxR cell. Also, regulation of cell cycle checkpoints, RNA polymerase complex, and DNA binding transcription activator activity was negatively enriched in Menin-null DtxR cells. Interestingly, several gene sets were significantly enhanced in DtxR (**Figure 3.13C**), this time were negatively enriched in the Menin knockout model (**Figure 3.14C).** For example, mTOR, Unfolded Protein Response, E2F Targets, and G2M Checkpoints, were negatively enriched ($NES<0$, $p<0.05$) in Menin ablation, unlike the DtxR vs P comparison. In **Figure 3.14D**, we provided GSEA enrichment plots in the same gene sets as **Figure 3.13D**, however, this time Menin ablation reversed the enrichment profile of these gene sets, showing negative NES scores. In our further

analysis, we specifically focused on these gene sets and examined them from multiple perspectives.

Since Menin depletion significantly stalled DtxR growth, we became interested in identifying genes that were oppositely regulated between the initial and subsequent comparisons. Therefore, we aimed to understand the changes that occurred during the acquisition of drug resistance and following Menin ablation. We overlapped two studies and sorted out upregulated genes in DtxR and downregulated genes in Menin knockout, and found 330 upregulated genes in DtxR, had decreased expression upon Menin silencing. Similarly, 468 genes which were downregulated in DtxR, had upregulated upon Menin knockout (**Figure 3.15B**). The most significantly reverted genes upon Menin knockout were presented in **Figure 3.15C**. Also, detailed genes enriched under the selected GSEA pathway were given in **Table 3.1.**

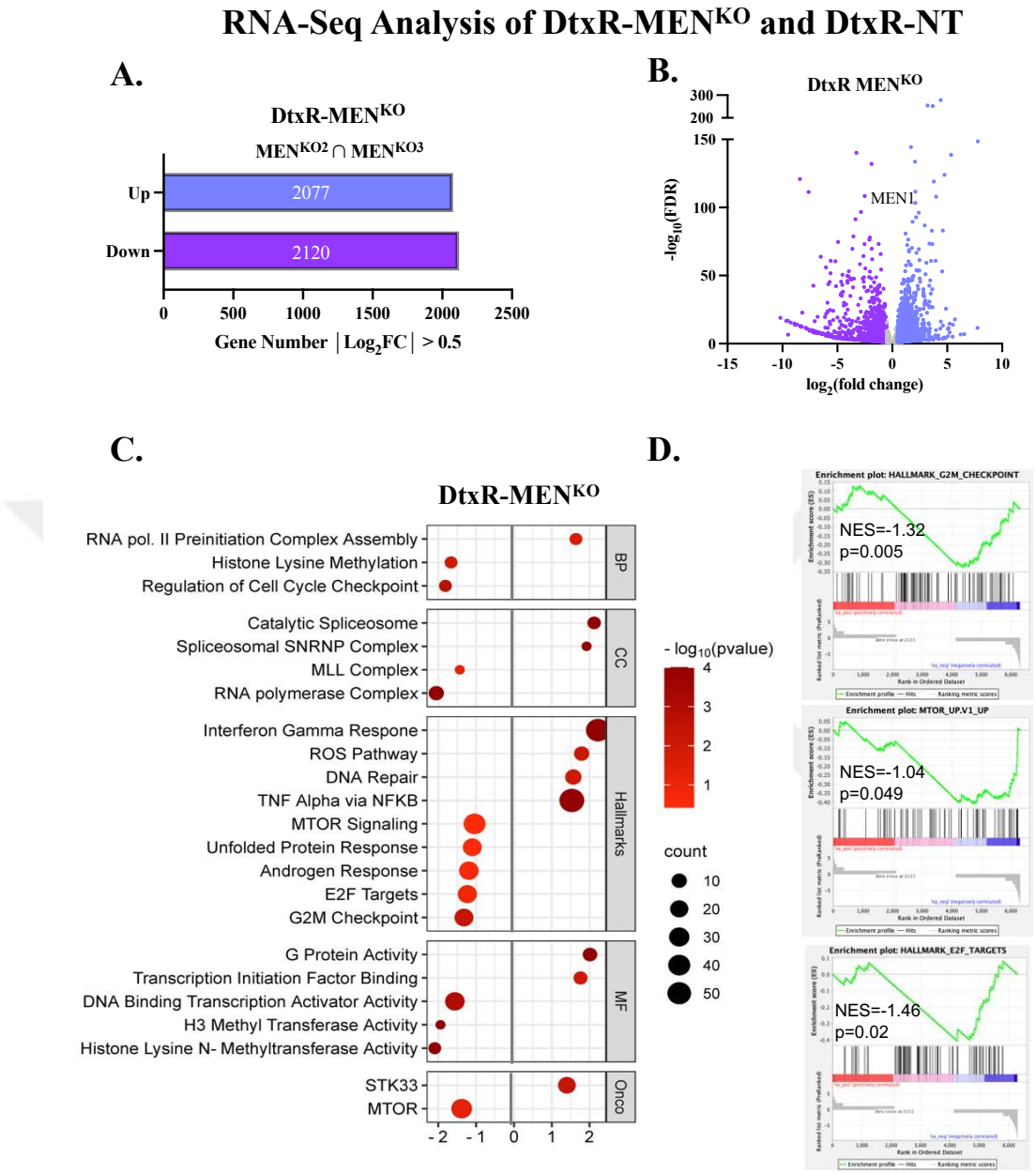

Figure 3. 14: RNA-seq analysis of Menin knockout in DtxR cells

A. The graph shows the number of up or downregulated genes in Menin knockout DtxR cells. **B.** Volcano plot representing each DEG, positioned depending on Log_2FC (x-axis) and -logFDR (y-axis) values. **C.** The bubble plot shows enriched pathways in different gene sets including, Hallmarks, BP, MF, CC, and Oncogenic pathways. Circle depicting the count of DEG in the relevant gene set, and color depicting, the significance of p-value. The bubble plot was visualized with the SRplot web server (https://www.bioinformatics.com.cn/en). **D.** Graphs showing Enrichment plots of chosen gene sets which significantly negatively enriched in Menin ablated DtxR cells.

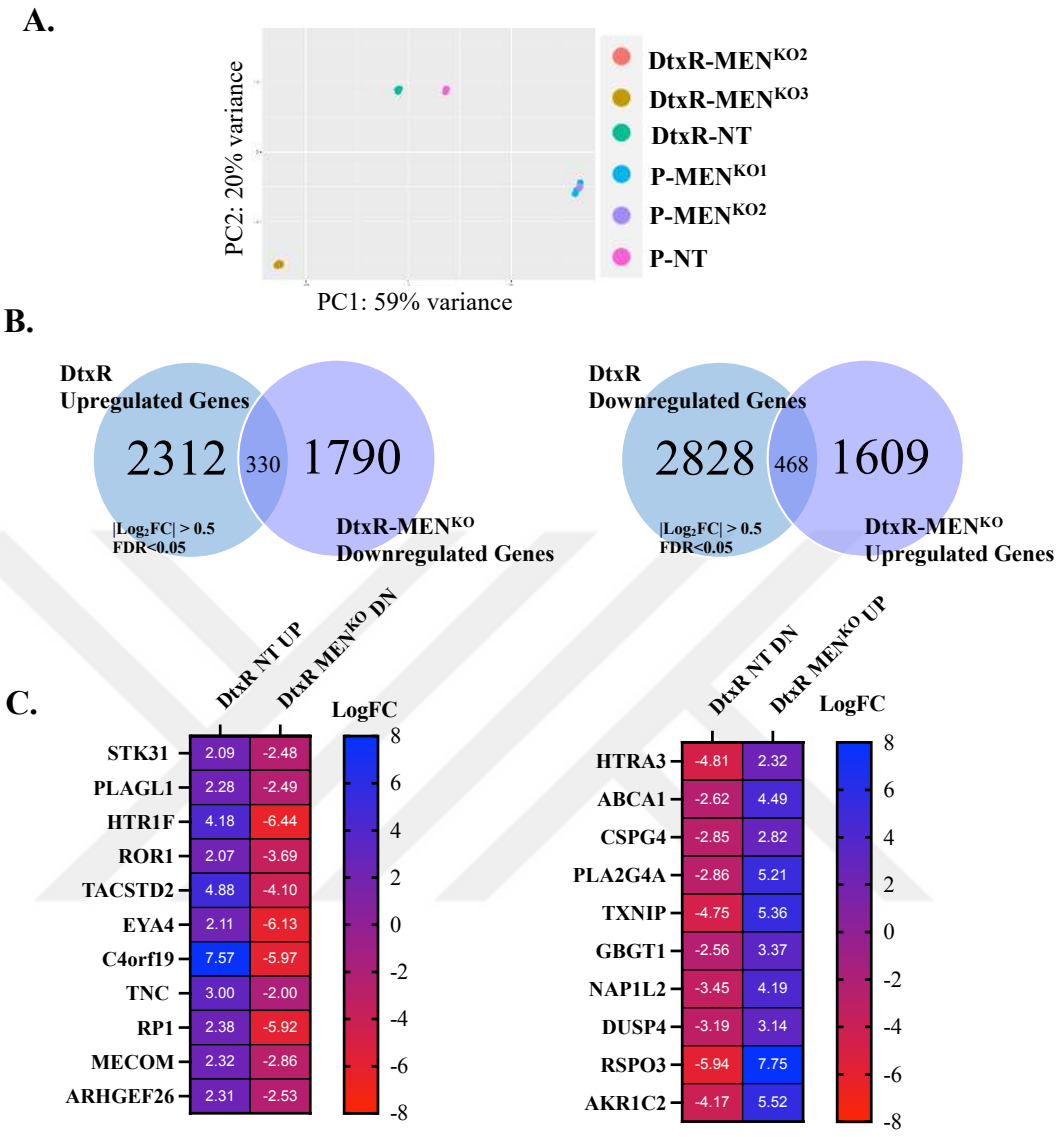

Figure 3. 15: Additional data including PCA plot of different Menin clones and genes showing reversed expression profiles.

A. PCA plot demonstrating the transcriptomic variances in two different clones of menin knockout and their controls in P and DtxR cells. **B.** Venn diagrams illustrating common DEGs however showing reversed expression patterns. **C.** Significantly up or down-regulated genes upon Menin knockout in DtxR cells.

Table 3. 1: Detailed enriched gene sets

Comparison / GSEA Analysis	DtxR vs P	DtxR-MEN^{KO} vs DtxR-NT
MTOR pathways	**NES: 1.77** HSPA5, DDIT3, NIBAN1, HSP90B1, CALR, NAMPT, BCAT1, SDF2L1, TES, HSPA4, GTF2H1, CDKN1A, AK4, CDC25A, PPP1R15A, RPN1, USO1, PLK1, ABCF2, MTHFD2, UBE2D3, HSPA9, HSPD1, ALDOA, UFM1, STIP1, PSMD13, TOMM40, SHMT2, ELOVL6, DDIT4, SLC1A15, ACTR3, EPRS1, PSMA3, ETF1, SLC2A1, ASNS, RIT1, NFKBIB, COPS5, IFRD1, HSPE1, TCEA1, PSMD14, PSAT1, PSMD12, SLC7A11, DHCR24, GOT1	**NES: -1.04** PSMD12, CTH, ATP6V1D, SLC2A3, CCNG1, INSIG1, AK4, CACYBP, FADS1, IDI1, HSP90B1, EDEM1, SCD, HMGCR, STARD4, CORO1A, HSPA5, TES, ERO1A, AURKA, SDF2L1, NUP205, GLRX, EPRS1, ADD3, ACLY, NUFIP1, ASNS, SC5D, CYP51A1, TMEM97, SQLE, HMGCS1, STC1, POLR3G, ITGB2
E2F targets	**NES: 2.78** TK1, PRDX4, PA2G4, EZH2, RAD51AP, CKS1B, NUDT21, CDKN1A, CDC20, CENPE, TRIP13, NME1, CSE1L, PRKDC, KPNA2, CDC25A, CDKN3, ZW10, ANP32E, PNN, PLK1, XRCC6, MTHFD2, DONSON, HUS1, ORC2, ASF1A, NOP56, PLK4, ING3, ORC6, HNRNPD, DCTPP1, TIPIN, GINS4, CTSP1, TACC3, PRIM2, SMC4, MAD2L1, RAN, MELK, HMGA1, PSMC3IP, H2AZ1, DIAPH3, NOLC1, TUBB, DDX39A, EXOSC8	**NES: -1.23** UBE2S, RFC1, ATAD2, KIF18B, TRIP13, PAN2, DSCC1, CDKN2C, LBR, SPC24, CKS2, EIF2S1, DEPDC1, UBE2T, AURKA, NUP205, CKS1B, DLGAP5, BARD1, TIMELESS, SMC4, ILF3, SPAG5, LYAR, CCP110
G2M targets	**NES: 2.08** ODC1, SAP30, TTK, EZH2, CKS1B, NSD2, HIF1A, CDC20, CENPE, NUP50, KPNA2, RBM14, CDC25A, CDKN3, PLK1, KIF20B, HUS1, DR1, NOTCH2, BUB3, SLC7A1, PLK4, ORC6, HNRNPD, CDC6, CCNA2, ATF5, ORC5, TACC3, PRIM2, SMC4, MAD2L1, E2F4, E2F3, HMGA1, H2AZ1, SLC7A5, NOLC1, FBXO5, KMT5A, DDX39A, MARCKS, DKC1, CCND1, SYNCRIP, JPT1, HSPA8, RAD21, E2F2, KIF15,	**NES: -1.31** RPS6KA5, SS18, RASAL2, NEK2, UCK2, CDKN2C, TENT4A, PRMT5, LBR, CKS2, CUL4A, AURKA, CKS1B, BARD1, SLC12A2, TLE3, KNL1, SMC4, ILF3, ODF2, POLQ, HOXC10, FOXN3, SQLE

On the other hand, Menin ablation did not induce a significant phenotypic change in parental cell growth. However, to understand the effects of Menin on parental cells we have also sequenced drug-naive cells as well. Similarly, we overlapped the genes in two clones (KO2 and KO3) and the common genes were selected for further studies. As shown in **Figure 3.16A**, Menin knockout in parental cells resulted in a higher number of DEGs. 3224 genes were upregulated and 3457 genes were downregulated in parental Menin knockout cells. Volcano plot depicted DEGs, similarly, Menin expression was significantly downregulated (**Figure 3.16B**). We have also evaluated the numbers of common DEGs in parental and resistant cells following Menin ablation. Interestingly, nearly half of DEGs in resistant cells were common with DEGs in parental Menin knockout. However, when we checked the GSEA analysis, the majority of the gene set enrichments were similar but, negatively regulated in parental Menin knockout. For example, mTOR, Unfolded Protein Response, E2F, and G2M Checkpoints had negative enrichment scores in Menin-ablated DtxR cells, however, they showed positive enrichment scores in Menin-null P cells.

Finally, we have performed a similar analysis on LEDGF-null parental and resistant cells. Compared to Menin-ablation, LEDGF deletion led to significantly fewer numbers of DEGs. For example, in parental cells, only 16 up, and 41 downregulated genes met the criteria of FDR<0.05 and $|Log_2FC|>0.5$ (**Figure 3.17A**). On the other hand, resistant cells showed 77 upregulated genes. Interestingly, the highest proportion of DEGs was observed in downregulated genes in DtxR cells, 727 genes were significantly downregulated (**Figure 3.17B**). This data indicated that LEDGF ablation alone did not have a major transcriptional effect on parental cells. However, LEDGF deletion resulted in significant transcriptional silencing on DtxR cells. When we overlapped DEGs, we observed that only 9 genes were common, hinting that LEDGF was bearing such versatile roles in these two cell lines (**Figure 3.17C**). As shown in volcano plots, LEDGF appeared to be the most significantly downregulated gene in P knockout cells, and the fourth downregulated gene in DtxR knockout cells (**Figure 3.17D-E**). We were unable to run a GSEA analysis on LEDGF-null parental cells, due to limited DEG numbers. On the other hand, DtxR cells showed negative enrichment on gene sets in

cell division, Glycolysis, mTOR, and Cyclin D1. In addition, ribosomal biogenesis and mitochondrial gene expression were positively enriched (**Figure 3.17F**).

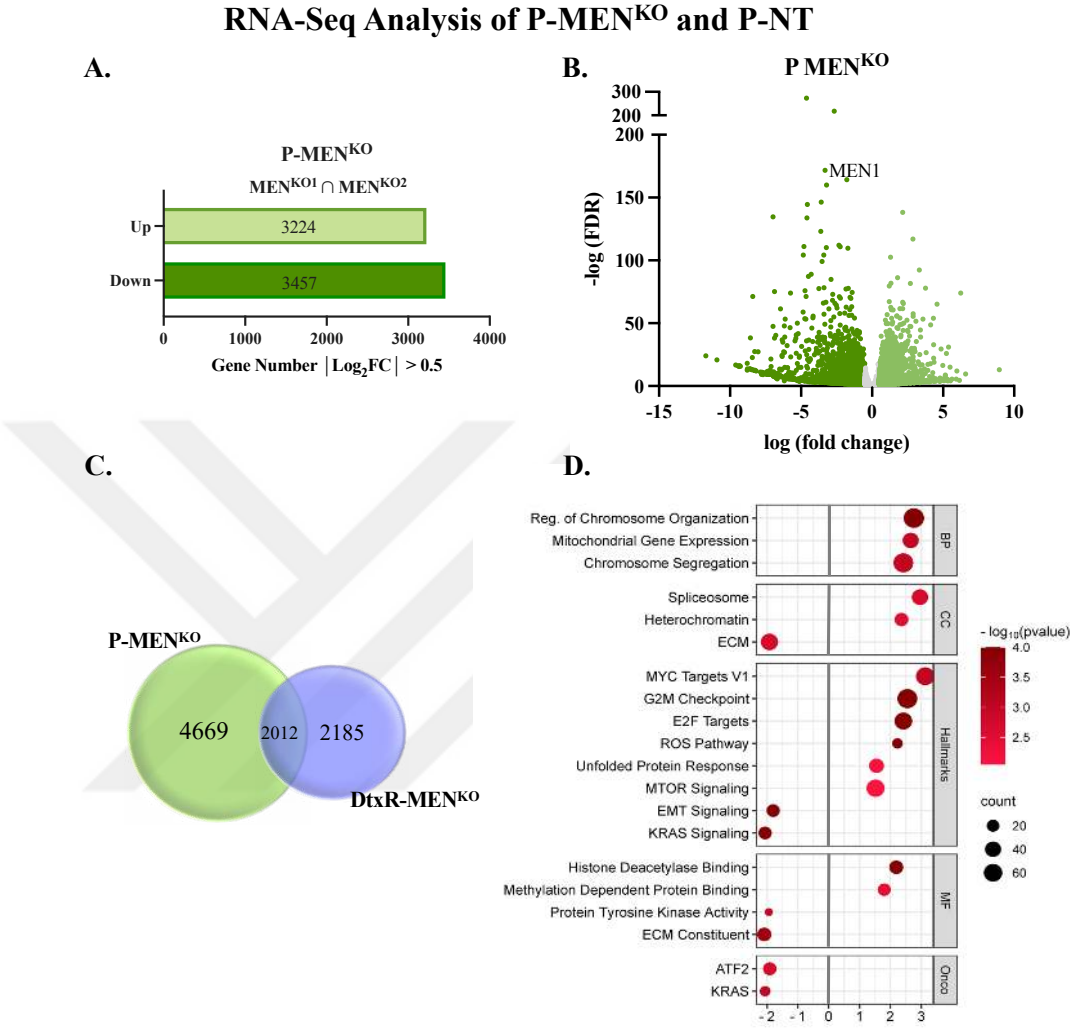

Figure 3. 16: RNA-seq analysis of Menin knockout in DtxR cells

A. Graph showing the number of up or downregulated genes in Menin knockout P cells. **B.** Volcano plot representing each DEG, positioned depending on Log_2FC (x-axis) and -logFDR (y-axis) values. **C.** Venn diagram showing common DEGs in P-MEN^{KO} and DtxR-MEN^{KO}. **D.** Bubble plot showing enriched pathways in different gene sets including, Hallmarks, BP, MF, CC, and Oncogenic pathways. Circle depicting the count of DEG in the relevant gene set, and color depicting, the significance of p-value. The bubble plot was visualized with the SRplot web server (https://www.bioinformatics.com.cn/en).

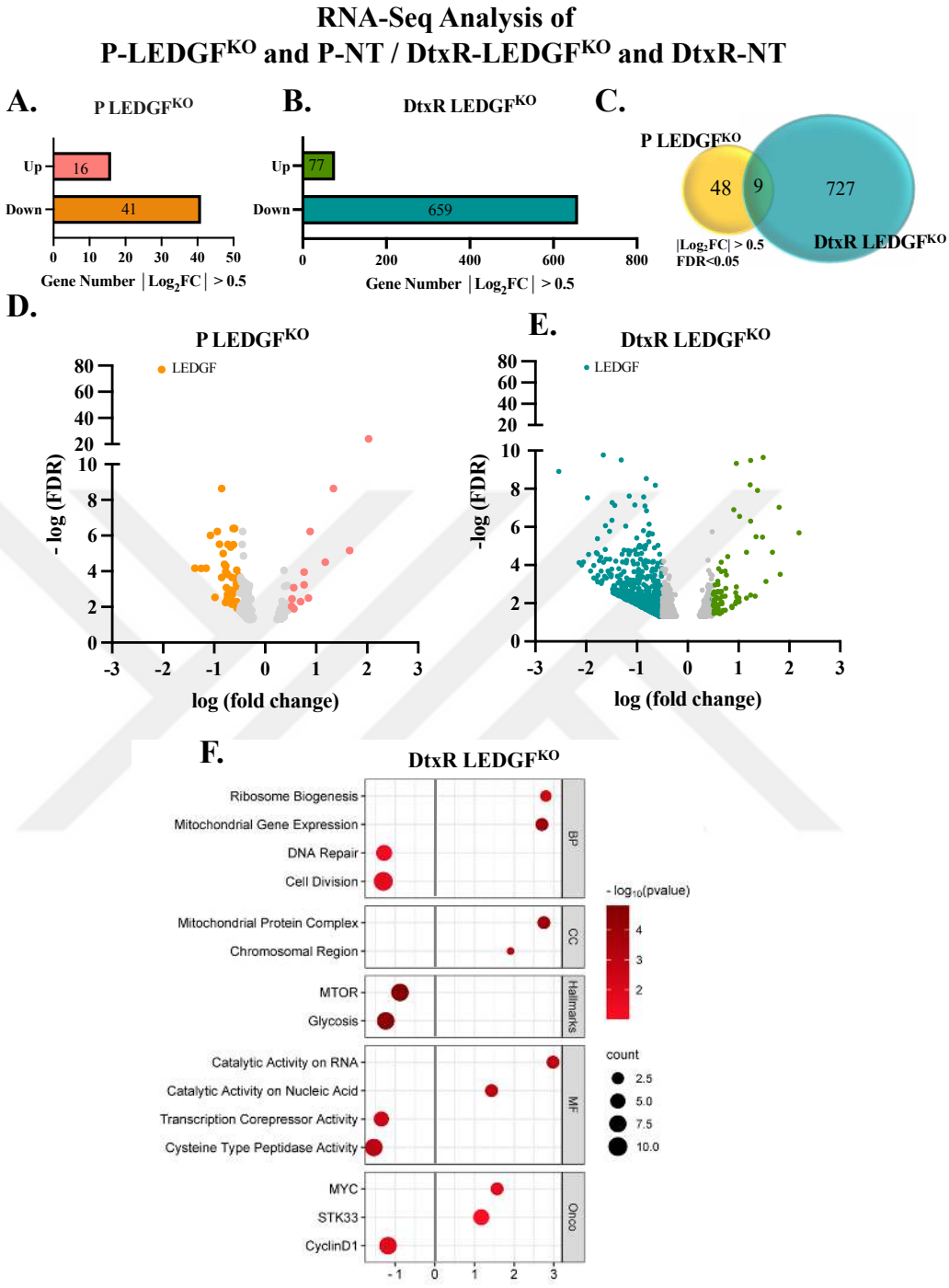

Figure 3. 17: RNA-seq analysis of LEDGF knockout in P and DtxR cells

A-B. Graph showing the number of up or downregulated genes in LEDGF ablated P and DtxR cells. **C.** Venn diagram showing common DEGs in P-LEDGF^{KO} and DtxR-LEDGF^{KO}. **D-E.** Volcano plot representing each DEG, positioned depending on Log_2FC (x-axis) and -logFDR (y-axis) values. **F.** Bubble plot showing enriched pathways in different gene sets including, Hallmarks, BP, MF, CC, and Oncogenic

pathways. Circle depicting the count of DEG in the relevant gene set, and color depicting, the significance of p-value. The bubble plot was visualized with the SRplot web server (https://www.bioinformatics.com.cn/en).

3.6 Menin is Required for the Acquisition of Drug Resistance

As we demonstrated Menin was essential within the cell growth regulation in DtxR cells, we also wanted to test whether Menin depletion was essential for the development of drug resistance phenotype. Therefore, we silenced Menin expression in parental cells, via shRNA-mediated transduction, and re-started the generation of resistance process, from the beginning (**Figure 3.18A**). Menin expression was constitutively silenced as validated in **Figure 3.18B**. Generation of drug resistance was initiated with cells receiving the first dose of Docetaxel (1 nM). Over time, cells were grown at increasing drug doses until reaching to 4th cycle (8 nM). At this stage, a significant fraction of parental cells lacking Menin expression, were unable to recover from the drug treatment, and cells continued to die with no further remaining population, however, the majority of the cells treated with shFF survived the drug cycle (**Figure 3.18C**). This data provided convincing evidence that Menin expression was required to have a drug-resistance phenotype. We therefore hypothesized that Menin is necessary and provides a favorable cellular environment for the drug-resistant phenotype to occur.

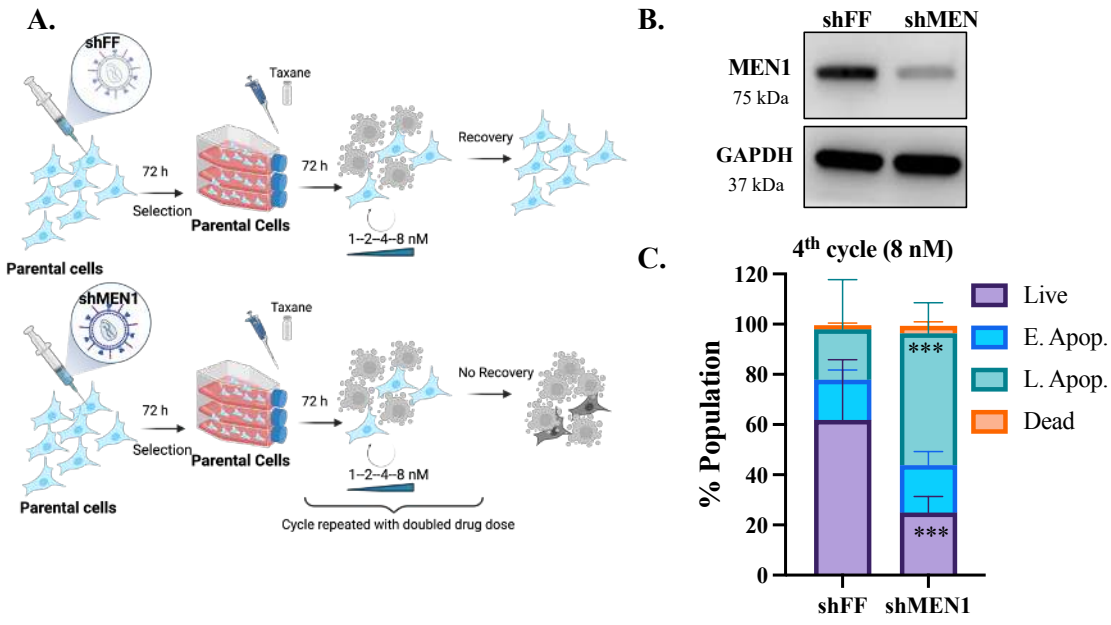

Figure 3. 18. Silencing Menin in Parental Cells and Re-generation of Drug Resistance

A. Schematic showing the experimental procedure of sh-targeted silencing in Menin and re-practicing Docetaxel treatment. **B.** Western blot indicating reduced Menin protein expression following treatment with relative shRNA. **C.** Graph showing Annexin V and PI stainings of parental cells following with relative shRNA and 8 nM of Docetaxel dose. Live cells represent negative staining for both markers, early apoptotic cells represent positive staining for Annexin V, late apoptotic cells represent positive staining for both markers and dead cells represent positive staining for PI. Graphs represent the average of ± standard deviation of two biological repeats. (One-way ANOVA, *** $p \leq 0.001$).

3.7 Menin Regulates mTOR Expression

In our RNA-seq analysis, we demonstrated that mTOR gene sets were upregulated in DtxR cells and reversed upon Menin ablation, which was also compatible with our RT-qPCR results (**Figure 3.19.A-B**). We have also restored Menin expression using Menin wild-type sequence and evaluated mTOR expression under Menin ablation and rescued conditions. Consistently, Menin rescue increased the expression of mTOR levels, supporting the idea of Menin acts on mTOR (**Figure 3.19C**). We have also examined mTOR's essentiality in our Dtx-resistant model, so we silenced mTOR using the shRNA method (**Figure 3.19D**). Upon mTOR silencing, DtxR cells completely failed to produce any colonies (**Figure 3.19E**). These results suggested Menin may lead to mTOR upregulation in DtxR to induce drug-resistant phenotype. mTOR is essential for the maintenance of the DtxR model, furthermore, Menin silencing reduced mTOR expression and therefore reduced tumor growth in resistant cells.

To test whether Menin transcriptionally regulates mTOR expression, we performed ChIP-qPCR. We initially tagged Menin and LEDGF proteins with a 3xFLAG tag and overexpressed this variant in our resistant cells (**Figure 3.19G**). Later on, we performed sonication (**Figure 3.19F**) and pulldown with FLAG antibody to analyze enriched DNA-binding sites of Menin and LEDGF. Our ChIP-qPCR analysis demonstrated Menin enrichment on mTOR promoter region (-500 bp, +100 bp) significantly (**Figure 3.19G**). These results strongly supported Menin's influence on mTOR expression.

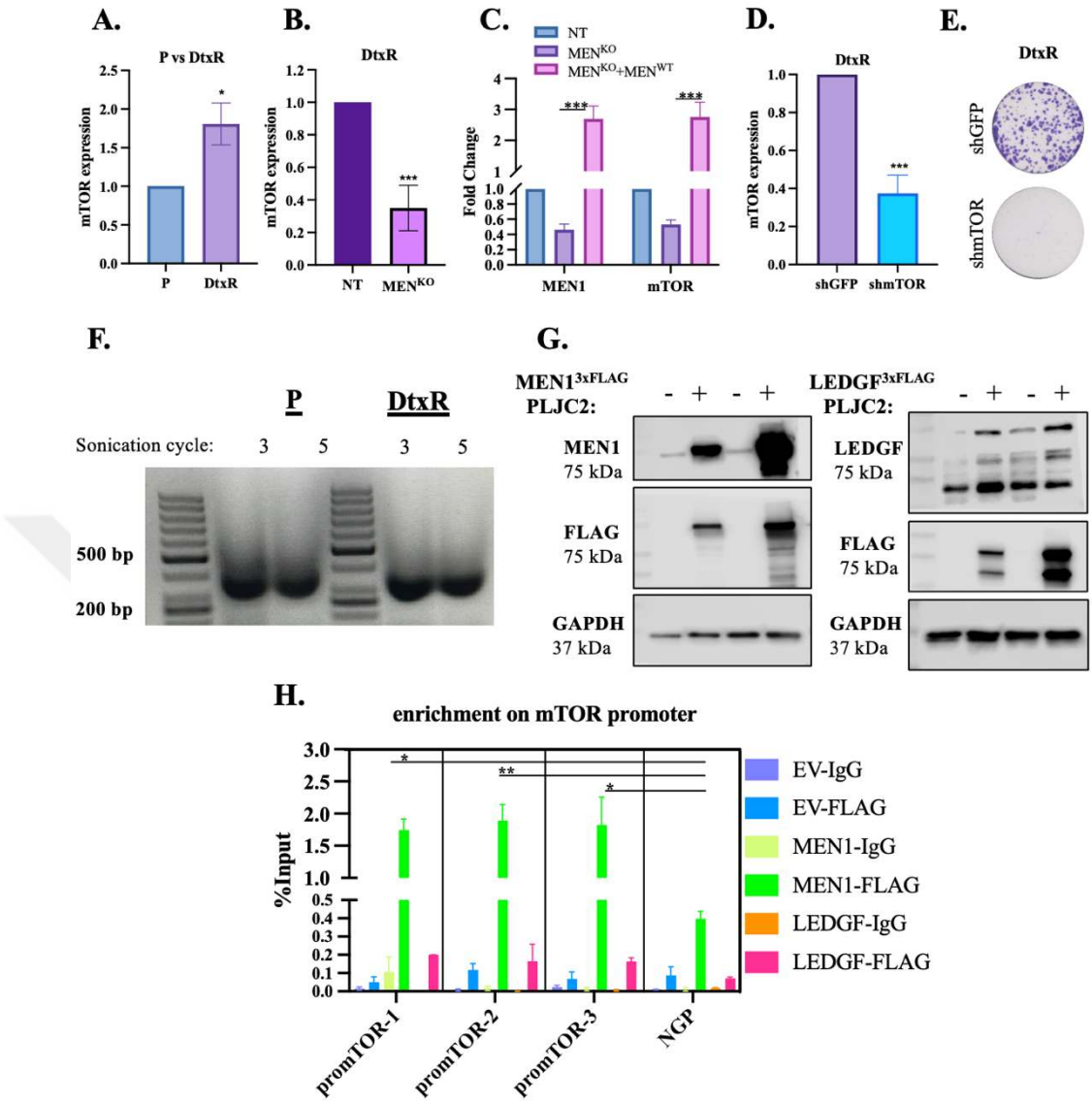

Figure 3. 19: Menin depletion reduces mTOR expression and Menin is enriched on mTOR promoter

A-B. RT-qPCR results showing mTOR expression in P and DtxR cells, and Menin-null cells. **C.** RT-qPCR results showing Menin and mTOR expression in Menin-depleted and rescued cells. **D.** mTOR expression levels following shRNA treatment. **E.** Colony formation results following mTOR silencing in DtxR cells. **F.** Agarose gel image showing sonicated DNA base pair for ChIP-qPCR. **G.** Western blot showing validation of FLAG-tagged MEN1, and LEDGF overexpression system. **H.** ChIP-qPCR results demonstrating Menin enrichment of mTOR promoter with three different primers amplifying TSS (-500 bp, +100 bp) region. NGP: Negative primer. Graphs represent the average of ± standard deviation of three bio logical repeats. (One-way ANOVA, *p≤0.05, **p≤ 0.01, *** p≤ 0.001).

3.8 mTOR silencing via Torin Synergizes with Dtx in Menin knockout cells

We first evaluated the Dtx response in Menin knockout cells, to do this we treated Menin-depleted cells with increased doses of Dtx. However, Menin depletion did not induce significant cell death, only the highest dose 250 nM sensitized Menin silenced cells (**Figure 3.20A-B**). Interestingly, the depletion of Menin using the KO model did not induce a significant reversion in Dtx response effectively as MLL-Menin inhibitors (**Figure 3.4**). To improve Dtx response, we combined mTOR inhibitor (Torin) with Dtx in Menin wild type and Menin KO cells. Interestingly, Menin depletion significantly improved Dtx and Torin response (**Figure 3.20C**). On the other hand, restoring Menin expression abolished this synergy, suggesting the importance of Menin depletion in this phenotype (**Figure 3.20D**). Increased synergy in Menin-null cells was also validated in enhanced levels of apoptotic cells (**Figure 3.20E**). Overall, our results highlighted mTOR's contribution to drug-resistant phenotype, as silencing mTOR improved Dtx response, and further mTOR silencing with Menin depletion, elevated this synergy.

3.9 Menin knockout cells show reduced cell growth and G1 Arrest

Slow-growing rates and lower division cycles were observed in Menin knockout cells. We reasoned that this phenotype was a result of limited growth signals derived from reduced mTOR pathways. Indeed, when we performed a competition assay, with an equally mixed population with Menin wildtype and knockout cells (**Figure 3.21A**), we observed a significant domination of wild-type cells in the population, as time progressed (**Figure 3.21B**). We therefore examined the cell cycle distribution of Menin knockout cells without a treatment. We analyzed cell cycle distribution with PI staining and observed a significant accumulation of Menin knockout cells in the G1 cell cycle (**Figure 3.21C**). These results also prompted us to test Menin's contribution to the regulation of cell cycle proteins. Initially, we tested protein levels of different cyclins in Menin-ablated cells. Consistently, Cyclin D1 protein levels were significantly lower in Menin knockout cells (**Figure 3.21D-E**). On the other hand, Cyclin E levels were observed to have a higher expression in Menin-ablated populations. (**Figure 3.21D-E).** These results indicate Menin depletion causes accumulation in the late G1 phase. Accordingly**,** our RNA-seq and qPCR results revealed a collective reduction in the expression of cell cycle affecting gene panel. For example, Cyclin D1, CEND1, and

CDK20 were significantly downregulated in Menin knockout cells. In addition, oncogene Myc and Myc target genes, NDRG1 were significantly downregulated in Menin-depleted cells (**Figure 3.21F**).

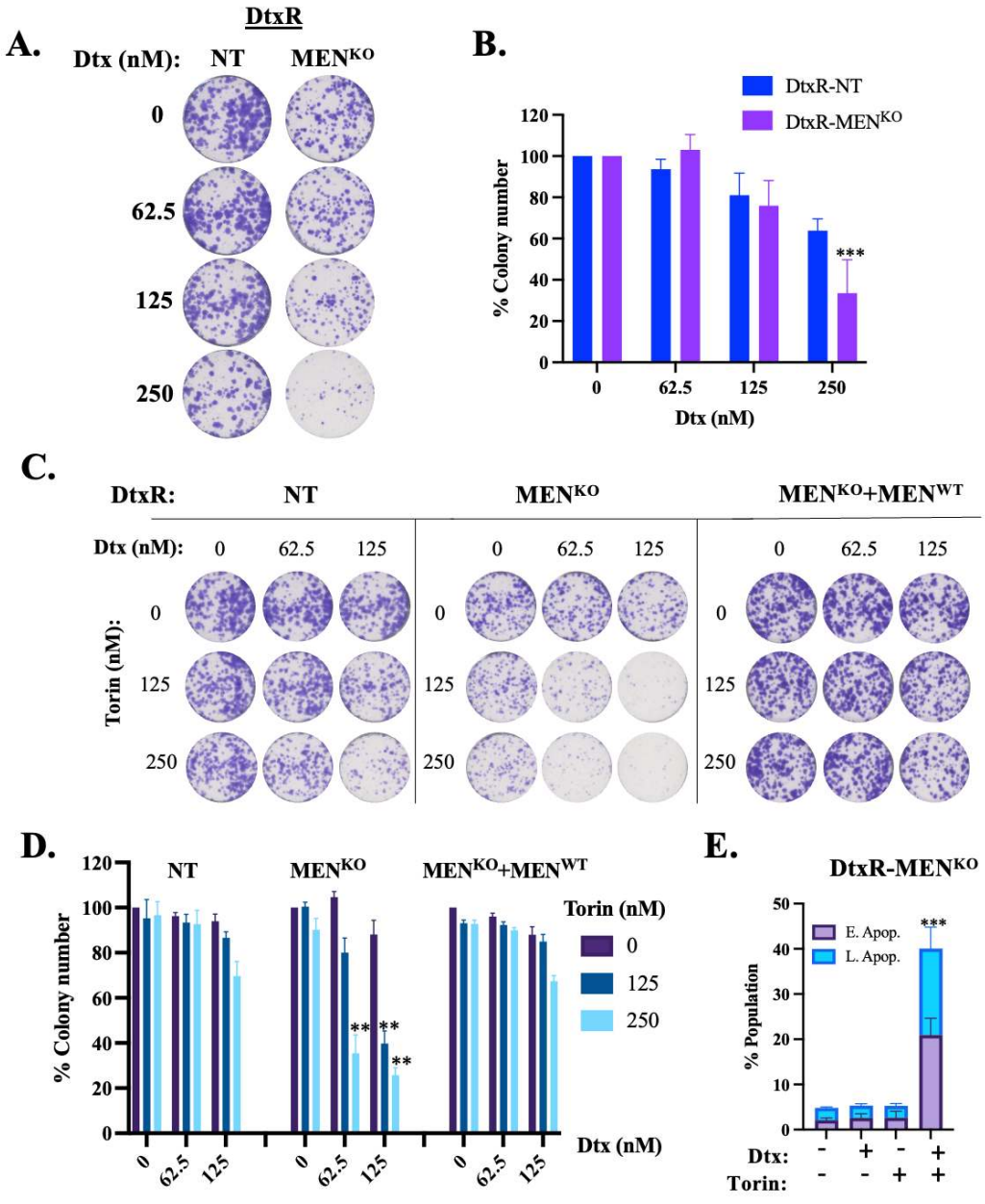

Figure 3. 20: mTOR silencing via Torin Synergizes with Dtx in Menin knockout cells

A. Dtx response via colony formation experiment in Menin wildtype and depleted DtxR cells. **B.** Graph showing normalized numbers of colonies. **C.** Colony formation analysis of Dtx and Torin combination treatment in Menin wildtype, knockout, and rescued cells. **D.** Graph showing normalized numbers of colonies, counted with CellCounter software

by Nghia Ho. **E.** Annexin V and PI stainings of Menin-depleted resistant cells following with Dtx (62.5 nM) and Torin (125 nM) combination. Early apoptotic cells represent positive staining for Annexin V, and late apoptotic cells represent positive stainings for both markers. Data represent the average of ± standard deviation of three biological repeats (One-way ANOVA, *p≤ 0.05, ** p≤0.01, *** p≤0.001).

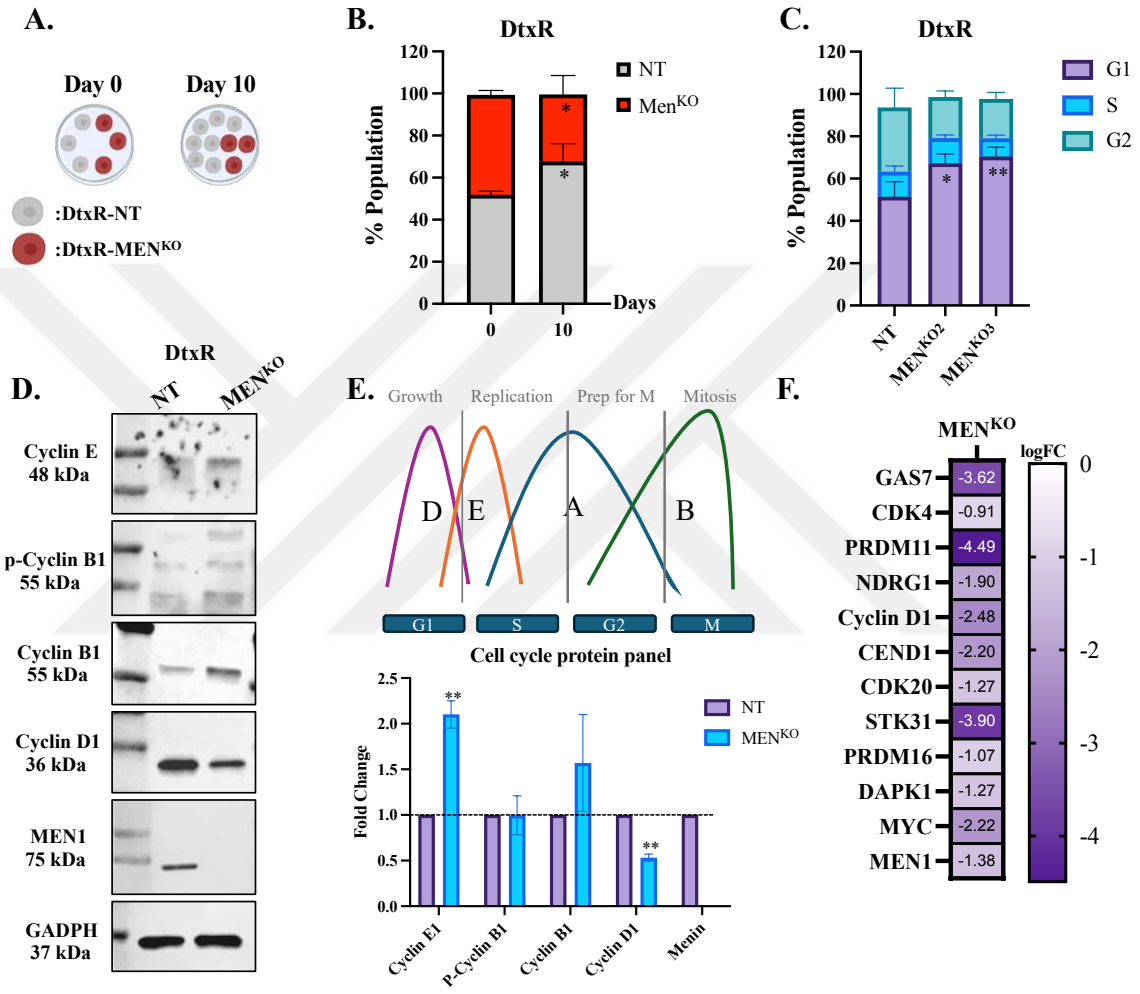

Figure 3. 21: Cell cycle profile of Menin knockout resistant cells

A. Cartoon showing the experimental setup of competition assay. **B.** Graph showing flow cytometry analysis of the distribution of an equally mixed population of Menin wildtype and knockout cells over 10 days. **C.** Flow cytometry analysis of cell cycle distribution in control and two knockout clones. **D.** Different cyclin protein levels in Menin knockout cells analyzed by western blot. **E.** Schematic showing peak levels of each Cyclin in different cell cycle phases and the graph showing normalized fold change quantification of western bands via Image J software. **F.** Heat map of reduced expression of different genes involved in cell cycle regulation in Menin knockout resistant cells. Data represent the average of ± standard deviation of three biological repeats (One-way ANOVA, *p≤ 0.05, ** p≤0.01, *** p≤0.001).

3.10 Menin is enriched on Cyclin D1 and CDK20 promoter

We observed a significant reduction in Cyclin D1 protein levels upon Menin silencing. Interestingly, other cell cycle-related proteins such as CEND1 and CDK20 were also significantly reduced upon Menin ablation. To test whether this was a direct interaction, we rescued Menin expression and evaluated the expression status of these aforementioned genes. Initially, we observed that reduced Cyclin D1 expression was recapitulated in the Menin rescue model (**Figure 3.22A**). Also, Menin rescuing significantly increased CEND1 and CDK20 expression in DtxR cells (**Figure 3.22B**). These data motivated us to examine the presence of Menin on the promoter regions of the indicated factors. Utilizing our 3xFLAG tag system, we performed Menin and LEDGF pulldown and ChIP-qPCR. Our results showed strong enrichment of Menin on CDK20 and Cyclin D1 promoter regions with 3 sets of primers targeting the TSS (-500 bp, +100 bp) region (**Figure 3.22C-D**). These data indicate Menin is contributes to cell division by regulating Cyclin D1 and CDK20 expression in the DtxR model.

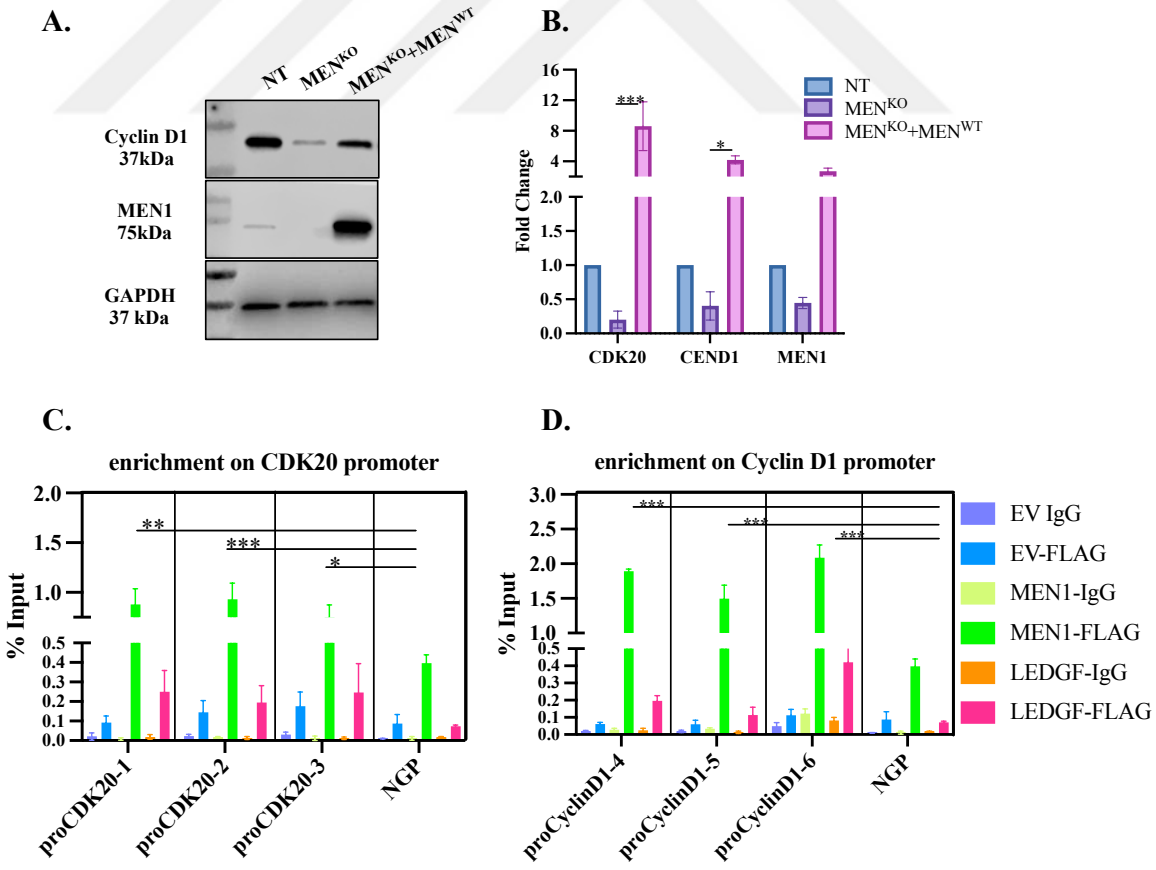

Figure 3.22: Menin rescue restores Cyclin D1 and CDK20 expression, Menin is also enriched on CDK20 and CEND1 promoter

A. Western blot showing Cyclin D1 protein levels in Menin knockout and Menin rescue DtxR cells. **B.** RT-qPCR showing CDK20 and CEND1 expression in Menin knockout and Menin rescue DtxR cells. **C-D.** ChIP-qPCR results demonstrating Menin enrichment of CDK20 and Cyclin D1 promoter with three different primers amplifying TSS (-500 bp, +100 bp) region. NGP: Negative primer. Graphs represent the average of ± standard deviation of three biological repeats. (One-way ANOVA, *p≤0.05, **p≤ 0.01, *** p≤ 0.001).

ChIP-qPCR analysis revealed significant enrichment of Menin on target sequences, however, in any case, LEDGF was not demonstrating a strong enrichment compared to negative primers. However, reduced cell cycling phenotype (reduced cell growth) was also observed in LEDGF^{KO} DtxR cells as well (**Figure 3.10**). Therefore, we examined cell cycle distribution in LEDGF ablated cells, and we acquired a slight increase (7% higher) in G1 levels (**Figure 3.23A**). Similarly, LEDGF ablated cells also showed reduced Cyclin D1 levels (**Figure 3.23B**). The negative enrichment on mTOR gene sets may have stalled the cell growth and division as shown in **Figure 3.17** in the LEDGF^{KO} model.

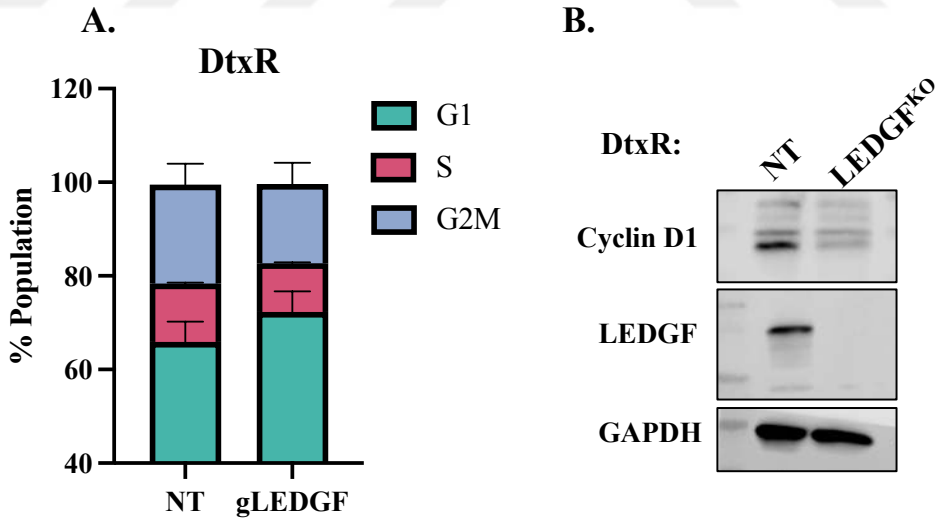

Figure 3. 23: LEDGF silencing also increases G1 levels and reduces Cyclin D1 protein

A. Graph showing flow cytometry analysis of cell cycle distribution in control and LEDGF knockout cells. **B.** Western blot showing Cyclin D1 protein levels in LEDGF knockout DtxR cells. Graphs represent the average of ± standard deviation of two biological repeats.

3.11 Epigenetic screening on Menin knockout DtxR cells

Since Menin regulates H3K4 methylation through its interaction via MLL and has also been reported to read H3K79me2 marks [Dreijerink et al., 2006, Lin et al., 2023], we hypothesized that Menin knockout may confer further epigenetic vulnerabilities. To identify potential targets, we performed an epigenetic screening on Menin WT and KO resistant cells. 30 drugs resulted in 10% differences in Menin knockout cells, and we identified them as hits. As classified, HMT inhibitors, BRD/BET inhibitors, WDR5 inhibitors, HDAC inhibitors, and several HAT inhibitors reduced cell viability in Menin-null cells. On the other hand, Menin-null cells showed less sensitivity for HDM inhibitors, DNMT inhibitors, CDK4 inhibitors, and PLK4 inhibitors (**Figure 3.24**). We were unable to find an inhibitor which considerable induced major variations in drug response except for Ryuvidine. This might have occurred due to the experimental setup with the acute treatment model, and prolonging the course of the treatment process may improve therapy response. Interestingly, Ryuvidine has high off-target effects and has been shown to inhibit SET8, KDM5B, and CDK4/6 [Blum et al., 2014, Lang et al., 2015, Mitsui et al., 2019]. To distinguish which one of the Ryuvidine targets is responsible for the observed phenotype, we tried other SET8 and KDM5B inhibitors. However, we did not observe any significant change in our Menin knockout cells. However, due to the observed low cell cycling phenotype, we hypothesized this reduced sensitivity may be driven by CDK4/6 inhibition. Therefore, we tested other CDK4/6 inhibitors such as Palbociclib, Abemaciclib, CINK4, and Ribociclib by acute (cell viability) and prolonged treatment (colony formation) (**Figure 3.25A-B**). In both cases, Menin-null cells showed reduced sensitivity to CDK4/6 inhibitors. We speculate that due to their low rate of cell division, Menin-null cells were protected from CDK4/6 inhibitors.

Another significant target that we were interested in was MYC; since MYC was significantly enriched in GSEA analysis in the DtxR model, it caught our attention (**Figure 3.26A**). Interestingly, under Menin silenced or knockout conditions, MYC expression was significantly reduced (**Figure 3.26B**). In literature, Menin enrichment on MYC promoter was repeatedly demonstrated [Wu et al., 2017, Luo et al., 2021]. Our ChIP-qPCR analysis also validated the Menin occupancy on MYC promoter in our

DtxR model (**Figure 3.26C**). We hypothesized Menin could be another factor that enables drug resistance, we therefore overexpressed MYC in Menin presence and absence conditions in P and DtxR cells. Myc overexpression was validated through RT-qPCR, in both cell lines (**Figure 3.27A**). MYC overexpression resulted in increased proliferation in P cells as expected, however, MYC overexpressed DtxR cells underwent cell death, independent from their Menin status (**Figure 3.27B**). We have also demonstrated significant upregulation of ABCB1 in our DtxR model, but neither RNA-seq nor GSEA analysis yielded a significant association with Menin silencing and ABCB1 expression, indeed Menin pulldown did not exhibit a significant enrichment on ChIP-qPCR (**Figure 3.28B**).

Additionaly, we have investigated several genes that were significantly down or upregulated upon Menin ablation. We evaluated Menin's occupancy in their promoter region depending on the online ChIP-seq database ChIP-Atlas (**Table 3.2**). By utilizing a combinational approach with our RNA-seq analysis and literature ChIP-seq data, we pointed out some genes that might be useful for future studies focusing on Menin's role in drug resistance and prostate cancer.

3.12 Menin and mTOR Expressions in Patient-Derived Clinical Data

Finally, Menin and mTOR correlation was investigated in clinical datasets with cBioPortal, we observed that MEN1 and mTOR had a very weak correlation in prostate adenocarcinoma; however as the disease relapses, and switches to metastatic state, MEN1 and mTOR correlation significantly improved to moderate correlation state depending on the increased pearson correlation (**Figure 3.29**). This finding underscores the importance of Menin and mTOR in patients with potentially resistant tumors. Furthermore, we examined the available data regarding the taxane response of patients with various cancers, such as breast and uterine. The results indicated that patients exhibiting lower expressions of Menin or mTOR responded more favorably to taxanes, whereas higher expressions of these markers were associated with a non-responsive state (**Figure 3.30**). Although not all studies achieved statistically significant p-values, which might be due to limited sample size, it is noteworthy that lower Menin and mTOR expressions may correlate with the clinical response to taxane therapies.

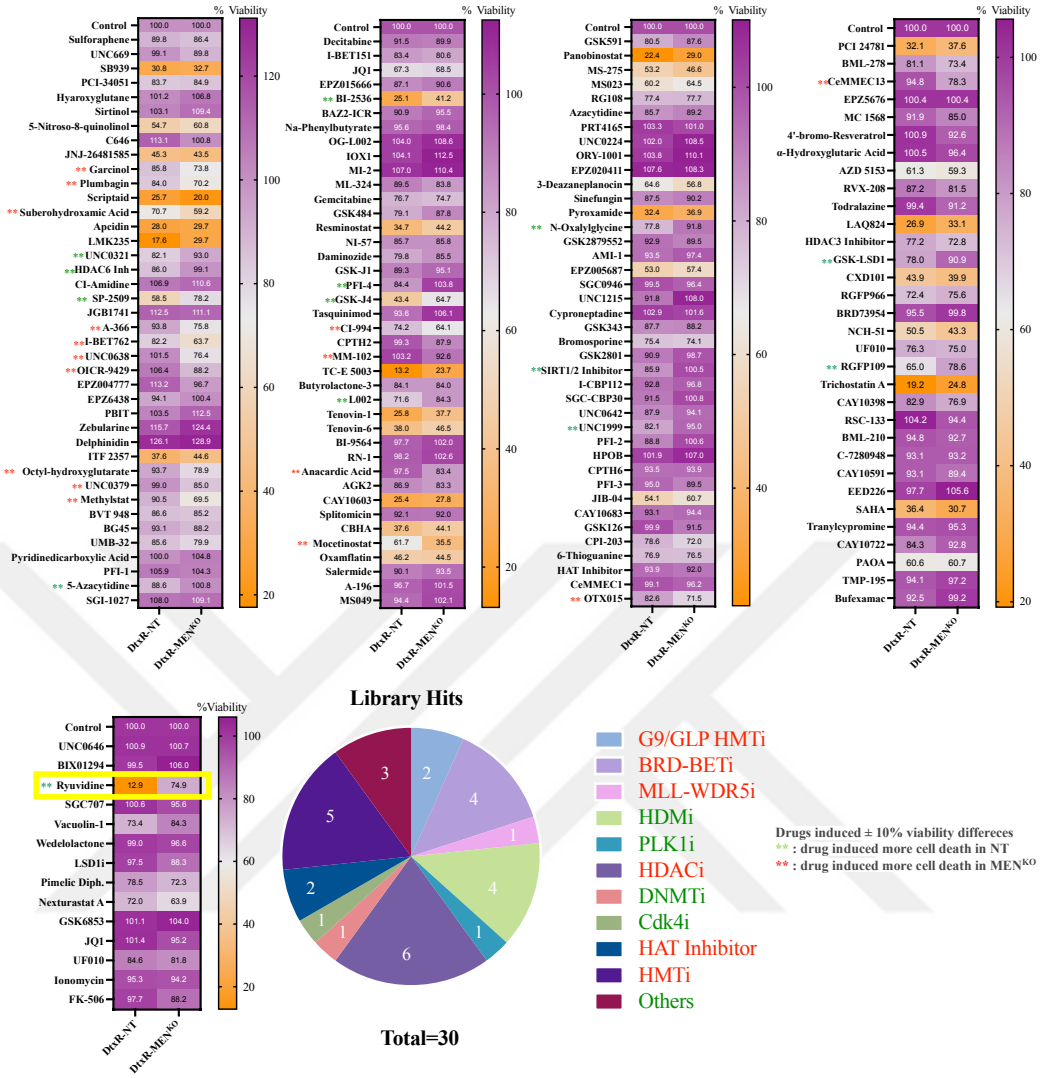

Figure 3. 24: Epigenetic screening on Menin-null DtxR cells and potential hits

Heat maps showing the cell viability results of control and Menin-depleted DtxR cells against 174 chemicals targeting an epigenetic modifier. Pie chart representing the distribution of potential hits that induced a change in the cell viability higher than 10%. Cell viability was assessed with the SRB test, red labeling indicates higher cell death in Menin knockout cells, and green labeling indicates higher cell death in control cells.

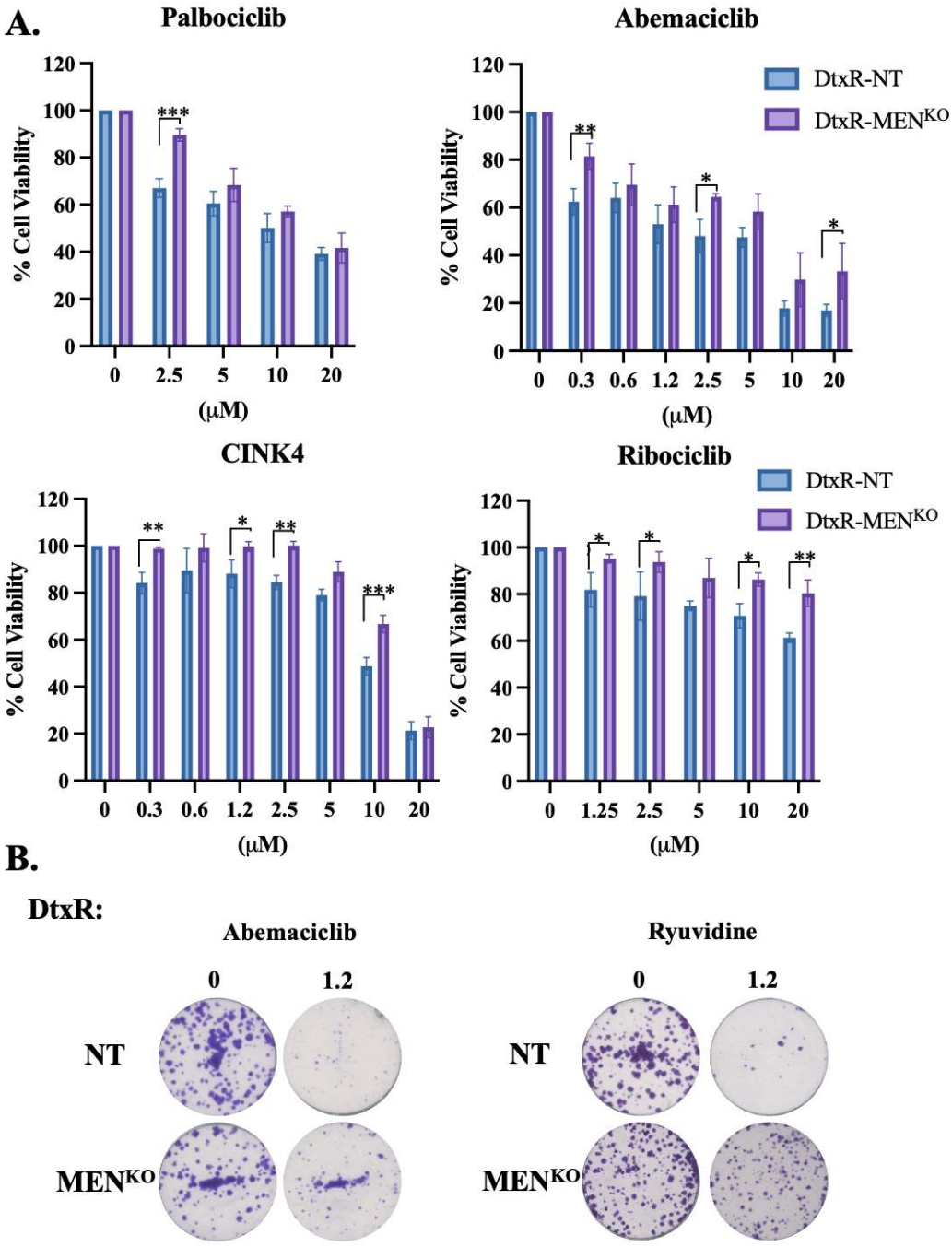

Figure 3. 25: Menin-depleted cells show lower sensitivity for CDK4/6 inhibitors

A. Graphs showing SRB cell viability results of control and Menin-depleted cells, following the treatment with Palbociclib, Abemaciclib, CINK4, and Ribociclib. **B.** Colony formation results of control and Menin-depleted cells following the treatment with Abemaciclib and Ryuvidine. Graphs represent the average of ± standard deviation of three biological repeats. (One-way ANOVA, *p≤0.05, **p≤ 0.01, *** p≤ 0.001).

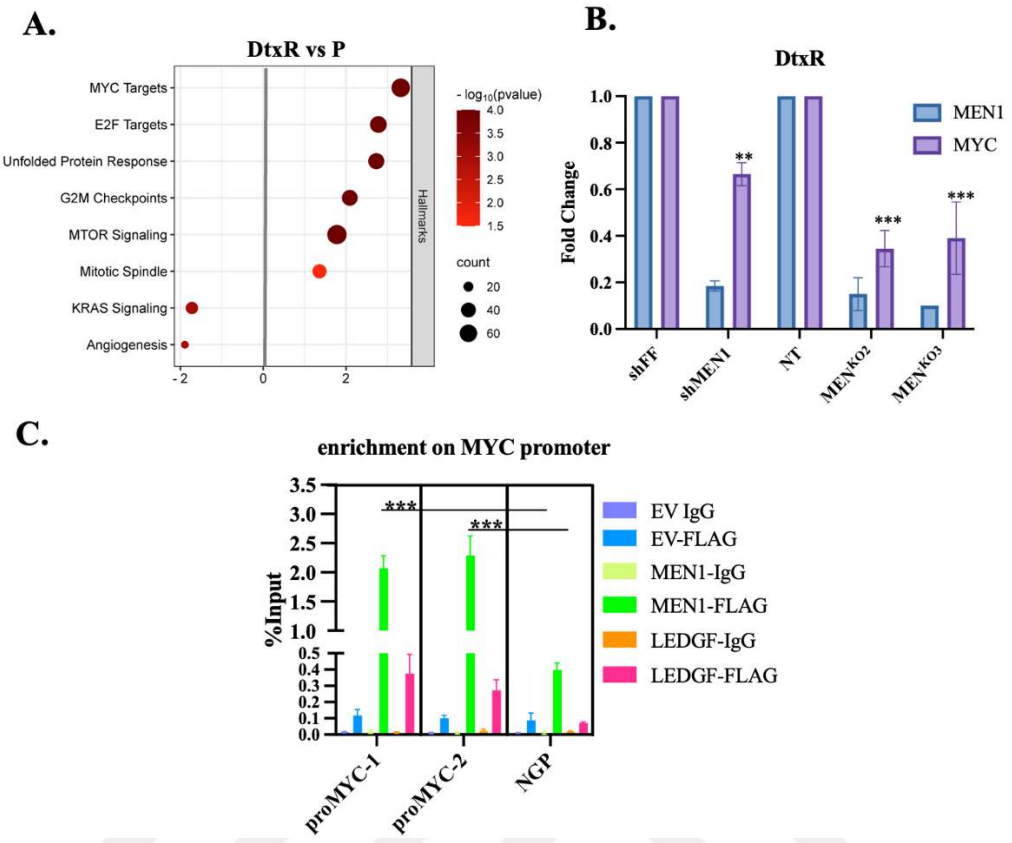

Figure 3. 26: Menin silencing significantly reduces MYC expression and Menin is enriched on MYC promoter

A. Bubble plot showing enriched pathways in different gene sets in Hallmarks pathway in DtxR cells. Circle depicting the count of DEG in the relevant gene set, and color depicting, the significance of p-value. The bubble plot was visualized with the SRplot web server (https://www.bioinformatics.com.cn/en). **B.** RT-qPCR showing MYC expression in Menin knockout and shMenin DtxR cells. **C.** ChIP-qPCR results demonstrating Menin enrichment of MYC promoter with two different primers amplifying TSS (-500 bp, +100 bp) region. NGP: Negative primer. Graphs represent the average of ± standard deviation of three biological repeats. (One-way ANOVA, *p≤0.05, **p≤ 0.01, *** p≤ 0.001).

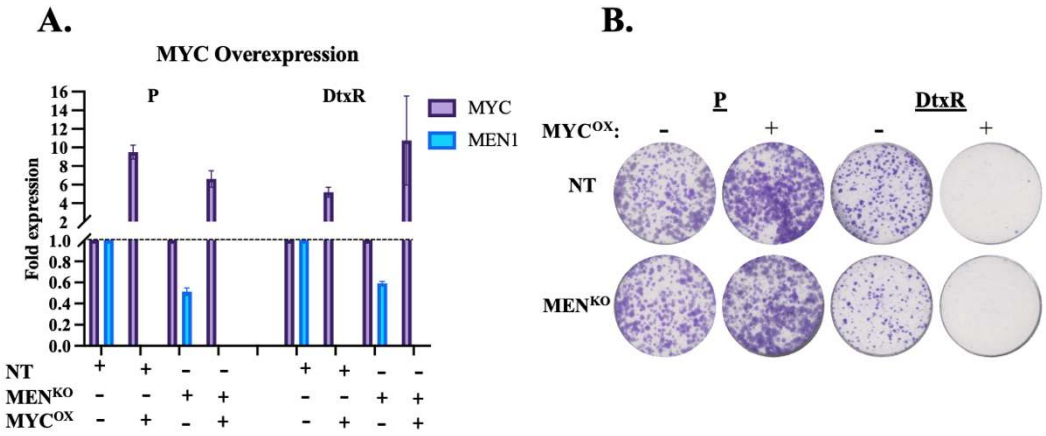

Figure 3. 27: DtxR cells showed induced cell death upon MYC overexpression, regardless of their Menin expression

A. RT-qPCR showing MYC expression in MYC overexpressed Menin knockout and control DtxR cells. **B.** Colony formation results of control and Menin-depleted cells following the treatment with MYC overexpression. Graphs represent the average of ± standard deviation of three biological repeats.

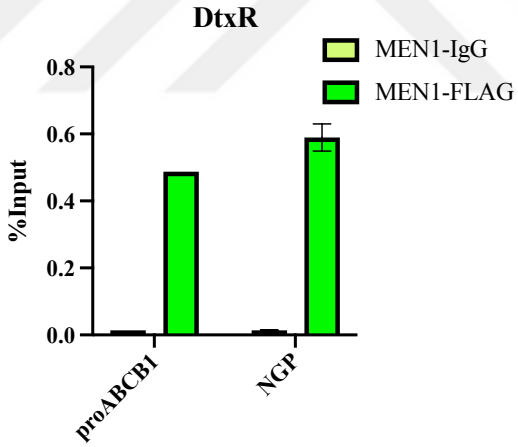

Figure 3. 28: Menin did not exhibit a significant enrichment on ABCB1 promoter

ChIP-qPCR results demonstrating Menin enrichment of ABCB1 promoter with specific primers amplifying upstream promoter region and compared to negative primer. NGP: Negative primer.

Table 3. 2: Predicted genes regulated by Menin

LogFC (DtxR-MEN^{KO})	Gene Name	Menin DNA Binding	LogFC (DtxR-MEN^{KO})	Gene Name	Menin DNA Binding
-8.40	COL5A2	●●●●	2.05	MARCKS	●
-8.35	TSPAN18	●	2.05	COL4A1	●●
-8.19	COBL	●	2.09	TP53I3	●●●●
-7.70	DAPK1	●●●	2.12	SOCS1	●●●●
-7.21	COL5A1	●	2.15	SCN9A	●
-7.08	ST6GALNAC3	●	2.26	ABCG2	●●
-6.90	CDK20	●	2.42	GOLT1A	●●
-6.97	SLC6A11	●	2.45	ACSM3	●●●
-5.64	PRDM16	●	2.57	GAP43	●
-5.60	PRDM11	●●●	2.71	DPP4	●●
-5.18	NDRG1	●●	2.80	APC	●
-4.49	MGMT	●	2.81	BAHCC1	●●
-4.28	QPRT	●	2.82	MT1F	●
-4.25	SOX4	●●	2.90	ARID5B	●
-4.19	PDZD2	●	3.02	HES1	●
-4.08	NR6A1	●●	3.04	SNAI	●
-3.54	MYO1D	●	3.10	ADAM12	●
-3.35	FMN2	●	3.26	ABCA8	●
-2.96	CHRM4	●	3.32	KIT	●
-2.90	MAPK4	●	3.45	HCP5	●
-2.61	TXNL1	●	3.50	CASP4	●
-2.55	ARHGAP44	●	5.36	TXNIP	●●●
-2.45	NR4A1	●●	7.75	RSPO3	●
-2.41	GREB1L	●			
-2.34	SLFN11	●●●			
-2.33	GAS7	●●●			
-2.35	MOB3B	●●			
-2.01	COL25A1	●			

Menin ChIP-seq was performed on:

- Erythroblasts
- K-562
- MV-4-11
- AML
- MCF-7
- OCI-AML3
- HCT-116

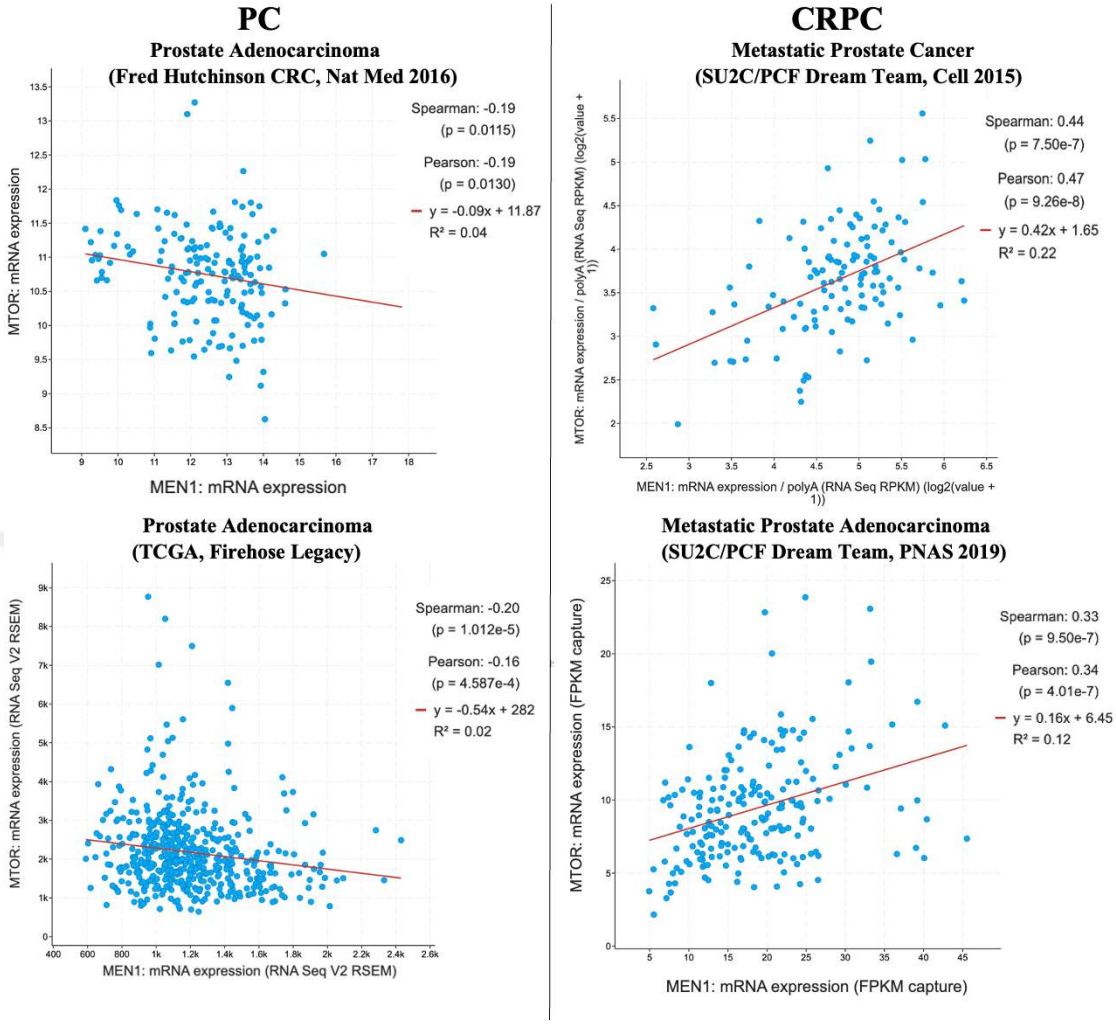

Pearson correlation coefficient values
0.01-0.19 very weak correlation
0.20-0.39 weak correlation
0.40-0.59 moderate correlation
0.60-0.79 strong correlation
0.79-0.99 very strong correlation

Figure 3. 29: Clinical data on PC and CRPC studies showing correlation status with MEN1 and mTOR expression

The left panel shows a very weak and weak correlation between MEN1 and mTOR in prostate adenocarcinoma studies. The right panel shows a moderate correlation between MEN1 and mTOR in metastatic prostate cancer. Prostate Adenocarcinoma (Fred Hutchinson CRC, Nat Med 2016), Prostate Adenocarcinoma (TCGA, Firehose Legacy), Metastatic Prostate Cancer (SU2C/PCF Dream Team, Cell 2015), Metastatic Prostate Cancer (SU2C/PCF Dream Team, PNAS 2019) data was obtained from cbioportal.org.

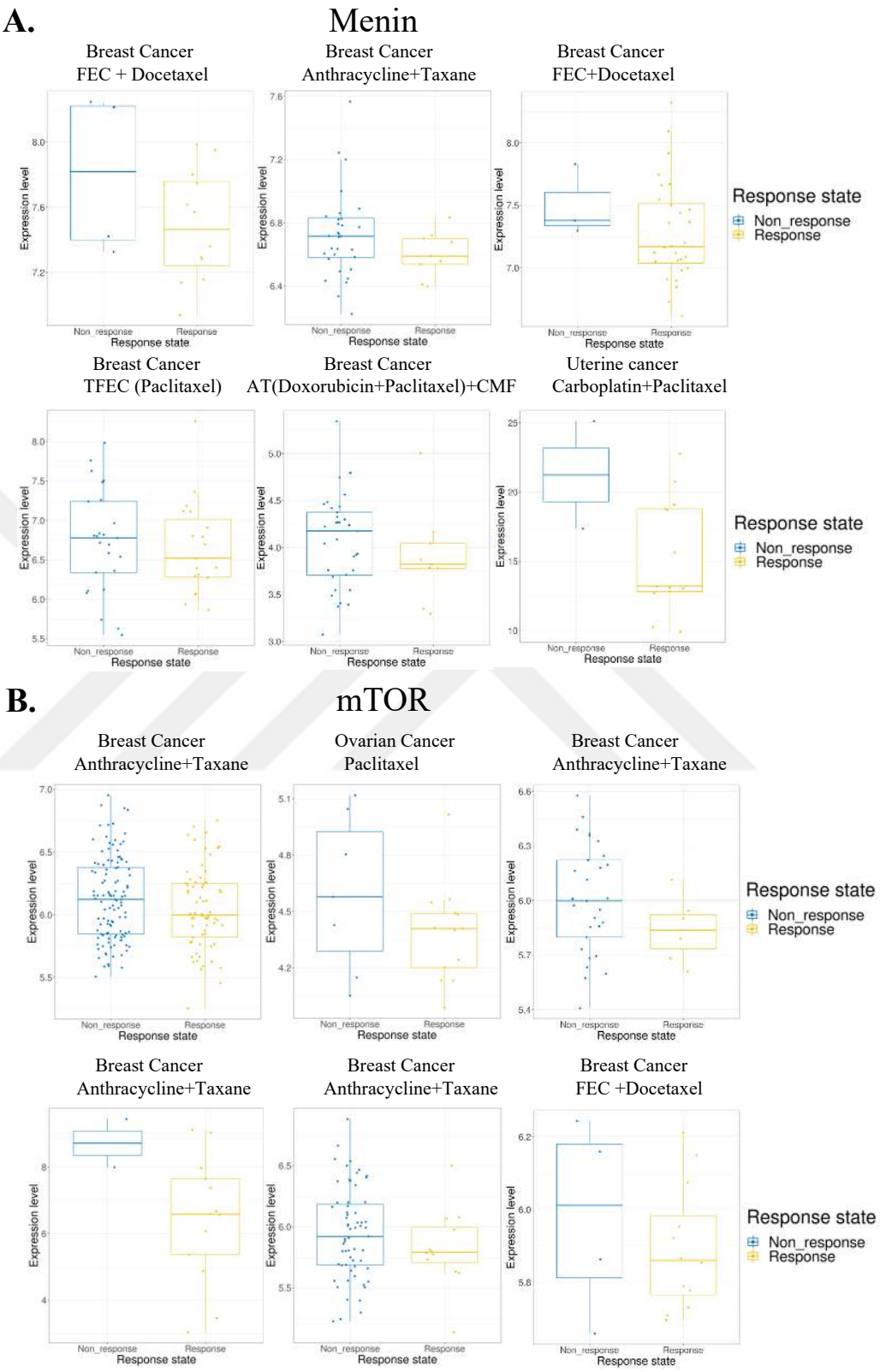

Figure 3. 30: Lower Menin and mTOR expressions appeared to be associated with taxane response in patient-derived clinical transcriptome data.

Graphs showing the response states of cancer patients to different taxane treatments and their relative expressions of Menin and mTOR. In cohorts of cancer patients exhibiting positive response to taxane treatment, relatively lower expression levels of Menin and mTOR are observed compared to the non-responsive patients. Data was obtained from the Cancer Treatment Response Gene Signature Data Base (CTR-DB).

Our findings elucidate several key points regarding the epigenetic regulations that confer Docetaxel (Dtx) resistance in castration-resistant prostate cancer (CRPC). Notably, we discovered that MLL-Menin inhibitors markedly enhance the efficacy of Dtx when used in combination therapies (**Figures 3.3** and **Figure 3.4**). We identified the Menin protein as a critical factor that suppresses Dtx-resistant (DtxR) cell proliferation. Additionally, rescue experiments with Menin mutants highlighted LEDGF as another significant factor, which diminishes colony formation in DtxR cells (**Figures 3.9** and **3.10**). RNA-seq analysis unveiled the molecular pathways activated by the ablation of Menin and LEDGF, with mTOR being notably upregulated during the resistance process and subsequently significantly downregulated upon depletion of Menin and LEDGF (**Figure 3.13**, **Figure 3.14**, and **Figure 3.17**). Parental cells necessitated Menin expression for the development of drug resistance, and mTOR emerged as an essential factor for the survival of DtxR cells (**Figures 3.18** and **Figure 3.19**). Our rescue and ChIP-qPCR experiments confirmed that Menin promotes DtxR growth by modulating mTOR expression (**Figure 3.19**). Indeed, Menin ablation significantly enhanced the therapeutic response to both Dtx and mTOR inhibition via Torin (**Figure 3.20**). Menin-depleted cells exhibited G1 cell cycle arrest and decreased levels of Cyclin D1 and CDK20 (**Figure 3.21**). Intriguingly, reactivation of Menin led to increased expression of Cyclin D1 and CDK20, with Menin found to be enriched on the promoters of these genes (**Figure 3.22**). Furthermore, Menin-ablated cells displayed a slight resistance to CDK4/6 inhibitors, attributable to their phenotype of reduced division rates (**Figures 3.24** and **Figure 3.25**).

Finally, clinical data provided a moderate correlation between Menin and mTOR in advanced CRPC patients, also lower Menin and mTOR levels were associated with better response to taxanes in patients with various tumors (**Figure 3.29** and **Figure 3.30**).

Chapter 4

DISCUSSION

Therapy resistance often manifests through a reduction in treatment efficacy, necessitating a thorough investigation of the underlying causes for each specific cancer type and associated medication. Prostate cancer (PC) serves as a suitable model for drug resistance studies due to its potential to relapse at various stages. Following prostatectomy, most patients initially receive anti-androgens, but the disease can progress to a castration-resistant (CR) stage that is non-responsive. At this point, patients are typically administered Docetaxel therapy; however, approximately half of the patients inevitably develop therapy resistance within the ensuing years [Lohiya et al., 2016]. Post-Docetaxel resistance, CRPC patients are often unsuitable for surgical intervention, prompting research groups to replicate the resistance model in cell culture [Liu et al., 2020]. To generate our Docetaxel resistance model, we employed the dose increment method, involving 3 days of drug treatment followed by 7-10 days of drug-free culturing. This approach closely mimics the actual chemotherapy process and minimizes cellular stress by avoiding constant drug exposure, a method that other groups might impose [Das Thakur et al., 2013; Tanneau et al., 2020]. A common problem in resistance mechanisms is the increased activity of ABCB1 pumps, and targeting these proteins with inhibitors such as verapamil is challenging due to off-target effects and side effects on immune system [Wang et al., 2020]. Additionally, resistance can be triggered by mechanisms other than ABCB1, requiring detailed studies for each type of cancer and drug. Significant progress is being made in understanding the epigenetic processes behind resistance, even reaching phase trials in combination therapies [Morel et al., 2020]. Therefore, we aimed to explore Docetaxel resistance from an epigenetic perspective. We first validated our drug-resistant cells (**Figure 3.2**) and, similar to other studies, observed a significant enrichment in ABCB1 activity (**Figure 3.7**) [Zhu et al., 2013]. The ABCB1 aspect of our resistance model was extensively studied in our earlier publication [Cevatemre et al., 2024], where we identified BRPF complexes as regulators of ABCB1 expression. In that study, we demonstrated the

synergy between BRPF inhibitors and Docetaxel, underscoring the essential role of BRPF in resistant cells. BRPF was enriched on the ABCB1 promoter, and BRPF inhibition halted ABCB1 activity, as evidenced by the Calcein assay.

In this thesis, we also observed increased ABCB1 activity (**Figure 3.7A**). Interestingly, CbzR cells exhibited genomic amplification, whereas DtxR cells did not (**Figure 3.7B**). As previously reported, silencing ABCB1 via siRNA significantly restored the response to taxane, underscoring ABCB1's critical role in our resistance model (**Figure 3.7C-D**). However, our investigation into the interaction between Menin and ABCB1 revealed a mechanism distinct from BRPF. Menin depletion using CRISPR did not result in a significant change in ABCB1 mRNA levels. Although MLL-Menin inhibitors displayed strong synergy with Docetaxel and inhibited ABCB1 activity upon MI-2 treatment, as evidenced by the Calcein assay (**Figures 3.4** and **Figure 3.7F**), Menin knockout alone did not produce similar synergy (showing only a slight decrease at 250 nM) (**Figure 3.20A**) with Docetaxel as observed with BRPF inhibition. Additionally, Menin was not enriched on the ABCB1 promoter in DtxR cells (**Figure 3.28**). These cumulative findings suggest that Menin's role in resistance operates through a pathway other than ABCB1.

Our epigenetic screen identified five groups of epigenetic modifiers capable of reversing Docetaxel (Dtx) resistance. As reported by our study [Cevatemre et al., 2024], which includes MLL-Menin inhibitors, BRPF inhibitors, CBP/P300 inhibitors, PRMT5 inhibitors, and SIRT activators, all of which exhibited significant synergistic effects. This thesis focuses deeply on the analysis of MLL-Menin inhibitors. We initially utilized MI-2 and subsequently expanded our panel to include MI-3, MI-136, and MI-463. Chemically, MI-2 and MI-3 are very similar, while MI-136 and MI-463 are closely related in molecular shape. Additionally, we identified the MLL-WDR5 inhibitor WDR5-0103, which demonstrated significant synergy (**Figure 3.4**). Consistent with our findings, Wu et al., 2022, published a study showing that WDR5-0103 effectively halts the drug-refractory phenotype of ABCB1 across multiple tumor cell lines, including colon, ovary, and lung, without altering ABCB1 expression.

It is important to note that these inhibitors exhibit minimal effects when used alone but significantly enhance sensitivity when combined with Docetaxel (Dtx) (**Figures 3.4** and **Figure 3.5**). Our findings indicate that Dtx-resistant (DtxR) cells, which typically do not respond to Dtx due to the drug-refractory phenotype, show a notable increase in G2/M arrest and apoptosis when MLL-Menin inhibitors are administered concurrently with Dtx, achieving the expected outcomes of a successful taxol treatment (**Figure 3.6**). While several studies have thoroughly investigated how MLL-Menin inhibitors improve therapy response in leukemias [Thomas, 2024], to the best of our knowledge, we are the first to report the synergy of MLL-Menin inhibitors with Dtx in solid tumors.

VCap, LNCaP, 22Rv1, Du145, and PC-3 cells are commonly used cell lines in prostate cancer studies, and we summarized their AR expressions in **Table 4.1**. While Du145, PC-3, 22Rv1, VCap cells (AR-negative / AR-negative / AR-positive / AR-mutant, respectively) are considered as CRPC, LNCaP cells (AR-positive) are considered as PC since they are sensitive to Enzalutamide treatment. Interestingly, Malik et al., 2015, evaluated the effects of MLL and Menin inhibitors on AR-positive cell lines such as LNCaP, VCaP, and 22Rv1, and reported a significant reduction in tumor growth. They have also referred to a diminished growth of Du145 cells on shMEN1 (AR negative), however did not follow a profound investigation. Furthermore, Kim et al., 2022, revealed reduced proliferation and increased apoptosis of Du145, PC-3, LNCaP, and 22Rv1 cells with siMEN1 and MLL-Menin inhibitor MI-503. However, these data were not compatible with our results, as Menin inhibitors alone did not induce CRPC death, and Menin knockout did not affect the colony growth in our parental Du145 cells (**Figure 3.5** and **Figure 3.9**).

Table 4. 1: Commonly used cell lines in prostate cancer studies

Cell Line	AR-Status	Location	Derived from
LNCaP	AR (+)	Lymph node metastasis	lymph node of a 50-year-old, White, with diagnosis of metastatic prostate carcinoma.
VCaP	AR (+) / AR-v7 (+)	Prostate epithelial	isolated from a White, 59-year-old, male patient with prostate cancer.
22Rv1	AR (+)	Prostate epithelial	human prostate carcinoma epithelial cell line derived from a xenograft that was serially propagated in mice
PC-3	AR (-)	Bone metastasis	initiated from a bone metastasis of a grade IV prostatic adenocarcinoma from a 62-year-old, White, male.
Du145	AR (-)	Brain metastasis	isolated from the brain of a 69-year-old, White, male with prostate cancer.

As previously mentioned, we evaluated the expression patterns of MLL inhibitors (targeting Menin or WDR5) in prostate adenocarcinoma (PRAD) using the Wanderer tool. Our analysis revealed that MLL expression was decreased in PRAD patient samples, whereas Menin and WDR5 expressions were elevated (**Figure 3.8B**). Numerous studies have documented the aberrant expression of MLL, Menin, and WDR5 across various tumor types, which we have summarized in **Table 4.2**.

Table 4. 2: Reported overexpressed MLL partners in different cancers

OX'ed Gene	Related Cancer	Reference
MLL	Glioblastoma	Gallo et al., 2013
MLL-m	Bladder Cancer	Wu et al., 2016
MLL	Acute Myeloid Leukemia	Pajuelo Gamez, et al., 2007
Menin	Hepatocellular Carcinoma	Xu et al., 2013
Menin	Glioblastoma	Wang et al., 2020
Menin	Breast Cancer	Nguyen et al., 2021
Menin	Prostate Cancer	Bourefis et al., 2022
WDR5	Breast Cancer	Dai et al., 2015
WDR5	Bladder Cancer	Chen et al., 2015
WDR5	Leukemia	Ge et al., 2016
WDR5	Colorectal Cancer	Tan et al., 2017
WDR5	Colon Cancer	Neilsen et al., 2018
WDR5	Head-Neck Sq. Cell Carci.	Wu et al., 2018
WDR5	Hepatocellular Carcinoma	Cui et al., 2018
WDR5	Gastric Cancer	Sun et al., 2018
WDR5	Oesophageal Sq.Cell Carci.	Huang et al., 2020
WDR5	Prostate Cancer	Zhou et al., 2021
WDR5	Non-small Lung Cancer	Li et al., 2022

When we silenced these three factors, we encountered the essentiality of MLL and WDR5 for our CRPC model (**Figure 3.8C-D**). On the other hand, Menin silencing only affected Dtx-resistant CRPC cells. We then focused on Menin mRNA levels, among advanced PRAD patients. Indeed, Menin expression was significantly upregulated in patients with Gleason scores 8 and 9 (compared to 6) (**Figure 3.11**). On the other hand, Ortiz-Hernandez et al., 2021, reported Menin overexpression in DtxR-resistant CRPC cells. Although we showed high essentiality of Menin in our Dtx-resistant model with CRISPR knockout, our RNA-seq results did not show a significant increase in Menin expression between drug-naive and resistant cells.

We isolated two single clones of Menin-null parental cells, and also 3 single clones of Menin-depleted DtxR cells. Compared to their control (non-targeting guide), Menin protein levels were extinct in the knockout conditions. While Menin depletion did not trigger a significant reduction in colony-forming ability in parental cells, it significantly halted the colony-formation capacity in the two Menin KO resistant clones (**Figure 9**). We have selected the third clone of Menin-null resistant population, for the convenience of the further experimental course. For our rescue experiments, we have selected several Menin mutants that previously reported to break interaction with binding partners such as MLL, and LEDGF. P12L mutant of Menin was reported to abrogate the LEDGF interaction site [Agarwal et al., 1999, Hughes et al., 2004], which substantially failed to rescue the phenotype (**Figure 3.10 C-D**). Based on these data, we evaluated the potential contributions of LEDGF via CRISPR-cas9. Similar to Menin, LEDGF knockout specifically affected the colony growth of DtxR-resistant cells (**Figure 3.10 E-G**). Supportively, Ortiz-Hernandez et al., 2021, revealed siRNA siRNA-mediated silencing of LEDGF and Menin, diminished the 3D tumorsphere formation in the DtxR CRPC model. Later on, the group revealed that LEDGF was contributing to drug-resistant phenotype via interacting with glucocorticoid (dexamethasone, cortisol, or prednisone) receptors (Sanchez-Hernandez et al., 2023). The group also provided some data revealing the synergy between GR modulators and Dtx. However, our LEDGF-depleted DtxR model did not provide a significant enrichment on GR regulation.

We have shown increased LEDGF mRNA levels in prostate cancer patients with the Gleason score of 10 (compared to 6) (**Figure 3.11**). Interestingly, without a resistance mechanism, Mediavilla-Varela et, 2009, demonstrated that transfecting drug-naive PC-3 cells with LEDGF overexpression vector stalled cell death upon Dtx treatment. LEDGF overexpression has been shown in other cancer types as well. Yin et al., 2017 identified LEDGF as a poor prognostic marker in cervical tumors. They indicated a reversed correlation between LEDGF expression and survival rate. On the other hand, Basu et al., 2012, tested LEDGF expression in different tumor types and their normal conjugates in the surrounding tissue. They revealed that prostate, thyroid, liver, uterus, breast, and colon tumor samples showed higher expression of LEDGF mRNA.

Rescue experiments with Menin mutants also showed a potential role of MLL-Menin interaction on drug-resistant phenotype. Menin mutants which were unable to interact with MLL, also could not restore the observed phenotype significantly (**Figure 3.10 C-D**). This data pointed out that Menin might be among the mechanisms that regulate the development of resistance at the transcriptional level through its interaction with MLL. Transcriptional regulation via targeting MLL and Menin interaction has been suggested as a clinical therapy method in acute myeloid leukemia. In cases with KMT2A translocations or NPM1 mutation, small molecule inhibition of MLL-Menin reduces HOXA9 and MEIS1 expression, which drives leukemogenesis [Grembecka et al., 2012, Shi et al., 2012, Fiskus et al., 2022, Thomas, 2024]. Furthermore, HDAC inhibition with Chidamide improved the therapy response of MLL-Menin inhibitors via disturbing DNA repair in AML [Ye et al., 2019]. On the other hand, MLL-Menin inhibition with MI-463 induced cell death in TNBC through targeting PI3K signaling [Zhang et al., 2020]. Another study focusing on breast cancer revealed that MLL-Menin interaction was essential for oxidative phosphorylation and MI-503 downregulated several genes in glycolysis, and Menin silencing caused attenuated ATP production [Chou et al., 2020]. Additionally, MLL-Menin silencing resulted in transcriptional regulation of the Rasgrf1 gene and stalled oncogenic activity in lung cancer [Zhu et al., 2022]. MLL-Menin axis also regulated Wnt-dependent tumorigenesis of head and neck cancer, which MI-503 diminished tumor propagating cells in vivo [Zhu et al., 2019]. Similarly, in endometrial tumors, organoid growth was stalled with MI-136, through reduced hypoxia and HIF-α pathways. Additionally, Menin was enriched on the promoter of several genes such as NOS2, NOS3, and PFKFB3 which are the targets of HIF-α regulation [Chen et al., 2021]. Finally, as we mentioned earlier, MLL-Menin silencing reduces the tumorigenic potential of AR-positive prostate cancer through AR-downstream genes [Malik et al., 2015].

In addition to the N-terminus complexes of MLL (Menin/LEDGF), we also investigated the effects of C-terminus complexes of MLL, including; ASH2L, CBP, P300, Rbbp5, and SET proteins (**Figure 3.12**). Interestingly, as a partner protein of trithorax group genes (TrxGs), ASH2L has been focused on through its interaction with MLL and, therefore reported to have a binding affinity with AR [Grasso et al., 2012, Malik et al.,

2015]. ASH2L has been reported to have an oncogenic activity through MYC and Ras [Lüscher-Firzlaff, et al., 2008, Ullius et al., 2014]. In addition, in breast cancer, ASH2L was reported to enhance ERα activity through GATA3 [Qi et al., 2014]. Furthermore, ASH2L and ERα coactivity were also reported in endometrial tumors [Zeng et al., 2019]. ASH2L activity was also demonstrated through the HOXC8 axis in re-arranged leukemias [Wu et al., 2020]. Our group recently evaluated ASH2L as an essential factor for glioblastoma growth [Ozyerli-Goknar, et al., 2023]. ASH2L undoubtedly participates in many oncogenic activities along with its function of histone methylation [Clermont et al., 2013]. Our results highlighted that DtxR cells were slightly more sensitive to ASH2L inhibition (**Figure 3.12**), so apart from AR regulation, its effects on CRPC can be further investigated.

Besides ASH2L, the CBP/P300 axis is commonly studied in prostate cancer. Initially, this histone acetyltransferase complex was targeted via siRNA, and caspase-dependent cell death mechanisms were upregulated in AR-positive and negative prostate cancer cell lines. The same study revealed that p300 suppression reduced invasion potential and p65 levels in PC-3 and LNCaP cells [Santer et al., 2011]. Similar to this, interaction with CBP/P300 and AR downstream genes was established in Ianculescu et al., 2012 and Jin et al., 2017. CBP/P300 inhibitors also induce synergy with PD-L1 antibody treatment in PC [Liu et al., 2021]. CBP/p300 activity was even considered as a biomarker in circulating tumor cells in patients with PC [Filon et al., 2023]. We have also indicated significant reversion of Dtx resistance via CBP/p300 inhibition in AR-negative Dtx-resistant CRPC cells in our latest study [Cevatemre et al., 2024]. Additionally, our DtxR cells showed higher essentiality of p300 silencing (**Figure 3.12**).

Rbbp5 complexes were identified in a limited number of PC studies. Rbbp5-dependent expressional regulation of snail protein was identified to trigger EMT pathways in PC [Li et al., 2016]. Also, lncRNA-dependent regulation of Rbbp5 was reported to promote an oncogenic effect on PC [Xie et al., 2021]. However, elaborative defined roles of Rbbp5 were identified in cases of other tumor types such as Wnt pathways in melanoma cells [Yang et al., 2023]. In our DtxR model, Rbbp5 silencing did not yield a significant

reduction in colony-forming capacity (**Figure 3.12**). Finally, SET1A has been studied through its major role in H3K4 methylation activity. SET1A was recently found to be the regulator of FOXM1, a specific transcription factor, essential for cell proliferation in CRPC cells [Yang et al., 2020]. Clinical significance of SET1A was reported in NSLC cancers, indeed SET1A activity was essential for S phase transition and DNA replication-related gene maintenance [Kang et al., 2021]. Induced SET1A activity was reported to have a poorer prognosis along with RUVBL1 in PDAC [Ishii et al., 2023]. SET1A also seems to be the contributor to metastasis in breast and gastric cancer [Salz et al., 2015, Wu et al., 2021]. Additionally, in tamoxifen-resistant breast cancers, SET1A overexpression conferred ERα mediated insensitivity for the therapy response [Kim et al., 2020]. Each day, literature data is accumulating that supports targeting drug resistance through HMT inhibitors [South, 2012, Wu et al., 2020, Yang et al., 2021]. Interestingly, in our model, SET1A silencing through CRISPR-cas9, majorly affected DtxR cells, indicating a direct or indirect regulation of SET1A in Dtx resistant mechanism (**Figure 3.12**).

In the next step, we performed RNA-seq analysis for further identification of transcriptomic differences in our varied cell models. Our initial comparison was between P and DtxR cells (**Figure 3.13**). Mitochondrial gene regulation and ribosomal biogenesis were significantly enriched in BP and CC pathways. During resistance progress, the ECM constituent was negatively enriched, we identified this feature with an adhesion experiment (paper under revision). According to this data, as cells gained drug refractory phenotype, they also showed low adhering characteristics. On the other hand, growth factor binding gene sets were negatively enriched in the DtxR model, which was compatible considering that DtxR cells grow slowly. Dysregulations in microtubule assembly and tubulin synthesis have been reported in taxol-resistant models [Barlow et al., 2002, Galletti et al., 2020]. Mutations in alpha or beta-tubulin are observed in resistance against microtubule-targeting drugs such as colcemid [Hari et al., 2003]. In our model, we have not tested whether our resistant cells held a microtubule mutation, however, another negative enrichment was observed in kinesin activity (a motor protein moves along the MTFs). We should also note that the MI-2 and Dtx combination resulted in G2/M arrest (via inhibition of depolymerized

microtubules), a common mechanism observed as a result of the successful binding of Dtx and beta-tubulin. In this case, when appropriate conditions are provided (following drug uptake), Dtx does not appear to have any obstacle to binding to beta-tubulins, suggesting that our DtxR-resistant model has a lower chance of retaining tubulin mutations. Additionally, MYC target genes were significantly upregulated in the DtxR model, indeed MYC and drug resistance interaction have been studied in detail. Enhanced MYC was reported to trigger therapy resistance against mTOR inhibitors in breast cancer [Bhin et al., 2023]. MYC silencing, reverted therapy resistance in AML and multiple myeloma [Pan et al., 2014, Li et al., 2014, Faruq et al., 2022]. MYC was reported to promote AR-independent tumor progress in PC [Gao et al., 2013], MYC overexpression also conferred drug resistance in neuroendocrine PC by miRNA regulation [Yin et al., 2019], and resistance to BET inhibitors in CPRC [Coleman et al., 2019]. MYC and Menin regulation was previously published in the concept of oncogenic activation, Menin was enriched on MYC promoter and enhances the expression of downtargets of MYC [Wu et al., 2017, Luo et al., 2021]. In this work, we also provided MYC and Menin interaction; MYC-related pathways were activated in DtxR cells, and upon Menin knockout MYC expression was halted, and correlatively with the literature, Menin was enriched on MYC promoter in DtxR cells (**Figure 3.26**). However, rescue experiments with MYC overexpression in DtxR cells failed due to an upregulated apoptosis mechanism (**Figure 3.27**). High cell death phenotype was reported upon MYC overexpressing normal and malignant cells [Neiman et al., 1991, Hoffman and Lieberman, 2008]. There could be several theories explaining this condition, initially, responding to ectopic MYC expression could be influenced by the amount of growth factor presence, however, in restricted growth stimuli, elevated MYC, may initiate controlled cell death [Gibson et al., 1995]. Therefore cells may undergo different pathways upon MYC overexpression, depending on their response capacity to growth factors. In fact, our GSEA analysis showed that resistant cells were negatively enriched in response to growth factor binding (**Figure 3.13C**). An additional option might be the background levels of MYC, in P and DtxR cells. The DtxR model already showed increased expression of MYC targets, and additional overexpression might trigger the activation of other subsets of target genes, ultimately resulting in cellular death. Overall, overexpression of MYC led to cell death in our resistant cells, even

though we were able to successfully restore MYC levels. Although, we were unable to identify Menin's role in resistance through MYC, undoubtedly, MYC was one of the important factors contributing to resistance.

mTOR was significantly upregulated in the DtxR model, which drew our attention, due to its notable reversion on Menin knockout (**Figure 3.14**). mTOR and drug resistance were elaborated on in detail by Jiang and Liu, 2008. 30 to 80 percent of different human malignancies have hyperactivated PI3K/Akt/mTOR signaling. Therefore, clinical trials are being conducted to test targeted therapeutics using either dual PI3K/mTOR or single mTOR inhibition [Murugan, 2019]. mTOR activation was presented to confer drug resistance in breast and ovarian cancer [Dong et al., 2021, Foster et al., 2010]. Similar to our study, activated mTOR was reported in oxaliplatin-treated cell lines and patient-derived xenografts in colon cancer, and synergistic effects of oxaliplatin with an mTOR inhibitor were published in Lu et al., 2017. Besides oxaliplatin, tankyrase inhibitors also demonstrated significant synergy with mTOR inhibitors in colon cancer [Mashima et al., 2017]. Additionally, abnormal activation of mTOR also caused sorafenib resistance in AML [Lindbland et al., 2016].

There have been several clues for us to link Menin and mTOR association; firstly, mTOR was upregulated during resistance progress (**Figure 3.13, Figure 3.19A)** and mTOR gene sets were negatively enriched on Menin knockout DtxR model (**Figure 3.14**, **Figure 3.19B**). Additionally, rescuing Menin expression also restored mTOR mRNA levels (**Figure 3.19C**). Secondly, parental cells required Menin expression to gain drug refractory phenotype (**Figure 3.18**), and similar to Menin, mTOR expression was indefeasible for DtxR maintenance (**Figure 3.19E**). Furthermore, additional depletion of Menin, improved Dtx response and mTOR inhibition (**Figure 3.20D**). Finally, an online database revealing ChIP-seq data provided Menin enrichment on mTOR promoter in different leukemia cell lines (ChIP-atlas ID: SRX11712604, SRX14030471, SRX4046307, SRX11712604, SRX14030482, SRX11712606). Cumulatively, these data prompted us to elaborate on Menin’s presence on mTOR promoter. As expected, Menin pulldown in DtxR cells, showed positive enrichment on mTOR promoter region (**Figure 3.19H**).

Other intriguing gene set analyses were E2F targeting and G2M Checkpoints; interestingly, these factors were positively enriched on the DtxR model and reversed upon Menin knockout (**Figure 3.13, Figure 3.14**). Elevation of E2F-regulated genes was previously reported by Alla et al., 2012 and Rosenfeldt et al., 2014, through their contribution to ABC pump activation. E2F overexpression was also involved in drug-resistant phenotype in gastric cancer, and silencing E2F improved therapy response [Yan et al., 2014, Yan et al., 2014]. On the other hand, the depletion of cell cycle-regulating genes was coherent with our wet lab analysis (**Figure 3.21**). Our Menin knockout cells showed elongated periods of doubling time, and the majority of cells were accumulated in the G1 cycle, also E2F targets were negatively enriched. This slowdown in the cell division rate could be a following effect of reduced mTOR-driven growth signals. When we checked cyclin levels upon Menin knockout (without a synchronization), we observed a consistent reduction of Cyclin D1 and an increase of Cyclin E1 (**Figure 3.21D-E**). Cyclin D1 and E1 dynamism is important in switching to the G1-S phase (**Figure 3.21E**). In the late G1, Cyclin D1 levels drop, while E1 levels rise and peak in the S phase [Hume et al., 2020], these results validate the slow-growing phenotype from the competition assay and also cell cycle analysis (**Figure 3.21**). A similar study focused on Cyclin D1 degradation and G1 cell cycle arrest in ovarian cancers within increased conditions of Cyclin E1 [Masamha and Benbrook, 2009]. Cyclin D1 activates Rb phosphorylation by binding to Cdk4/6, this phosphorylation induces the release of E2F and triggers the transcription of several genes necessary for DNA replication and the initiation of the G1 to S phase switch [Seville et al., 2005]. Cyclin D1 amplification or overexpression is observed in several tumors, and Cyclin D1 reduction via RNA-based silencing reverses tumorigenic phenotype *in vivo* [Tashiro et al., 2007, Deharvengt et al., 2010]. Indeed, overexpression of Cyclin D1 shortens G1 phase duration in non-cancer cells, therefore cancer cells may favor the overactivity of Cyclin D1 to maintain rapid cell division phenotype [Won et al., 1992, Jiang et al., 1993]. Additionally, Averous et al., 2008, reported that mTOR silencing through Rapamycin caused a reduction in Cyclin D1 levels in MCF-7 cells. Compatible with these findings our DtxR Menin knockout cells showed reduced mTOR levels and as a consequence, reduced Cylin D1 levels with extended cell cycle durations. Furthermore, regaining Menin expression increased Cyclin D1 protein levels **Figure 3.22A**. Another

possible mechanism could be a direct regulation of Cylin D1 by Menin since Menin and cell cycle regulation has been studied earlier. Indeed, we have provided supporting data showing the significant enrichment of Menin on Cyclin D1 promoter (**Figure 3.22D**).

Menin has been reported to affect cell cycle regulation through Cyclin-dependent kinase inhibitors via histone methylation in normal pancreatic cells; in the study, Menin suppressed the growth of beta cells through p27 and p18 expression [Karnik et al., 2005]. In another study, performed with MEFs, Menin was stalling the G2/M transition through Cyclin B2 reduction [Wu et al., 2010]. These studies contributed to the emergence of Menin's tumor suppressor features. However, as we mentioned earlier, in multiple tumor cells, Menin has caused oncogenic effects in several aspects [Yokoyama et al., 2005, Grembecka et al., 2012, Dreijerink et al., 2017, Luo et al., 2021]. Here, we provide supporting data demonstrating a possible direct regulation of Menin in cell cycle control via Cyclin D1, in Dtx-resistant CRPC. Interestingly, in addition to Cyclin D1, Menin was also enriched around the promoter regions of an upper kinase CDK20 (also known as CCRK or CAKkinasep42), involved in cell cycle regulation (**Figure 3.22C**). CDK20 expression was significantly downregulated upon Menin knockout and recovered upon Menin rescue (**Figure 3.22B**). CDK20 is a cyclin activating kinase (CAK), through its activating role on CDK2, to initiate G1-S transition, it also regulates G0-G1 activity in collaboration with Cyclin D1 [Liu and Galaktionov, 2004, Ng et al., 2007, Tian et al., 2012, Lai et al., 2020]. Cumulatively, Cyclin D1 and CDK20 reduction helped the explanation of the stalled phenotype of G1-S transition in Menin-null DtxR cells. We have also identified Menin enrichment on these promoters via ChIP-qPCR experiments, indicating Menin's direct involvement in the process. Additionally, Menin knockout cells showed less sensitivity to CDK4/6 inhibitors, which are designed to interrupt, actively dividing cells

On the other hand, LEDGF depletion is essential on DtxR cells, furthermore reduced mTOR and Cyclin D1 gene set enrichments were observed in the RNA-seq analysis (**Figure 3.17**). Cyclin D1 protein levels were also significantly downregulated in LEDGF knockout cells (**Figure 3.23**). Similar to Menin, LEDGF has a DNA binding motif, from the N-terminal PWWP (which is known to mediate DNA binding),

however, we did not observe a significant LEDGF enrichment on any of the target gene promoter regions in our pulldown experiments. Interestingly, Menin mutants which were unable to bind LEDGF, could not rescue the phenotype. This data suggesting that LEDGF contributes to the essentiality in DtxR cells, without showing direct binding to DNA. According to our results, the enrichment of Menin in the TSS region indicates its importance in the regulation of target genes. Designing an experimental setup with an overexpressed MENP12L mutant (causing loss of interaction between Menin and LEDGF) and performing ChIP-qPCR may elucidate the question of whether LEDGF and Menin interaction is required to activate the role of Menin in the regulation of transcription. Overall, our data provided a detailed mechanism on how Menin and LEDGF complexes confer Dtx resistance on CRPC cell lines.

Chapter 5

CONCLUSION

In this work, we focused on the epigenetic aspects of Dtx resistance in CRPC. We first generated our Dtx-resistant cells via the dose increment method and validated our DtxR model. Through an epigenetic drug screen, we discovered that MLL-Menin inhibitors can effectively reverse Dtx resistance. We examined the targets of MLL inhibitors one by one and found out that the DtxR cells were super sensitive to Menin depletion. As we tested different Menin mutations, we identified LEDGF as another factor that significantly reduces cell growth in the DtxR model. Our RNA-seq analysis uncovered molecular pathways participating in Menin and LEDGF ablation. According to our GSEA analysis, mTOR gene sets were positively enriched during the acquisition of drug resistance; however, significantly reverted upon Menin and LEDGF-null cells. Regenerating drug resistance failed in Menin-depleted parental cells, suggesting the necessity of Menin for the maintenance of drug resistance.

mTOR emerged as a crucial factor for the survival of DtxR cells. Menin-depleted cells exhibited reduced mTOR expression, and this depletion triggered a synergistic response when combined with Torin (an mTOR inhibitor) and Dtx in our resistant model. Restoring Menin expression reinstated mTOR mRNA levels and eliminated the observed synergy. Additionally, Menin was found to be enriched in the mTOR promoter region (-500 bp to +100 bp).

Menin-depleted cells waned in the competition assay and showed a high percentage of G1 cell cycle state. Two important factors promoting G1-S transition, Cyclin D1 and CDK20 were significantly lowered in Menin-depleted cells, and Menin rescuing reverted the expression patterns of these targets. It’s interesting to note that, Menin also occupied the promoter region (-500 bp, +100 bp) of Cyclin D1 and CDK20. This slow growth rate observed in Menin ablated cells also provided a slight resistance against

CDK4/6 inhibitors. Lastly, we concluded our key points in **Figure 5.1**, we hope that this study will provide mechanistic insights into Menin's role on Dtx resistant CRPC.

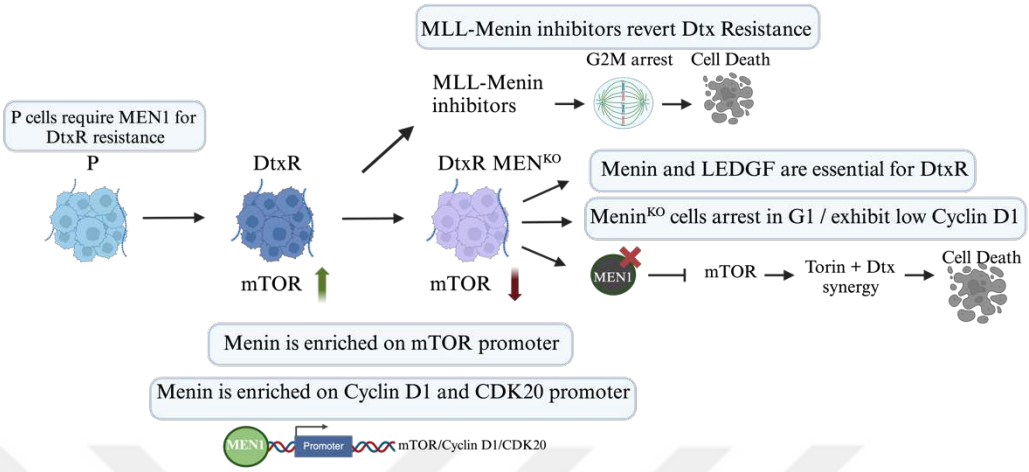

Figure 5. 1: Graphical abstract summarizing the key findings of the study.

BIBLIOGRAPHY

Abal, M., J.M. Andreu, and I. Barasoain, Taxanes: microtubule and centrosome targets, and cell cycle-dependent mechanisms of action. Curr Cancer Drug Targets, 2003. 3(3): p. 193-203.

Abidi, A. (2013). Cabazitaxel: A novel taxane for metastatic castration-resistant prostate cancer-current implications and future prospects. Journal of Pharmacology and Pharmacotherapeutics, 4(4), 230-237.

Adhikari, S., Bhattacharya, A., Adhikary, S., Singh, V., Gadad, S. S., Roy, S., & Das, C. (2022). The paradigm of drug resistance in cancer: an epigenetic perspective. Bioscience Reports, 42(4), BSR20211812.

Agarwal, S. K., Guru, S. C., Heppner, C., Erdos, M. R., Collins, R. M., Park, S. Y., … & Burns, A. L. (1999). Menin interacts with the AP1 transcription factor JunD and represses JunD-activated transcription. Cell, 96(1), 143-152.

Agoulnik, I. U., & Weigel, N. L. (2008). Androgen receptor coactivators and prostate cancer. Hormonal Carcinogenesis V, 245-255.

Alla, V., Kowtharapu, B. S., Engelmann, D., Emmrich, S., Schmitz, U., Steder, M., & Pützer, B. M. (2012). E2F1 confers anticancer drug resistance by targeting ABC transporter family members and Bcl-2 via the p73/DNp73-miR-205 circuitry. *Cell cycle*, *11*(16), 3067-3078.

Amente, S., Bertoni, A., Morano, A., Lania, L., Avvedimento, E. V., & Majello, B. (2010). LSD1-mediated demethylation of histone H3 lysine 4 triggers Myc-induced transcription. Oncogene, 29(25), 3691-3702.

Amin, A. G., Jeong, S. W., Gillick, J. L., Sursal, T., Murali, R., Gandhi, C. D., & Jhanwar-Uniyal, M. (2021). Targeting the mTOR pathways using novel ATP-competitive inhibitors, Torin1, Torin2 and XL388, in the treatment of glioblastoma. International Journal of Oncology, 59(4), 1-9.

Armstrong, A. J., Shen, T., Halabi, S., Kemeny, G., Bitting, R. L., Kartcheske, P., … & George, D. J. (2013). A phase II trial of temsirolimus in men with castration-resistant metastatic prostate cancer. Clinical genitourinary cancer, 11(4), 397-406.

Asatiani, E., Huang, W. X., Wang, A., Rodriguez Ortner, E., Cavalli, L. R., Haddad, B. R., & Gelmann, E. P. (2005). Deletion, methylation, and expression of the NKX3. 1 suppressor gene in primary human prostate cancer. Cancer research, 65(4), 1164-1173.

Averous, J., Fonseca, B. D., & Proud, C. G. (2008). Regulation of cyclin D1 expression by mTORC1 signaling requires eukaryotic initiation factor 4E-binding protein 1. *Oncogene*, *27*(8), 1106-1113.

Ayton, P. M., & Cleary, M. L. (2001). Molecular mechanisms of leukemogenesis mediated by MLL fusion proteins. Oncogene, 20(40), 5695-5707.

Azad, A. A., Volik, S. V., Wyatt, A. W., Haegert, A., Le Bihan, S., Bell, R. H., … & Chi, K. N. (2015). Androgen receptor gene aberrations in circulating cell-free DNA: biomarkers of therapeutic resistance in castration-resistant prostate cancer. Clinical cancer research, 21(10), 2315-2324.

Bacolod, M. D. (2021). The epigenetic factors that drive Cancer drug resistance. Current Cancer Drug Targets, 21(4), 269-273.

Barata, P. C., Cooney, M., Mendiratta, P., Gupta, R., Dreicer, R., & Garcia, J. A. (2019). Phase I/II study evaluating the safety and clinical efficacy of temsirolimus and bevacizumab in patients with chemotherapy refractory metastatic castration-resistant prostate cancer. *Investigational new drugs*, *37*, 331-337.

Barlow, S. B., Gonzalez-Garay, M. L., & Cabral, F. (2002). Paclitaxel-dependent mutants have severely reduced microtubule assembly and reduced tubulin synthesis. *Journal of Cell Science*, *115*(17), 3469-3478.

Basu, A., Rojas, H., Banerjee, H., Cabrera, I. B., Perez, K. Y., De León, M., & Casiano, C. A. (2012). Expression of the stress response oncoprotein LEDGF/p75 in human cancer: a study of 21 tumor types. PloS One, 7(1), e30132.

Baylin, S.B. and P.A. Jones, Epigenetic Determinants of Cancer. Cold Spring Harb Perspect Biol, 2016. 8(9).

Beeram, M., Tan, Q. T., Tekmal, R. R., Russell, D., Middleton, A., & DeGraffenried, L. A. (2007). Akt-induced endocrine therapy resistance is reversed by inhibition of mTOR signaling. Annals of Oncology, 18(8), 1323-1328.

Berns, K., Horlings, H. M., Hennessy, B. T., Madiredjo, M., Hijmans, E. M., Beelen, K., … & Bernards, R. (2007). A functional genetic approach identifies the PI3K pathways as a major determinant of trastuzumab resistance in breast cancer. Cancer cell, 12(4), 395-402.

Berry, W., Dakhil, S., Modiano, M., Gregurich, M., & Asmar, L. (2002). Phase III study of mitoxantrone plus low dose prednisone versus low dose prednisone alone in patients with asymptomatic hormone refractory prostate cancer. The Journal of urology.

Beuvink, I., Boulay, A., Fumagalli, S., Zilbermann, F., Ruetz, S., O'Reilly, T., … & Thomas, G. (2005). The mTOR inhibitor RAD001 sensitizes tumor cells to DNA-damaged induced apoptosis through inhibition of p21 translation. Cell, 120(6), 747-759.

Bhin, J., Yemelyanenko, J., Chao, X., Klarenbeek, S., Opdam, M., Malka, Y., … & Wessels, L. F. (2023). MYC is a clinically significant driver of mTOR inhibitor resistance in breast cancer. *Journal of Experimental Medicine*, *220*(11), e20211743.

Biersack, B., Nitzsche, B., & Höpfner, M. (2022). HDAC inhibitors with potential to pathways drug resistance in castration-resistant prostate cancer. Cancer Drug Resistance, 5(1), 64.

Bitting, R. L., & Armstrong, A. J. (2013). Targeting the PI3K/Akt/mTOR 98athways in castration-resistant prostate cancer. Endocrine-related cancer, 20(3), R83-R99.

Blokken, J., De Rijck, J., Christ, F., & Debyser, Z. (2017). Protein-protein and protein–chromatin interactions of LEDGF/p75 as novel drug targets. Drug Discovery Today: Technologies, 24, 25-31.

Borkin, D., He, S., Miao, H., Kempinska, K., Pollock, J., Chase, J., … & Grembecka, J. (2015). Pharmacologic inhibition of the Menin-MLL interaction blocks progression of MLL leukemia in vivo. Cancer cell, 27(4), 589-602.

Bortul, R., Tazzari, P. L., Cappellini, A., Tabellini, G., Billi, A. M., Bareggi, R., … & Martelli, A. M. (2003). Constitutively active Akt1 protects HL60 leukemia cells from TRAIL-induced apoptosis through a mechanism involving NF-κB activation and cFLIPL up-regulation. Leukemia, 17(2), 379-389.

Bose, R., & Ma, C. X. (2021). Breast cancer, HER2 mutations, and overcoming drug resistance. New England Journal of Medicine, 385(13), 1241-1243.

Bourefis, A., Berredjem, H., Djeffal, O., Le, T. K., Giusiano, S., & Rocchi, P. (2022). HSP27/Menin Expression as New Prognostic Serum Biomarkers of Prostate Cancer Aggressiveness Independent of PSA. *Cancers*, *14*(19), 4773.

Bumbaca, B., & Li, W. (2018). Taxane resistance in castration-resistant prostate cancer: mechanisms and therapeutic strategies. Acta Pharmaceutica Sinica B, 8(4), 518-529.

Bradshaw, D. M., & Arceci, R. J. (1998). Clinical relevance of transmembrane drug efflux as a mechanism of multidrug resistance. Journal of Clinical Oncology, 16(11), 3674-3690.

Brooke, G. N., & Bevan, C. L. (2009). The role of androgen receptor mutations in prostate cancer progression. Current genomics, 10(1), 18-25.

Brown, R., Curry, E., Magnani, L., Wilhelm-Benartzi, C. S., & Borley, J. (2014). Poised epigenetic states and acquired drug resistance in cancer. Nature Reviews Cancer, 14(11), 747-753.

Bryant, R. J., Cross, N. A., Eaton, C. L., Hamdy, F. C., & Cunliffe, V. T. (2007). EZH2 promotes proliferation and invasiveness of prostate cancer cells. The Prostate, 67(5), 547-556.

Cai, C., Chen, S., Ng, P., Bubley, G. J., Nelson, P. S., Mostaghel, E. A., … & Balk, S. P. (2011). Intratumoral de novo steroid synthesis activates androgen receptor in castration-resistant prostate cancer and is upregulated by treatment with CYP17A1 inhibitors. Cancer research, 71(20), 6503-6513.

Canella, A., Van Belle, S., Brouns, T., Nigita, G., Carlon, M. S., Christ, F., & Debyser, Z. (2022). LEDGF/p75-mediated chemoresistance of mixed-lineage leukemia involves cell survival pathways and super enhancer activators. Cancer Gene Therapy, 29(2), 133-140.

Cao, F., Chen, Y., Cierpicki, T., Liu, Y., Basrur, V., Lei, M., & Dou, Y. (2010). An Ash2L/RbBP5 heterodimer stimulates the MLL1 methyltransferase activity through coordinated substrate interactions with the MLL1 SET domain. PloS one, 5(11), e14102.

Carling, T., Correa, P., Hessman, O., Hedberg, J., Skogseid, B., Lindberg, D., … & Åkerström, G. (1998). Parathyroid MEN1 gene mutations in relation to clinical characteristics of nonfamilial primary hyperparathyroidism. *The Journal of Clinical Endocrinology & Metabolism*, *83*(8), 2960-2963.

Castillo, V., Valenzuela, R., Huidobro, C., Contreras, H. R., & Castellon, E. A. (2014). Functional characteristics of cancer stem cells and their role in drug resistance of prostate cancer. International journal of oncology, 45(3), 985-994.

Cevatemre, B., Bulut, I., Dedeoglu, B., Isiklar, A., Syed, H., Bayram, O. Y., … & Acilan, C. (2024). Exploiting epigenetic targets to 100athways taxane resistance in prostate cancer. Cell Death & Disease, 15(2), 132.

Chandrasekar, T., Yang, J. C., Gao, A. C., & Evans, C. P. (2015). Mechanisms of resistance in castration-resistant prostate cancer (CRPC). Translational andrology and urology, 4(3), 365.

Chekmarev, J., Azad, M. G., & Richardson, D. R. (2021). The oncogenic signaling disruptor, NDRG1: molecular and cellular mechanisms of activity. Cells, 10(9), 2382.

Chen, X., Thakkar, H., Tyan, F., Gim, S., Robinson, H., Lee, C., … & Srivastava, R. K. (2001). Constitutively active Akt is an important regulator of TRAIL sensitivity in prostate cancer. Oncogene, 20(42), 6073-6083.

Chen YX, Yan J, Keeshan K, Tubbs AT, Wang H, Silva A, Brown EJ, Hess JL, Pear WS, Hua X. The tumor suppressor menin regulates hematopoiesis and myeloid transformation by influencing Hox gene expression. Proc Natl Acad Sci U S A. 2006;103:1018–1023.

Chen, Y., Li, J., Yu, X., Li, S., Zhang, X., Mo, Z., & Hu, Y. (2013). APC gene hypermethylation and prostate cancer: a systematic review and meta-analysis. European Journal of Human Genetics, 21(9), 929-935.

Chen, X., Ma, Q., Shang, Z., & Niu, Y. (2020). Super-enhancer in prostate cancer: transcriptional disorders and therapeutic targets. NPJ precision oncology, 4(1), 31.

Chen, J., Zhao, L., Peng, H., Dai, S., Quan, Y., Wang, M., … & Na, F. (2021). An organoid-based drug screening identified a menin-MLL inhibitor for endometrial cancer through regulating the HIF 100athways. *Cancer Gene Therapy*, *28*(1), 112-125.

Chen, E. J., Sowalsky, A. G., Gao, S., Cai, C., Voznesensky, O., Schaefer, R., … & Taplin, M. E. (2015). Abiraterone treatment in castration-resistant prostate cancer selects for progesterone responsive mutant androgen receptors. Clinical cancer research, 21(6), 1273-1280.

Chen, X., Xie, W., Gu, P., Cai, Q., Wang, B., Xie, Y., … & Huang, J. (2015). Upregulated WDR5 promotes proliferation, self-renewal and chemoresistance in 101athway cancer via mediating H3K4 trimethylation. *Scientific reports*, *5*(1), 8293.

Cherif, C., Nguyen, D. T., Paris, C., Le, T. K., Sefiane, T., Carbuccia, N., … & Rocchi, P. (2022). Menin inhibition suppresses castration-resistant prostate cancer and enhances chemosensitivity. Oncogene, 41(1), 125-137.

Chiam, K., Ricciardelli, C., & Bianco-Miotto, T. (2014). Epigenetic biomarkers in prostate cancer: Current and future uses. Cancer letters, 342(2), 248-256.

Cho, S., et al., Epigenetic methylation and expression of caspase 8 and survivin in hepatocellular carcinoma. Pathol Int, 2010. 60(3): p. 203-11.

Chou, C. W., Tan, X., Hung, C. N., Lieberman, B., Chen, M., Kusi, M., … & Huang, T. H. M. (2020). Menin and menin-associated proteins coregulate cancer energy metabolism. Cancers, 12(9), 2715.

Choy, G., Liu, J. W., Chandra, D., & Tang, D. G. (2005). Cell survival signaling during apoptosis: implications in drug resistance and anti-cancer therapeutic development. Advances in Targeted Cancer Therapy, 115-145.

Claessens, F., Helsen, C., Prekovic, S., Van den Broeck, T., Spans, L., Van Poppel, H., & Joniau, S. (2014). Emerging mechanisms of enzalutamide resistance in prostate cancer. *Nature reviews urology*, *11*(12), 712-716.

Clark, A. S., West, K., Streicher, S., & Dennis, P. A. (2002). Constitutive and inducible Akt activity promotes resistance to chemotherapy, trastuzumab, or tamoxifen in breast cancer cells. Molecular cancer therapeutics, 1(9), 707-717.

Clermont, P. L., Crea, F., & Helgason, C. D. (2013). Trithorax Genes in Prostate Cancer. In *Advances in Prostate Cancer*. IntechOpen.

Coleman, D. J., Gao, L., Schwartzman, J., Korkola, J. E., Sampson, D., Derrick, D. S., … & Alumkal, J. J. (2019). Maintenance of MYC expression promotes de novo resistance to BET bromodomain inhibition in castration-resistant prostate cancer. *Scientific reports*, *9*(1), 3823.

Conteduca, V., Hess, J., Yamada, Y., Ku, S. Y., & Beltran, H. (2021). Epigenetics in prostate cancer: clinical implications. Translational andrology and urology, 10(7), 3104.

Coutinho, I., Day, T. K., Tilley, W. D., & Selth, L. A. (2016). Androgen receptor signaling in castration-resistant prostate cancer: a lesson in persistence. Endocrine-related cancer, 23(12), T179-T197.

Cui, Z., Li, H., Liang, F., Mu, C., Mu, Y., Zhang, X., & Liu, J. (2018). Effect of high WDR5 expression on the hepatocellular carcinoma prognosis. *Oncology letters*, *15*(5), 7864-7870.

Dai, X., Guo, W., Zhan, C., Liu, X., Bai, Z., & Yang, Y. (2015). WDR5 expression is prognostic of breast cancer outcome. *PloS One*, *10*(9), e0124964.

Daniels T, Zhang J, Gutierrez I, Elliot ML, Yamada B, et al. (2005) Antinuclear autoantibodies in prostate cancer: immunity to LEDGF/p75, a survival protein highly expressed in prostate tumors and cleaved during apoptosis. Prostate 62: 14–26.

Das Thakur, M., Salangsang, F., Landman, A. S., Sellers, W. R., Pryer, N. K., Levesque, M. P., … & Stuart, D. D. (2013). Modelling vemurafenib resistance in melanoma reveals a 102athways to forestall drug resistance. Nature, 494(7436), 251-255.

Daugaard, M., Baude, A., Fugger, K., Povlsen, L. K., Beck, H., Sørensen, C. S., … & Jäättelä, M. (2012). LEDGF (p75) promotes DNA-end resection and homologous recombination. Nature structural & molecular biology, 19(8), 803-810.

De Carvalho, D. D., Sharma, S., You, J. S., Su, S. F., Taberlay, P. C., Kelly, T. K., … & Jones, P. A. (2012). DNA methylation screening identifies driver epigenetic events of cancer cell survival. Cancer cell, 21(5), 655-667.

Debes, J. D., Schmidt, L. J., Huang, H., & Tindall, D. J. (2002). p300 mediates androgen-independent transactivation of the androgen receptor by interleukin 6. Cancer research, 62(20), 5632-5636.

Deharvengt, S. J., Gunn, J. R., Pickett, S. B., & Korc, M. (2010). Intratumoral delivery of shRNA targeting 102athwa D1 attenuates pancreatic cancer growth. *Cancer gene therapy*, *17*(5), 325-333.

Dengler, J., Von Bubnoff, N., Decker, T., Peschel, C., & Duyster, J. (2005). Combination of imatinib with 102athways102 or RAD001 acts synergistically only in Bcr-Abl-positive cells with moderate resistance to imatinib. Leukemia, 19(10), 1835-1838.

Ding, L., Getz, G., Wheeler, D. A., Mardis, E. R., McLellan, M. D., Cibulskis, K., … & Wilson, R. K. (2008). Somatic mutations affect key pathways in lung adenocarcinoma. Nature, 455(7216), 1069-1075.

Dong, C., Wu, J., Chen, Y., Nie, J., & Chen, C. (2021). Activation of PI3K/AKT/mTOR 103athways causes drug resistance in breast cancer. Frontiers in pharmacology, 12, 628690.

Dou Y, Milne TA, Ruthenburg AJ, Lee S, Lee JW, Verdine GL, Allis CD, Roeder RG. Regulation of MLL1 H3K4 methyltransferase activity by 103athways components. Nat Struct Mol Biol. 2006;13:713–719.

Dreijerink, K. M., Mulder, K. W., Winkler, G. S., Höppener, J. W., Lips, C. J., & Timmers, H. T. M. (2006). Menin links estrogen receptor activation to histone H3K4 trimethylation. Cancer research, 66(9), 4929-4935.

Dreijerink, K. M., Groner, A. C., Vos, E. S., Font-Tello, A., Gu, L., Chi, D., … & Brown, M. (2017). Enhancer-mediated oncogenic function of the menin tumor suppressor in breast cancer. *Cell reports*, *18*(10), 2359-2372.

Duesberg, P., R. Stindl, and R. Hehlmann, Explaining the high mutation rates of cancer cells to drug and multidrug resistance by chromosome reassortments that are catalyzed by aneuploidy. Proc Natl Acad Sci U S A, 2000. 97(26): p. 14295-300.

Dunwell, T., Hesson, L., Rauch, T. A., Wang, L., Clark, R. E., Dallol, A., … & Latif, F. (2010). A genome-wide screen identifies frequently methylated genes in haematological and epithelial cancers. Molecular cancer, 9, 1-12.

Easwaran, H., Tsai, H. C., & Baylin, S. B. (2014). Cancer epigenetics: tumor heterogeneity, plasticity of stem-like states, and drug resistance. Molecular cell, 54(5), 716-727.

Eder, I. E., Culig, Z., Putz, T., Nessler-Menardi, C., Bartsch, G., & Klocker, H. (2001). Molecular biology of the androgen receptor: from molecular understanding to the clinic. *European urology*, *40*(3), 241-251.

Egger, G., Liang, G., Aparicio, A., & Jones, P. A. (2004). Epigenetics in human disease and prospects for epigenetic therapy. Nature, 429(6990), 457-463.

El Ashkar, S., Schwaller, J., Pieters, T., Goossens, S., Demeulemeester, J., Christ, F., … & De Rijck, J. (2018). LEDGF/p75 is dispensable for hematopoiesis but essential for MLL-rearranged leukemogenesis. Blood, The Journal of the American Society of Hematology, 131(1), 95-107.

Ellinger, J., Kahl, P., Von Der Gathen, J., Rogenhofer, S., Heukamp, L. C., Gütgemann, I., … & von Ruecker, A. (2010). Global levels of histone modifications predict prostate cancer recurrence. The Prostate, 70(1), 61-69.

Ellis, L., Ku, S., Ramakrishnan, S., Lasorsa, E., Azabdaftari, G., Godoy, A., & Pili, R. (2013). Combinatorial antitumor effect of HDACs and the PI3K-Akt-mTOR pathways inhibition in a Pten deficient model of prostate cancer. Oncotarget, 4(12), 2225.

Ernst, P., Wang, J., & Korsmeyer, S. J. (2002). The role of MLL in hematopoiesis and leukemia. Current opinion in hematology, 9(4), 282-287.

Eteleeb, A. M., Thunuguntla, P. K., Gelev, K. Z., Tang, C. Y., Rozycki, E. B., Miller, A., … & Maher, C. A. (2022). LINC00355 regulates p27KIP expression by binding to MENIN to induce proliferation in late-stage relapse breast cancer. NPJ Breast Cancer, 8(1), 49.

Faruq, O., Zhao, D., Shrestha, M., Vecchione, A., Zacksenhaus, E., & Chang, H. (2022). Targeting an MDM2/MYC axis to 104athways drug resistance in multiple myeloma. *Cancers*, *14*(6), 1592.

Filon, M., Yang, B., Purohit, T. A., Schehr, J., Singh, A., Bigarella, M., … & Jarrard, D. F. (2023). Development of a multiplex assay to assess activated p300/CBP in circulating prostate tumor cells. *Oncotarget*, *14*, 738.

Fingar, D. C., Richardson, C. J., Tee, A. R., Cheatham, L., Tsou, C., & Blenis, J. (2004). mTOR controls cell cycle progression through its cell growth effectors S6K1 and 4E-BP1/eukaryotic translation initiation factor 4E. Molecular and cellular biology.

Fiskus, W., Boettcher, S., Daver, N., Mill, C. P., Sasaki, K., Birdwell, C. E., … & Bhalla, K. N. (2022). Effective Menin inhibitor-based combinations against AML with MLL rearrangement or NPM1 mutation (NPM1c). Blood cancer journal, 12(1), 5.

Foster, D. A., Yellen, P., Xu, L., & Saqcena, M. (2010). Regulation of G1 cell cycle progression: distinguishing the restriction point from a nutrient-sensing cell growth checkpoint (s). Genes & cancer, 1(11), 1124-1131.

Foster, H., Coley, H. M., Goumenou, A., Pados, G., Harvey, A., & Karteris, E. (2010). Differential expression of mTOR 104athways104 components in drug resistance in ovarian cancer. Anticancer research, 30(9), 3529-3534.

Francipane, M. G., & Lagasse, E. (2013). Selective targeting of human colon cancer stem-like cells by the mTOR inhibitor Torin-1. Oncotarget, 4(11), 1948.

Galletti, G., Zhang, C., Gjyrezi, A., Cleveland, K., Zhang, J., Powell, S., … & Giannakakou, P. (2020). Microtubule engagement with taxane is altered in taxane-resistant gastric cancer. *Clinical Cancer Research*, *26*(14), 3771-3783.

Gallo, M., Ho, J., Coutinho, F. J., Vanner, R., Lee, L., Head, R., … & Dirks, P. B. (2013). A tumorigenic MLL-homeobox network in human glioblastoma stem cells. *Cancer research*, *73*(1), 417-427.

Gan, X., Wang, J., Wang, C., Sommer, E., Kozasa, T., Srinivasula, S., … & Wu, D. (2012). PRR5L degradation promotes mTORC2-mediated PKC-δ phosphorylation and cell migration downstream of Gα12. Nature cell biology, 14(7), 686-696.

Gang, D., Hongwei, H., Hedai, L., Ming, Z., Qian, H., & Zhijun, L. (2013). The tumor suppressor protein menin inhibits NF-κB-mediated transactivation through recruitment of Sirt1 in hepatocellular carcinoma. Molecular biology reports, 40, 2461-2466.

Gao, L., Schwartzman, J., Gibbs, A., Lisac, R., Kleinschmidt, R., Wilmot, B., … & Alumkal, J. (2013). Androgen receptor promotes ligand-independent prostate cancer progression through c-Myc upregulation. *PloS one*, *8*(5), e63563.

Gao, L., Han, B., & Dong, X. (2022). The Androgen Receptor and Its Crosstalk With the Src Kinase During Castrate-Resistant Prostate Cancer Progression. Frontiers in Oncology, 12, 905398.

Ge H, Si Y, Roeder RG (1998) Isolation of cDNAs encoding novel transcription coactivators p52 and p75 reveals an alternate regulatory mechanism of transcriptional activation. EMBO J 17: 6723–6729.

Ge, Z., Song, E. J., Kawasawa, Y. I., Li, J., Dovat, S., & Song, C. (2016). WDR5 high expression and its effect on tumorigenesis in leukemia. *Oncotarget*, *7*(25), 37740.

George, D. J., Halabi, S., Healy, P., Jonasch, D., Anand, M., Rasmussen, J., … & Armstrong, A. J. (2020, March). Phase 2 clinical trial of TORC1 inhibition with everolimus in men with metastatic castration-resistant prostate cancer. In Urologic Oncology: Seminars and Original Investigations (Vol. 38, No. 3, pp. 79-e15). Elsevier.

Gibson, A. W., Cheng, T., & Johnston, R. N. (1995). Apoptosis induced by c-myc overexpression is dependent on growth conditions. *Experimental cell research*, *218*(1), 351-358.

Goldstein, L. J. (1996). MDR1 gene expression in solid tumours. European journal of cancer, 32(6), 1039-1050.

Golob-Schwarzl, N., Krassnig, S., Toeglhofer, A. M., Park, Y. N., Gogg-Kamerer, M., Vierlinger, K., … & Haybaeck, J. (2017). New liver cancer biomarkers: PI3K/AKT/mTOR 106athways members and eukaryotic translation initiation factors. European Journal of Cancer, 83, 56-70.

Grasso, C. S., Wu, Y. M., Robinson, D. R., Cao, X., Dhanasekaran, S. M., Khan, A. P., … & Tomlins, S. A. (2012). The mutational landscape of lethal castration-resistant prostate cancer. *Nature*, *487*(7406), 239-243.

Grembecka, J., He, S., Shi, A., Purohit, T., Muntean, A. G., Sorenson, R. J., … & Cierpicki, T. (2012). Menin-MLL inhibitors reverse oncogenic activity of MLL fusion proteins in leukemia. Nature chemical biology, 8(3), 277-284.

Gremke, N., Polo, P., Dort, A., Schneikert, J., Elmshäuser, S., Brehm, C., … & Stiewe, T. (2020). mTOR-mediated cancer drug resistance suppresses autophagy and generates a druggable metabolic vulnerability. Nature communications, 11(1), 4684.

Guerrero-Zotano, A., Mayer, I. A., & Arteaga, C. L. (2016). PI3K/AKT/mTOR: role in breast cancer progression, drug resistance, and treatment. Cancer and Metastasis Reviews, 35, 515-524.

Gurung, B., Feng, Z., Iwamoto, D. V., Thiel, A., Jin, G., Fan, C. M., … & Hua, X. (2013). Menin epigenetically represses Hedgehog signaling in MEN1 tumor syndrome. Cancer research, 73(8), 2650-2658.

Guo, Z., Yang, X., Sun, F., Jiang, R., Linn, D. E., Chen, H., … & Qiu, Y. (2009). A novel androgen receptor splice variant is up-regulated during prostate cancer progression and promotes androgen depletion–resistant growth. Cancer research, 69(6), 2305-2313.

Guo, M., Peng, Y., Gao, A., Du, C., & Herman, J. G. (2019). Epigenetic heterogeneity in cancer. Biomarker research, 7, 1-19.

Hååg, P., Bektic, J., Bartsch, G., Klocker, H., & Eder, I. E. (2005). Androgen receptor down regulation by small interference RNA induces cell growth inhibition in androgen sensitive as well as in androgen independent prostate cancer cells. *The Journal of steroid biochemistry and molecular biology*, *96*(3-4), 251-258.

Hara, T., Ushio, K., Nishiwaki, M., Kouno, J., Araki, H., Hikichi, Y., … & Yamaoka, M. (2010). A mutation in β-tubulin and a sustained dependence on androgen receptor 106athways106 in a newly established docetaxel-resistant prostate cancer cell line. Cell biology international, 34(2), 177-184.

Hari, M., Wang, Y., Veeraraghavan, S., & Cabral, F. (2003). Mutations in α-and β-tubulin that stabilize microtubules and confer resistance to colcemid and vinblastine. *Molecular cancer therapeutics*, *2*(7), 597-605.

Harris, W. P., Mostaghel, E. A., Nelson, P. S., & Montgomery, B. (2009). Androgen deprivation therapy: progress in understanding mechanisms of resistance and optimizing androgen depletion. Nature clinical practice Urology, 6(2), 76-85.

Herman, J. G., Umar, A., Polyak, K., Graff, J. R., Ahuja, N., Issa, J. P. J., … & Baylin, S. B. (1998). Incidence and functional consequences of hMLH1 promoter hypermethylation in colorectal carcinoma. Proceedings of the National Academy of Sciences, 95(12), 6870-6875.

Helsen, C., Van den Broeck, T., Voet, A., Prekovic, S., Van Poppel, H., Joniau, S., & Claessens, F. (2014). Androgen receptor antagonists for prostate cancer therapy. Endocrine-related cancer, 21(4), T105-T118.

Hientz, K., Mohr, A., Bhakta-Guha, D., & Efferth, T. (2017). The role of p53 in cancer drug resistance and targeted chemotherapy. Oncotarget, 8(5), 8921.

Hoffman, B., & Liebermann, D. A. (2008). Apoptotic signaling by c-MYC. *Oncogene*, *27*(50), 6462-6472.

Housman, G., Byler, S., Heerboth, S., Lapinska, K., Longacre, M., Snyder, N., & Sarkar, S. (2014). Drug resistance in cancer: an overview. Cancers, 6(3), 1769-1792.

Hsieh, A. C., Liu, Y., Edlind, M. P., Ingolia, N. T., Janes, M. R., Sher, A., … & Ruggero, D. (2012). The translational landscape of mTOR 107athways107 steers cancer initiation and metastasis. Nature, 485(7396), 55-61.

Huang, T. S., Myklebust, L. M., Kjarland, E., Gjertsen, B. T., Pendino, F., Bruserud, Ø., … & Lillehaug, J. R. (2007). LEDGF/p75 has increased expression in blasts from chemotherapy-resistant human acute myelogenic leukemia patients and protects leukemia cells from apoptosis in vitro. Molecular cancer, 6, 1-13.

Huang, J., Gurung, B., Wan, B., Matkar, S., Veniaminova, N. A., Wan, K., … & Lei, M. (2012). The same pocket in menin binds both MLL and JUND but has opposite effects on transcription. *Nature*, *482*(7386), 542-546.

Huang, D., Chen, X., Chen, X., Qu, Y., Wang, Y., Yang, Y., & Cheng, Y. (2020). WDR5 promotes proliferation and correlates with poor prognosis in oesophageal squamous cell carcinoma. *OncoTargets and therapy*, 10525-10534.

Hume, S., Dianov, G. L., & Ramadan, K. (2020). A unified model for the G1/S cell cycle transition. *Nucleic acids research*, *48*(22), 12483-12501.

Hughes, C. M., Rozenblatt-Rosen, O., Milne, T. A., Copeland, T. D., Levine, S. S., Lee, J. C., … & Meyerson, M. (2004). Menin associates with a trithorax family histone methyltransferase complex and with the hoxc8 locus. Molecular cell, 13(4), 587-597.

Hyun, K., Jeon, J., Park, K., & Kim, J. (2017). Writing, erasing and reading histone lysine methylations. Experimental & molecular medicine, 49(4), e324-e324.

Ianculescu, I., Wu, D. Y., Siegmund, K. D., & Stallcup, M. R. (2012). Selective roles for cAMP response element-binding protein binding protein and p300 protein as coregulators for androgen-regulated gene expression in advanced prostate cancer cells. *Journal of Biological Chemistry*, *287*(6), 4000-4013.

Imachi, H., Murao, K., Dobashi, H., Bhuyan, M. M., Cao, X., Kontani, K., … & Yamauchi, A. (2010). Menin, a product of the MENI gene, binds to estrogen receptor to enhance its activity in breast cancer cells: possibility of a novel predictive factor for tamoxifen resistance. Breast cancer research and treatment, 122, 395-407.

Ishii, T., Akiyama, Y., Shimada, S., Kabashima, A., Asano, D., Watanabe, S., … & Tanaka, S. (2023). Identification of a novel target of SETD1A histone methyltransferase and the clinical 108athways108nce in pancreatic cancer. Cancer Science, 114(2), 463-476.

Izumi, K., & Chang, C. (2013). Targeting inflammatory cytokines-androgen receptor (AR) signaling with ASC-J9® to better battle prostate cancer progression. *Oncoimmunology*, *2*(12), e26853.

James, N. D., Sydes, M. R., Clarke, N. W., Mason, M. D., Dearnaley, D. P., Spears, M. R., … & Parmar, M. K. (2016). Addition of 108athways108, zoledronic acid, or both to first-line long-term hormone therapy in prostate cancer (STAMPEDE): survival results from an adaptive, multiarm, multistage, platform randomised controlled trial. *The Lancet*, *387*(10024), 1163-1177.

Jernberg, E., Bergh, A., & Wikström, P. (2017). Clinical relevance of androgen receptor alterations in prostate cancer. Endocrine connections, 6(8), R146-R161.

Jhanwar-Uniyal, M., Amin, A. G., Cooper, J. B., Das, K., Schmidt, M. H., & Murali, R. (2017). Discrete signaling mechanisms of mTORC1 and mTORC2: Connected yet

apart in cellular and molecular aspects. Advances in 109athways109n regulation, 64, 39-48.

Ji, H. (2010). Mechanistic insights into acquired drug resistance in epidermal growth factor receptor mutation-targeted lung cancer therapy. Cancer science, 101(9), 1933-1938.

Jiang, B. H., & Liu, L. Z. (2008). Role of mTOR in anticancer drug resistance: perspectives for improved drug treatment. Drug resistance updates, 11(3), 63-76.

Jiang, W., Kahn, S. M., Zhou, P. I. N. G., Zhang, Y. J., Cacace, A. M., Infante, A. S., … & Weinstein, I. B. (1993). Overexpression of 109athwa D1 in rat fibroblasts causes abnormalities in growth control, cell cycle progression and gene expression. *Oncogene*, *8*(12), 3447-3457.

Jih, G., Iglesias, N., Currie, M. A., Bhanu, N. V., Paulo, J. A., Gygi, S. P., … & Moazed, D. (2017). Unique roles for histone H3K9me states in RNAi and heritable silencing of transcription. Nature, 547(7664), 463-467.

Jin, W., Liao, X., Lv, Y., Pang, Z., Wang, Y., Li, Q., … & Huang, L. (2017). MUC1 induces acquired chemoresistance by upregulating ABCB1 in EGFR-dependent manner. Cell death & disease, 8(8), e2980-e2980.

Jin, L., Garcia, J., Chan, E., de la Cruz, C., Segal, E., Merchant, M., … & Gascoigne, K. E. (2017). Therapeutic targeting of the CBP/p300 bromodomain blocks the growth of castration-resistant prostate cancer. *Cancer research*, *77*(20), 5564-5575.

Johnson, S. M., Gulhati, P., Rampy, B. A., Han, Y., Rychahou, P. G., Doan, H. Q., … & Evers, B. M. (2010). Novel expression patterns of PI3K/Akt/mTOR signaling pathways components in colorectal cancer. Journal of the American College of Surgeons, 210(5), 767-776.

Kahl, P., Gullotti, L., Heukamp, L. C., Wolf, S., Friedrichs, N., Vorreuther, R., … & Buettner, R. (2006). Androgen receptor coactivators lysine-specific histone demethylase 1 and four and a half LIM domain protein 2 predict risk of prostate cancer recurrence. Cancer research, 66(23), 11341-11347.

Kampan, N. C., Madondo, M. T., McNally, O. M., Quinn, M., & Plebanski, M. (2015). Paclitaxel and its evolving role in the management of ovarian cancer. BioMed research international, 2015(1), 413076.

Kandoth, C., McLellan, M. D., Vandin, F., Ye, K., Niu, B., Lu, C., … & Ding, L. (2013). Mutational landscape and 110athways110nce across 12 major cancer types. Nature, 502(7471), 333-339.

Kang, Z., Jänne, O. A., & Palvimo, J. J. (2004). Coregulator recruitment and histone modifications in transcriptional regulation by the androgen receptor. Molecular Endocrinology, 18(11), 2633-2648.

Kang, J. Y., Park, J. W., Hwang, Y., Hahm, J. Y., Park, J., Park, K. S., & Seo, S. B. (2021). The H3K4 methyltransferase SETD1A is required for proliferation of non-small cell lung cancer cells by promoting S-phase progression. *Biochemical and Biophysical Research Communications*, *561*, 120-127.

Karatas, H., Townsend, E. C., Bernard, D., Dou, Y. & Wang, S. Analysis of the binding of mixed lineage leukemia 1 (MLL1) and histone peptides to WD repeat domain 5 (WDR5) for the design of inhibitors of the MLL1–WDR5 interaction. J. Med. Chem. 53, 5179–5185 (2010).

Kartner, N., Riordan, J. R., & Ling, V. (1983). Cell surface P-glycoprotein associated with multidrug resistance in mammalian cell lines. Science, 221(4617), 1285-1288.

Kato, I., Kasukabe, T., & Kumakura, S. (2020). Menin-MLL inhibitors induce ferroptosis and enhance the anti-proliferative activity of auranofin in several types of cancer cells. International Journal of Oncology, 57(4), 1057-1071.

Katona, B. W., Glynn, R. A., Paulosky, K. E., Feng, Z., Davis, C. I., Ma, J., … & Hua, X. (2019). Combined menin and EGFR inhibitors synergize to suppress colorectal cancer via EGFR-independent and calcium-mediated repression of SKP2 transcription. Cancer research, 79(9), 2195-2207.

Ketkar, M., & Dutt, S. (2022). Epigenetic regulation towards acquired drug resistance in cancer. In Metabolism and Epigenetic Regulation: Implications in Cancer (pp. 473-502). Cham: Springer International Publishing.

Keyes, M., Crook, J., Morton, G., Vigneault, E., Usmani, N., & Morris, W. J. (2013). Treatment options for localized prostate cancer. *Canadian Family Physician*, *59*(12), 1269-1274.

Khan, M. W., Biswas, D., Ghosh, M., Mandloi, S., Chakrabarti, S., & Chakrabarti, P. (2015). mTORC2 controls cancer cell survival by modulating gluconeogenesis. Cell Death Discovery, 1(1), 1-12.

Kim, S. S., Lee, M. H., & Lee, M. O. (2020). Histone methyltransferases regulate the transcriptional expression of ERα and the proliferation of tamoxifen-resistant breast cancer cells. *Breast cancer research and treatment*, *180*, 45-54.

Kim, T., Jeong, K., Kim, E., Yoon, K., Choi, J., Park, J. H., … & Cho, E. J. (2022). Menin Enhances Androgen Receptor-Independent Proliferation and Migration of Prostate Cancer Cells. Molecules and cells, 45(4), 202-215.

Kobayashi, Y., Absher, D. M., Gulzar, Z. G., Young, S. R., McKenney, J. K., Peehl, D. M., … & Sherlock, G. (2011). DNA methylation profiling reveals novel biomarkers and important roles for DNA methyltransferases in prostate cancer. Genome research, 21(7), 1017-1027.

Kongkham, P. N., Northcott, P. A., Ra, Y. S., Nakahara, Y., Mainprize, T. G., Croul, S. E., … & Rutka, J. T. (2008). An epigenetic genome-wide screen identifies SPINT2 as a novel tumor suppressor gene in pediatric medulloblastoma. Cancer research, 68(23), 9945-9953.

Konishi, N., Nakamura, M., Kishi, M., Nishimine, M., Ishida, E., & Shimada, K. (2002). DNA hypermethylation status of multiple genes in prostate adenocarcinomas. Japanese journal of cancer research, 93(7), 767-773.

Kosaka, T., Miyajima, A., Shirotake, S., Suzuki, E., Kikuchi, E., & Oya, M. (2011). Long-term androgen ablation and pathways up-regulate phosphorylated Akt in castration-resistant prostate cancer. The Journal of Urology, 185(6), 2376-2381.

Krishna Vadlapatla, R., Dutt Vadlapudi, A., Pal, D., & K Mitra, A. (2013). Mechanisms of drug resistance in cancer chemotherapy: coordinated role and regulation of efflux transporters and metabolizing enzymes. Current pharmaceutical design, 19(40), 7126-7140.

Krivtsov, A. V., & Armstrong, S. A. (2007). MLL translocations, histone modifications, and Leukemia stem-cell development. Nature Reviews Cancer, 7(11), 823-833.

Kruczek, K., Ratterman, M., Tolzien, K., Sulo, S., Lestingi, T. M., & Nabhan, C. (2013). A phase II study evaluating the toxicity and efficacy of single-agent temsirolimus in chemotherapy-naïve castration-resistant prostate cancer. British journal of cancer, 109(7), 1711-1716.

Kudo, R., & Sagae, S. (1992). Treatment of recurrent ovarian cancer. Cancer & Chemotherapy, 19(12), 1991-1997.

Kuroda, K., Liu, H., Kim, S., Guo, M., Navarro, V., & Bander, N. H. (2009). Docetaxel down-regulates the expression of androgen receptor and prostate-specific antigen but not prostate-specific membrane antigen in prostate cancer cell lines: Implications for PSA surrogacy. The Prostate, 69(14), 1579-1585.

La, P., Silva, A. C., Hou, Z., Wang, H., Schnepp, R. W., Yan, N., … & Hua, X. (2004). Direct binding of DNA by tumor suppressor menin. Journal of Biological Chemistry, 279(47), 49045-49054.

Lai, L., Shin, G. Y., & Qiu, H. (2020). The role of cell cycle regulators in cell survival—dual pathways-dependent kinase 20 and p21cip1/waf1. *International journal of molecular sciences*, *21*(22), 8504.

Lang, E., Zelenak, C., Eberhard, M., Bissinger, R., Rotte, A., Ghashghaeinia, M., … & Qadri, S. M. (2015). Impact of 112athwa-dependent kinase CDK4 inhibition on eryptosis. Cellular physiology and biochemistry, 37(3), 1178-1186.

Lee Jr, J. T., Steelman, L. S., & McCubrey, J. A. (2004). Phosphatidylinositol 3′-kinase activation leads to multidrug resistance protein-1 expression and subsequent chemoresistance in advanced prostate cancer cells. Cancer research, 64(22), 8397-8404.

Lee, S., Choi, E. J., Jin, C., & Kim, D. H. (2005). Activation of PI3K/Akt 112athways by PTEN reduction and PIK3CA mRNA amplification contributes to cisplatin resistance in an ovarian cancer cell line. Gynecologic oncology, 97(1), 26-34.

Lee, S. H., Johnson, D., Luong, R., & Sun, Z. (2015). Crosstalking between androgen and PI3K/AKT signaling pathways in prostate cancer cells. Journal of Biological Chemistry, 290(5), 2759-2768.

Lei, H., Zhang, S. Q., Fan, S., Bai, H. R., Zhao, H. Y., Mao, S., & Xin, M. (2021). Recent progress of small molecule menin–MLL interaction inhibitors as therapeutic agents for acute leukemia. Journal of medicinal chemistry, 64(21), 15519-15533.

Leitz, J., Reuschenbach, M., Lohrey, C., Honegger, A., Accardi, R., Tommasino, M., … & Hoppe-Seyler, F. (2014). Oncogenic human papillomaviruses activate the tumor-associated lens epithelial-derived growth factor (LEDGF) gene. PloS pathogens, 10(3), e1003957.

Levina, E., Ji, H., Chen, M., Baig, M., Oliver, D., Ohouo, P., … & Shtutman, M. (2015). Identification of novel genes that regulate androgen receptor signaling and growth of androgen-deprived prostate cancer cells. Oncotarget, 6(15), 13088.

Li, L., Osdal, T., Ho, Y., Chun, S., McDonald, T., Agarwal, P., … & Bhatia, R. (2014). SIRT1 activation by a c-MYC oncogenic network promotes the maintenance and drug resistance of human FLT3-ITD acute myeloid leukemia stem cells. *Cell stem cell*, *15*(4), 431-446.

Li, D., Sun, H., Sun, W. J., Bao, H. B., Si, S. H., Fan, J. L., … & Yu, X. G. (2016). Role of RbBP5 and H3K4me3 in the vicinity of Snail transcription start site during epithelial-mesenchymal transition in prostate cancer cell. *Oncotarget*, *7*(40), 65553.

Li, F., Ng, W. L., Luster, T. A., Hu, H., Sviderskiy, V. O., Dowling, C. M., … & Wong, K. K. (2020). Epigenetic CRISPR screens identify Npm1 as a therapeutic vulnerability in non–small cell lung cancer. Cancer research, 80(17), 3556-3567.

Li, Z., Liang, N., Wang, N., Jia, Y., & Tian, C. (2022). WDR5 is a prognostic biomarker of brain metastasis from non-small cell lung cancer. *Frontiers in Oncology*, *12*, 1023776.

Liao, R. S., Ma, S., Miao, L., Li, R., Yin, Y., & Raj, G. V. (2013). Androgen receptor-mediated non-genomic regulation of prostate cancer cell proliferation. *Translational andrology and urology*, *2*(3), 187.

Liau, B. B., Sievers, C., Donohue, L. K., Gillespie, S. M., Flavahan, W. A., Miller, T. E., … & Bernstein, B. E. (2017). Adaptive chromatin remodeling drives glioblastoma stem cell plasticity and drug tolerance. Cell stem cell, 20(2), 233-246.

Liedtke, M., & Cleary, M. L. (2009). Therapeutic targeting of MLL. Blood, The Journal of the American Society of Hematology, 113(24), 6061-6068.

Liedtke, V., Schröder, C., Roggenbuck, D., Weiss, R., Stohwasser, R., Schierack, P., … & Schenk, L. (2021). LEDGF/p75 is required for an efficient DNA damage response. International Journal of Molecular Sciences, 22(11), 5866.

Lin, J., Wu, Y., Tian, G., Yu, D., Yang, E., Lam, W. H., … & Li, X. D. (2023). Menin “reads” H3K79me2 mark in a nucleosomal context. Science, 379(6633), 717-723.

Lindblad, O., Cordero, E., Puissant, A., Macaulay, L., Ramos, A., Kabir, N. N., … & Kazi, J. U. (2016). Aberrant activation of the PI3K/mTOR 113athways promotes resistance to sorafenib in AML. *Oncogene*, *35*(39), 5119-5131.

Liu, Y., Wu, C., & Galaktionov, K. (2004). p42, a novel 114athwa-dependent kinase-activating kinase in mammalian cells. Journal of Biological Chemistry, 279(6), 4507-4514.

Liu, Q., Chang, J. W., Wang, J., Kang, S. A., Thoreen, C. C., Markhard, A., … & Gray, N. S. (2010). Discovery of 1-(4-(4-propionylpiperazin-1-yl)-3-(trifluoromethyl) phenyl)-9-(quinolin-3-yl) benzo [h][1, 6] naphthyridin-2 (1 H)-one as a highly potent, selective mammalian target of 114athways114 (mTOR) inhibitor for the treatment of cancer. Journal of medicinal chemistry, 53(19), 7146-7155.

Liu, J., Huang, Y., Zhu, D., Dai, Y., Liu, D., Zhai, Y., … & Zhao, Q. (2020). Establishment and characterization of a docetaxel-resistant human prostate cancer cell line. Oncology letters, 20(5), 1-1.

Lohiya, V., Aragon-Ching, J. B., & Sonpavde, G. (2016). Role of chemotherapy and mechanisms of resistance to chemotherapy in metastatic castration-resistant prostate cancer. Clinical Medicine Insights: Oncology, 10, CMO-S34535.

Lonergan, P.E. and D.J. Tindall, Androgen receptor signaling in prostate cancer development and progression. J Carcinog, 2011. **10**: p. 20.

Lu, M., Zessin, A. S., Glover, W., & Hsu, D. S. (2017). Activation of the mTOR 114athways by oxaliplatin in the treatment of colorectal cancer liver metastasis. *PloS One*, *12*(1), e0169439.

Lu, C., Paschall, A. V., Shi, H., Savage, N., Waller, J. L., Sabbatini, M. E., … & Liu, K. (2017). The MLL1-H3K4me3 axis-mediated PD-L1 expression and pancreatic cancer 114athwa evasion. JNCI: journal of the National Cancer Institute, 109(6), djw283.

Lu, K., Tao, H., Si, X., & Chen, Q. (2018). The histone H3 lysine 4 presenter WDR5 as an oncogenic protein and novel epigenetic target in cancer. Frontiers in oncology, 8, 502.

Luo, W., Karpf, A. R., Deeb, K. K., Muindi, J. R., Morrison, C. D., Johnson, C. S., & Trump, D. L. (2010). Epigenetic regulation of vitamin D 24-hydroxylase/CYP24A1 in human prostate cancer. Cancer research, 70(14), 5953-5962.

Luo, Y., Vlaeminck-Guillem, V., Teinturier, R., Abou Ziki, R., Bertolino, P., Le Romancer, M., & Zhang, C. X. (2021). The scaffold protein menin is essential for activating the MYC locus and MYC-mediated androgen receptor transcription in

androgen receptor-dependent prostate cancer cells. *Cancer Communications*, *41*(12), 1427.

Lüscher-Firzlaff, J., Gawlista, I., Vervoorts, J., Kapelle, K., Braunschweig, T., Walsemann, G., … & Lüscher, B. (2008). The human trithorax protein hASH2 functions as an oncoprotein. *Cancer research*, *68*(3), 749-758.

Ma, X. M., & Blenis, J. (2009). Molecular mechanisms of mTOR-mediated translational control. Nature reviews Molecular cell biology, 10(5), 307-318.

Mahapatra, S., Klee, E. W., Young, C. Y., Sun, Z., Jimenez, R. E., Klee, G. G., … & Donkena, K. V. (2012). Global methylation profiling for risk prediction of prostate cancer. Clinical cancer research, 18(10), 2882-2895.

Maier, P., Spier, I., Laufs, S., Veldwijk, M. R., Fruehauf, S., Wenz, F., & Zeller, W. J. (2010). Chemoprotection of human hematopoietic stem cells by simultaneous lentiviral overexpression of multidrug resistance 1 and O6-methylguanine-DNA methyltransferaseP140K. Gene therapy, 17(3), 389-399.

Maira, S. M., Stauffer, F., Brueggen, J., Furet, P., Schnell, C., Fritsch, C., … & Garcia-Echeverria, C. (2008). Identification and characterization of NVP-BEZ235, a new orally available dual phosphatidylinositol 3-kinase/mammalian target of 115athways115 inhibitor with potent in vivo antitumor activity. Molecular cancer therapeutics, 7(7), 1851-1863.

Malekzadeh, K., Sobti, R. C., Nikbakht, M., Shekari, M., Hosseini, S. A., Tamandani, D. K., & Singh, S. K. (2009). Methylation patterns of Rb1 and Casp-8 promoters and their impact on their expression in 115athway cancer. Cancer investigation, 27(1), 70-80.

Malik, R., Khan, A., Asangani, I. et al. Targeting the MLL complex in castration-resistant prostate cancer. Nat Med 21, 344–352 (2015).

Marhold, M., Tomasich, E., El-Gazzar, A., Heller, G., Spittler, A., Horvat, R., … & Horak, P. (2015). HIF1α regulates mTOR signaling and viability of prostate cancer stem cells. Molecular Cancer Research, 13(3), 556-564.

Masamha, C. P., & Benbrook, D. M. (2009). Cyclin D1 degradation is sufficient to induce G1 cell cycle arrest despite 115athways115nce expression of 115athwa E2 in ovarian cancer cells. *Cancer research*, *69*(16), 6565-6572.

Mashima, T., Taneda, Y., Jang, M. K., Mizutani, A., Muramatsu, Y., Yoshida, H., … & Seimiya, H. (2017). mTOR signaling mediates resistance to tankyrase inhibitors in Wnt-driven colorectal cancer. *Oncotarget*, *8*(29), 47902.

Massie, C. E., Lynch, A., Ramos-Montoya, A., Boren, J., Stark, R., Fazli, L., … & Mills, I. G. (2011). The androgen receptor fuels prostate cancer by regulating central metabolism and biosynthesis. The EMBO journal, 30(13), 2719-2733.

Matkar S, Thiel A, Hua X. Menin: a scaffold protein that controls gene expression and cell signaling. Trends Biochem Sci. 2013 Aug;38(8):394-402. doi: 10.1016/j.tibs.2013.05.005. Epub 2013 Jul 10. PMID: 23850066; PMCID: PMC3741089.

McDonald, S., Brive, L., Agus, D. B., Scher, H. I., & Ely, K. R. (2000). Ligand responsiveness in human prostate cancer: structural analysis of mutant androgen receptors from LNCaP and CWR22 tumors. Cancer research, 60(9), 2317-2322.

Mediavilla-Varela, M., Pacheco, F. J., Almaguel, F., Perez, J., Sahakian, E., Daniels, T. R., … & Casiano, C. A. (2009). Docetaxel-induced prostate cancer cell death involves concomitant activation of caspase and lysosomal pathways and is attenuated by LEDGF/p75. *Molecular cancer*, *8*, 1-15.

Mellado, B., Jimenez, N., Marin-Aguilera, M., & Reig, O. (2016). Diving into cabazitaxel's mode of action: more than a taxane for the treatment of castration-resistant prostate cancer patients. Clinical genitourinary cancer, 14(4), 265-270.

Méreau, H., De Rijck, J., Čermáková, K., Kutz, A., Juge, S., Demeulemeester, J., … & Schwaller, J. (2013). Impairing MLL-fusion gene-mediated transformation by dissecting critical interactions with the lens epithelium-derived growth factor (LEDGF/p75). Leukemia, 27(6), 1245-1253.

Merseburger, A. S., Haas, G. P., & von Klot, C. A. (2015). An update on enzalutamide in the treatment of prostate cancer. *Therapeutic advances in urology*, *7*(1), 9-21.

Merson, S., Yang, Z. H., Brewer, D., Olmos, D., Eichholz, A., McCarthy, F., … & Clark, J. P. (2014). Focal amplification of the androgen receptor gene in hormone-naive human prostate cancer. British journal of cancer, 110(6), 1655-1662.

Milne, T. A., Briggs, S. D., Brock, H. W., Martin, M. E., Gibbs, D., Allis, C. D., & Hess, J. L. (2002). MLL targets SET domain methyltransferase activity to Hox gene promoters. Molecular cell, 10(5), 1107-1117.

Milne TA, Dou Y, Martin ME, Brock HW, Roeder RG, Hess JL. MLL associates specifically with a subset of transcriptionally active target genes. Proc Natl Acad Sci U S A. 2005 Oct 11;102(41):14765-70. doi: 10.1073/pnas.0503630102. Epub 2005 Sep 30. PMID: 16199523; PMCID: PMC1253553.

Milne TA, Hughes CM, Lloyd R, Yang Z, Rozenblatt-Rosen O, Dou Y, Schnepp RW, Krankel C, Livolsi VA, Gibbs D, et al. Menin and MLL cooperatively regulate expression of 117athwa-dependent kinase inhibitors. Proc Natl Acad Sci U S A. 2005;102:749–754.

Mitchell, A. V., Wu, L., James Block, C., Zhang, M., Hackett, J., Craig, D. B., … & Wu, G. (2022). FOXQ1 recruits the MLL complex to activate transcription of EMT and 117athways breast cancer metastasis. Nature Communications, 13(1), 6548.

Mitra, A., Mishra, L., & Li, S. (2015). EMT, CTCs and CSCs in tumor relapse and drug-resistance. Oncotarget, 6(13), 10697.

Mitsui, E., Yoshida, S., Shinoda, Y., Matsumori, Y., Tsujii, H., Tsuchida, M., … & Mizukami, T. (2019). Identification of 117athways117 as a KDM5A inhibitor. Scientific Reports, 9(1), 9952

Montanaro, L., & Pandolfi, P. P. (2004). Initiation of mRNA translation in oncogenesis: the role of eIF4E. Cell Cycle, 3(11), 1387-1389.

Montgomery, R. B., Mostaghel, E. A., Vessella, R., Hess, D. L., Kalhorn, T. F., Higano, C. S., … & Nelson, P. S. (2008). Maintenance of intratumoral androgens in metastatic prostate cancer: a mechanism for castration-resistant tumor growth. Cancer research, 68(11), 4447-4454.

Moore, L. D., Le, T., & Fan, G. (2013). DNA methylation and its basic function. Neuropsychopharmacology, 38(1), 23-38.

Morel, D., Jeffery, D., Aspeslagh, S., Almouzni, G., & Postel-Vinay, S. (2020). Combining epigenetic drugs with other therapies for solid tumours—past lessons and future promise. *Nature Reviews Clinical Oncology*, *17*(2), 91-107.

Murphy, T.M., et al., In silico analysis and DHPLC screening 117athways identifies novel apoptotic gene targets of aberrant promoter hypermethylation in prostate cancer. Prostate, 2011. 71(1): p. 1-17.

Murugan, A. K. (2019, December). mTOR: Role in cancer, metastasis and drug resistance. In Seminars in cancer biology (Vol. 59, pp. 92-111). Academic Press.

Nathan, N., Keppler-Noreuil, K. M., Biesecker, L. G., Moss, J., & Darling, T. N. (2017). Mosaic disorders of the PI3K/PTEN/AKT/TSC/mTORC1 signaling 118athways. Dermatologic clinics, 35(1), 51-60.

Neiman, P. E., Thomas, S. J., & Loring, G. (1991). Induction of apoptosis during normal and neoplastic B-cell development in the bursa of Fabricius. *Proceedings of the National Academy of Sciences*, *88*(13), 5857-5861.

Neilsen, B. K., Chakraborty, B., McCall, J. L., Frodyma, D. E., Sleightholm, R. L., Fisher, K. W., & Lewis, R. E. (2018). WDR5 supports colon cancer cells by promoting methylation of H3K4 and suppressing DNA damage. *BMC cancer*, *18*, 1-13.

Ng, S. S., Cheung, Y. T., An, X. M., Chen, Y. C., Li, M., Hoi-Yee Li, G., … & Lin, M. C. (2007). Cell cycle–related kinase: A novel candidate oncogene in human glioblastoma. *Journal of the National Cancer Institute*, *99*(12), 936-948.

Ngollo, M., Lebert, A., Daures, M., Judes, G., Rifai, K., Dubois, L., … & Bernard-Gallon, D. (2017). Global analysis of H3K27me3 as an epigenetic marker in prostate cancer progression. BMC cancer, 17, 1-8.

Nguyen, D. T., Le, T. K., Paris, C., Cherif, C., Audebert, S., Oluchi Udu-Ituma, S., … & Rocchi, P. (2021). Antisense oligonucleotide-based therapeutic against menin for triple-negative breast cancer treatment. Biomedicines, 9(7), 795.

Ni, L., Yang, C. S., Gioeli, D., Frierson, H., Toft, D. O., & Paschal, B. M. (2010). FKBP51 promotes assembly of the Hsp90 chaperone complex and regulates androgen receptor signaling in prostate cancer cells. Molecular and cellular biology, 30(5), 1243-1253.

Obinata, D., Takayama, K., Takahashi, S., & Inoue, S. (2017). Crosstalk of the androgen receptor with transcriptional collaborators: potential therapeutic targets for castration-resistant prostate cancer. *Cancers*, *9*(3), 22.

Okada, Y., Feng, Q., Lin, Y., Jiang, Q., Li, Y., Coffield, V. M., … & Zhang, Y. (2005). hDOT1L links histone methylation to leukemogenesis. Cell, 121(2), 167-178.

Ortiz-Hernandez, G. L., Sanchez-Hernandez, E. S., Ochoa, P. T., Elix, C. C., Alkashgari, H. R., McMullen, J. R., … & Casiano, C. A. (2021). The LEDGF/p75 integrase binding domain interactome contributes to the survival, clonogenicity, and tumorsphere formation of 118athways118-resistant prostate cancer cells. Cells, 10(10), 2723.

Osoba, D., Tannock, I. F., Ernst, D. S., & Neville, A. J. (1999). Health-related quality of life in men with metastatic prostate cancer treated with prednisone alone or mitoxantrone and prednisone. Journal of Clinical Oncology, 17(6), 1654-1654.

Ozyerli-Goknar, E., Kala, E. Y., Aksu, A. C., Bulut, I., Cingöz, A., Nizamuddin, S., … & Bagci-Onder, T. (2023). Epigenetic-focused CRISPR/Cas9 screen identifies (absent, small, or homeotic) 2-like protein (ASH2L) as a regulator of glioblastoma cell survival. *Cell Communication and Signaling*, *21*(1), 328.

Pajuelo-Gámez, J. C., Cervera, J., García-Casado, Z., Mena-Durán, A. V., Valencia, A., Barragán, E., … & Sanz, M. A. (2007). MLL amplification in acute myeloid leukemia. *Cancer genetics and cytogenetics*, *174*(2), 127-131.

Pagliarulo, V. (2018). Androgen deprivation therapy for prostate cancer. *Molecular & Diagnostic Imaging in Prostate Cancer: Clinical Applications and Treatment Strategies*, 1-30.

Pan, X. N., Chen, J. J., Wang, L. X., Xiao, R. Z., Liu, L. L., Fang, Z. G., … & Lin, D. J. (2014). Inhibition of c-Myc overcomes cytotoxic drug resistance in acute myeloid leukemia cells by promoting differentiation. *PloS one*, *9*(8), e105381.

Parikh, M., Liu, C., Wu, C. Y., Evans, C. P., Dall'Era, M., Robles, D., … & Pan, C. X. (2021). Phase Ib trial of reformulated niclosamide with abiraterone/prednisone in men with castration-resistant prostate cancer. Scientific reports, 11(1), 6377.

Passagne, I., Evrard, A., Depeille, P., Cuq, P., Cupissol, D., & Vian, L. (2006). O6-methylguanine DNA-methyltransferase (MGMT) overexpression in melanoma cells induces resistance to nitrosoureas and temozolomide but sensitizes to mitomycin C. Toxicology and applied pharmacology, 211(2), 97-105.

Patel, A., Dharmarajan, V., Vought, V. E., & Cosgrove, M. S. (2009). On the Mechanism of Multiple Lysine Methylation by the Human Mixed Lineage Leukemia Protein-1 (MLL1) Core Complex*♦. Journal of Biological Chemistry, 284(36), 24242-24256.

Peer, A., Gottfried, M., Sinibaldi, V., Carducci, M. A., Eisenberger, M. A., Sella, A., … & Keizman, D. (2014). Comparison of abiraterone acetate versus ketoconazole in patients with metastatic castration resistant prostate cancer refractory to 119athways119. The Prostate, 74(4), 433-440.

Petrylak, D. P., Tangen, C. M., Hussain, M. H., Lara Jr, P. N., Jones, J. A., Taplin, M. E., … & Crawford, E. D. (2004). Docetaxel and estramustine compared with mitoxantrone

and prednisone for advanced refractory prostate cancer. New England Journal of Medicine, 351(15), 1513-1520.

Pompeia, C., Hodge, D. R., Plass, C., Wu, Y. Z., Marquez, V. E., Kelley, J. A., & Farrar, W. L. (2004). Microarray analysis of epigenetic silencing of gene expression in the KAS-6/1 multiple myeloma cell line. Cancer research, 64(10), 3465-3473.

Pópulo, H., Lopes, J. M., & Soares, P. (2012). The mTOR 120athways120 120athways in human cancer. International journal of molecular sciences, 13(2), 1886-1918.

Pradeepa, M. M., Sutherland, H. G., Ule, J., Grimes, G. R., & Bickmore, W. A. (2012). Psip1/Ledgf p52 binds methylated histone H3K36 and splicing factors and contributes to the regulation of alternative splicing. PloS genetics, 8(5), e1002717.

Pradeepa, M. M., Taylor, G. C., & von Kriegsheim, A. (2017). Proteomic analysis of H3K36me3 and PSIP1/p75 (LEDGF) complexes reveal their wider role in DNA repair.

Rad, E., Murray, J. T., & Tee, A. R. (2018). Oncogenic 120athways120 through mechanistic target of 120athways120 (mTOR): a driver of metabolic transformation and cancer progression. Cancers, 10(1), 5.

Raith, F., O'Donovan, D. H., Lemos, C., Politz, O., & Haendler, B. (2023). Addressing the reciprocal crosstalk between the AR and the PI3K/AKT/mTOR signaling pathways for prostate cancer treatment. International Journal of Molecular Sciences, 24(3), 2289.

Ran, F. A. F. A., Hsu, P. D., Wright, J., Agarwala, V., Scott, D. A., & Zhang, F. (2013). Genome engineering using the CRISPR-Cas9 system. Nature protocols, 8(11), 2281-2308.

Reita, D., Bour, C., Benbrika, R., Groh, A., Pencreach, E., Guérin, E., & Guenot, D. (2019). Synergistic anti-tumor effect of mTOR inhibitors with irinotecan on colon cancer cells. Cancers, 11(10), 1581.

Richon, V. M., Sandhoff, T. W., Rifkind, R. A., & Marks, P. A. (2000). Histone deacetylase inhibitor selectively induces p21WAF1 expression and gene-associated histone acetylation. Proceedings of the National Academy of Sciences, 97(18), 1001.

Ríos-Colón, L., Cajigas-Du Ross, C. K., Basu, A., Elix, C., Alicea-Polanco, I., Sanchez, T. W., … & Casiano, C. A. (2017). Targeting the stress oncoprotein LEDGF/p75 to sensitize chemoresistant prostate cancer cells to taxanes. Oncotarget, 8(15), 24915.

Rosenfeldt, M. T., Bell, L. A., Long, J. S., O'prey, J., Nixon, C., Roberts, F., … & Ryan, K. M. (2014). E2F1 drives chemotherapeutic drug resistance via ABCG2. *Oncogene*, *33*(32), 4164-4172.

Ruthenburg AJ, Allis CD, Wysocka J. Methylation of lysine 4 on histone H3: intricacy of writing and reading a single epigenetic mark. Mol Cell. 2007 Jan 12;25(1):15-30. doi: 10.1016/j.molcel.2006.12.014. PMID: 17218268.

Salehan, M. R., & Morse, H. R. (2013). DNA damage repair and tolerance: a role in chemotherapeutic drug resistance. British journal of biomedical science, 70(1), 31-40.

Salz, T., Deng, C., Pampo, C., Siemann, D., Qiu, Y., Brown, K., & Huang, S. (2015). Histone methyltransferase hSETD1A is a novel regulator of metastasis in breast cancer. *Molecular Cancer Research*, *13*(3), 461-469.

Sánchez, C., Mendoza, P., Contreras, H. R., Vergara, J., McCubrey, J. A., Huidobro, C., & Castellon, E. A. (2009). Expression of multidrug resistance proteins in prostate cancer is related with cell sensitivity to chemotherapeutic drugs. The Prostate, 69(13), 1448-1459.

Sanchez-Hernandez, E. S., Ochoa, P. T., Suzuki, T., Ortiz-Hernandez, G. L., Unternaehrer, J. J., Alkashgari, H. R., … & Casiano, C. A. (2023). Glucocorticoid receptor regulates and interacts with LEDGF/p75 to 121athways 121athways121 resistance in prostate cancer cells. *Cells*, *12*(16), 2046.

Sapoznik, S., Cohen, B., Tzuman, Y., Meir, G., Ben-Dor, S., Harmelin, A., & Neeman, M. (2009). Gonadotropin-regulated lymphangiogenesis in ovarian cancer is mediated by LEDGF-induced expression of VEGF-C. *Cancer research*, *69*(24), 9306-9314.

Sarbassov, D. D., Ali, S. M., & Sabatini, D. M. (2005). Growing roles for the mTOR 121athways. Current opinion in cell biology, 17(6), 596-603.

Sauna, Z. E., & Ambudkar, S. V. (2001). Characterization of the catalytic cycle of ATP hydrolysis by human P-glycoprotein: the two ATP hydrolysis events in a single catalytic cycle are kinetically similar but affect different functional outcomes. Journal of Biological Chemistry, 276(15), 11653-11661.

Scacheri, P. C., Davis, S., Odom, D. T., Crawford, G. E., Perkins, S., Halawi, M. J., … & Collins, F. S. (2006). Genome-wide analysis of menin binding provides insights into MEN1 tumorigenesis. PloS genetics, 2(4), e51.

Scariano, J. K., Treat, E., Alba, F., Nelson, H., Ness, S. A., & Smith, A. Y. (2008). The SRD5A2 V89L polymorphism is associated with severity of disease in men with early onset prostate cancer. The Prostate, 68(16).

Schuettengruber, B., Martinez, A. M., Iovino, N. &Cavalli, G. Trithorax group proteins: switching genes on and keeping them active. Nature Rev. Mol. Cell Biol. 12, 799–814 (2011).

Sekhoacha, M., Riet, K., Motloung, P., Gumenku, L., Adegoke, A., & Mashele, S. (2022). Prostate cancer review: genetics, diagnosis, treatment options, and alternative approaches. *Molecules*, *27*(17), 5730.

Sekino, Y., & Teishima, J. (2020). Molecular mechanisms of 122athways122 resistance in prostate cancer. Cancer Drug Resistance, 3(4), 676.

Senisterra, G., Wu, H., Allali-Hassani, A., Wasney, G. A., Barsyte-Lovejoy, D., Dombrovski, L., … & Vedadi, M. (2013). Small-molecule inhibition of MLL activity by disruption of its interaction with WDR5. Biochemical Journal, 449(1), 151-159.

Shah, K. and R.M. Rawal, Genetic and Epigenetic Modulation of Drug Resistance in Cancer: Challenges and Opportunities. Curr Drug Metab, 2019. 20(14): p. 1114-1131.

Sharma, S. V., Lee, D. Y., Li, B., Quinlan, M. P., Takahashi, F., Maheswaran, S., … & Settleman, J. (2010). A chromatin-mediated reversible drug-tolerant state in cancer cell subpopulations. Cell, 141(1), 69-80.

Shi, A., Murai, M. J., He, S., Lund, G., Hartley, T., Purohit, T., … & Cierpicki, T. (2012). Structural insights into inhibition of the bivalent menin-MLL interaction by small molecules in leukemia. *Blood, The Journal of the American Society of Hematology*, *120*(23), 4461-4469.

Shin, Y. J., & Kim, J. H. (2012). The role of EZH2 in the regulation of the activity of matrix metalloproteinases in prostate cancer cells. PloS one, 7(1), e30393.

Shivapurkar, N., Toyooka, S., Eby, M. T., Huang, C. X., Sathyanarayana, U. G., Cunningham, H. T., … & Gazdar, A. (2002). Differential inactivation of caspase-8 in lung cancers. Cancer biology & therapy, 1(1), 65-69.

Sikand, K., Slaibi, J. E., Singh, R., Slane, S. D., and Shukla, G. C. (2010). MiR 488* inhibits androgen receptor expression in prostate carcinoma cells. Int. J. Cancer. 129, 810–819.

Singh, D. P., Fatma, N., Kimura, A., Chylack Jr, L. T., & Shinohara, T. (2001). LEDGF binds to heat shock and stress-related element to activate the expression of stress-related genes. Biochemical and Biophysical Research Communications, 283(4), 943-955.

Singh, P. K., Plumb, M. R., Ferris, A. L., Iben, J. R., Wu, X., Fadel, H. J., … & Levin, H. L. (2015). LEDGF/p75 interacts with mRNA splicing factors and targets HIV-1 integration to highly spliced genes. Genes & development, 29(21), 2287-2297.

Snoek, R., Cheng, H., Margiotti, K., Wafa, L. A., Wong, C. A., Wong, E. C., … & Rennie, P. S. (2009). In vivo knockdown of the androgen receptor results in growth inhibition and regression of well-established, castration-resistant prostate tumors. *Clinical Cancer Research*, *15*(1), 39-47.

South, P. F. (2012). *The Set1 histone H3K4 methyltransferase complex: A 123athways of gene expression, ergosterol homeostasis, and drug resistance* (Doctoral dissertation, Purdue University).

Spoelstra, E.C., et al., P-glycoprotein drug efflux pump involved in the mechanisms of intrinsic drug resistance in various colon cancer cell lines. Evidence for a saturation of active daunorubicin transport. Biochem Pharmacol, 1991. 41(3): p. 349-59.

Squillace, R. M., Miller, D., Wardwell, S. D., Wang, F., Clackson, T., & Rivera, V. M. (2012). Synergistic activity of the mTOR inhibitor ridaforolimus and the antiandrogen bicalutamide in prostate cancer models. International journal of oncology, 41(2), 425-432.

Stefani, C., Miricescu, D., Stanescu-Spinu, I. I., Nica, R. I., Greabu, M., Totan, A. R., & Jinga, M. (2021). Growth factors, PI3K/AKT/mTOR and MAPK signaling pathways in colorectal cancer pathogenesis: where are we now?. International journal of molecular sciences, 22(19), 10260.

Stephan, S., Datta, K., Wang, E., Li, J., Brekken, R. A., Parangi, S., … & Mukhopadhyay, D. (2004). Effect of 123athways123 alone and in combination with antiangiogenesis therapy in an orthotopic model of human pancreatic cancer. Clinical cancer research, 10(20), 6993-7000.

Strömberg, T., Dimberg, A., Hammarberg, A., Carlson, K., Osterborg, A., Nilsson, K., & Jernberg-Wiklund, H. (2004). Rapamycin sensitizes multiple myeloma cells to apoptosis induced by dexamethasone. Blood, 103(8), 3138-3147.

Suffness, M. (1993). Taxol: from discovery to therapeutic use. In Annual Reports in Medicinal Chemistry (Vol. 28, pp. 305-314). Academic Press.

Sun, S., Sprenger, C. C., Vessella, R. L., Haugk, K., Soriano, K., Mostaghel, E. A., … & Plymate, S. R. (2010). Castration resistance in human prostate cancer is conferred by a frequently occurring androgen receptor splice variant. The Journal of clinical investigation, 120(8), 2715-2730.

Sun, W., Guo, F., & Liu, M. (2018). Up-regulated WDR5 promotes gastric cancer formation by induced 124athwa D1 expression. *Journal of cellular biochemistry*, *119*(4), 3304-3316.

Sundarraj, J., Taylor, G. C., von Kriegsheim, A., & Pradeepa, M. M. (2017). H3K36me3 and PSIP1/LEDGF associate with several DNA repair proteins, suggesting their role in efficient DNA repair at actively transcribing loci. Wellcome Open Research, 2.

Sutherland, H. G., Newton, K., Brownstein, D. G., Holmes, M. C., Kress, C., Semple, C. A., & Bickmore, W. A. (2006). Disruption of Ledgf/Psip1 results in perinatal mortality and homeotic skeletal transformations. Molecular and cellular biology.

Sweeney, C. J., Chen, Y. H., Carducci, M., Liu, G., Jarrard, D. F., Eisenberger, M., … & DiPaola, R. S. (2015). Chemohormonal therapy in metastatic hormone-sensitive prostate cancer. *New England Journal of Medicine*, *373*(8), 737-746.

Szakács, G., Annereau, J. P., Lababidi, S., Shankavaram, U., Arciello, A., Bussey, K. J., … & Gottesman, M. M. (2004). Predicting drug sensitivity and resistance: profiling ABC transporter genes in cancer cells. Cancer cell, 6(2), 129-137.

Szwed, A., Kim, E., & Jacinto, E. (2021). Regulation and metabolic 124athways124 of mTORC1 and mTORC2. Physiological reviews, 101(3), 1371-1426.

Tashiro, E., Tsuchiya, A., & Imoto, M. (2007). Functions of 124athwa D1 as an oncogene and regulation of 124athwa D1 expression. *Cancer science*, *98*(5), 629-635.

Tan, X., Chen, S., Wu, J., Lin, J., Pan, C., Ying, X., … & Huang, W. (2017). PI3K/AKT-mediated upregulation of WDR5 promotes colorectal cancer metastasis by directly targeting ZNF407. *Cell death & disease*, *8*(3), e2686-e2686.

Tanneau, L., Karlsson, M. O., & Svensson, E. M. (2020). Understanding the drug exposure–response relationship of bedaquiline to predict efficacy for novel dosing regimens in the treatment of multidrug-resistant tuberculosis. British journal of clinical pharmacology, 86(5), 913-922.

Tannock, I. F., De Wit, R., Berry, W. R., Horti, J., Pluzanska, A., Chi, K. N., … & Eisenberger, M. A. (2004). Docetaxel plus prednisone or mitoxantrone plus prednisone for advanced prostate cancer. New England Journal of Medicine, 351(15), 1502-1512.

Taverna, S., Li, H., Ruthenburg, A. et al. How chromatin-binding modules interpret histone modifications: lessons from 125athways125nce pocket pickers. Nat Struct Mol Biol 14, 1025–1040 (2007).

Tazzari, P. L., Cappellini, A., Ricci, F., Evangelisti, C., Papa, V., Grafone, T., … & Martelli, A. M. (2007). Multidrug resistance-associated protein 1 expression is under the control of the phosphoinositide 3 kinase/Akt signal transduction network in human acute myelogenous leukemia blasts. Leukemia, 21(3), 427-438.

Thomas, C., Lamoureux, F., Crafter, C., Davies, B. R., Beraldi, E., Fazli, L., … & Zoubeidi, A. (2013). Synergistic targeting of PI3K/AKT 125athways and androgen receptor axis significantly delays castration-resistant prostate cancer progression in vivo. Molecular cancer therapeutics, 12(11), 2342-2355.

Thomas, X. (2024). Small Molecule Menin Inhibitors: Novel Therapeutic Agents Targeting Acute Myeloid Leukemia with KMT2A Rearrangement or NPM1 Mutation. *Oncology and Therapy*, *12*(1), 57-72.

Thoreen, C. C., Kang, S. A., Chang, J. W., Liu, Q., Zhang, J., Gao, Y., … & Gray, N. S. (2009). An ATP-competitive mammalian target of 125athways125 inhibitor reveals 125athways125-resistant 125athways125 of mTORC1. Journal of Biological Chemistry, 284(12), 8023-8032.

Tian, T., Li, X., & Zhang, J. (2019). mTOR signaling in cancer and mTOR inhibitors in solid tumor targeting therapy. International journal of molecular sciences, 20(3), 755.

Tian, Y., Wan, H., & Tan, G. (2012). Cell cycle-related kinase in carcinogenesis. *Oncology Letters*, *4*(4), 601-606.

Tolkach, Y., Zarbl, R., Bauer, S., Ritter, M., Ellinger, J., Hauser, S., … & Kristiansen, G. (2021). DNA promoter methylation and ERG regulate the expression of CD24 in prostate cancer. The American journal of pathology, 191(4), 618-630.

Tomiyasu, H., Goto-Koshino, Y., Fujino, Y., Ohno, K., & Tsujimoto, H. (2014). Epigenetic regulation of the ABCB1 gene in drug-sensitive and drug-resistant lymphoid tumour cell lines obtained from canine patients. The Veterinary Journal, 199(1), 103-109.

Turner, N. C., & Reis-Filho, J. S. (2012). Genetic heterogeneity and cancer drug resistance. The lancet oncology, 13(4), e178-e185.

Ueda, T., Mawji, N. R., Bruchovsky, N., & Sadar, M. D. (2002). Ligand-independent activation of the androgen receptor by interleukin-6 and the role of steroid receptor coactivator-1 in prostate cancer cells. Journal of Biological Chemistry, 277(41), 38087-38094.

Ullius, A., Lüscher-Firzlaff, J., Costa, I. G., Walsemann, G., Forst, A. H., Gusmao, E. G., … & Lüscher, B. (2014). The interaction of MYC with the trithorax protein ASH2L promotes gene transcription by regulating H3K27 modification. *Nucleic acids research*, *42*(11), 6901-6920.

Varambally, S., Dhanasekaran, S. M., Zhou, M., Barrette, T. R., Kumar-Sinha, C., Sanda, M. G., … & Chinnaiyan, A. M. (2002). The polycomb group protein EZH2 is involved in progression of prostate cancer. Nature, 419(6907), 624-629.

Visakorpi, T., Hyytinen, E., Koivisto, P., Tanner, M., Keinänen, R., Palmberg, C., … & Kallioniemi, O. P. (1995). In vivo amplification of the androgen receptor gene and progression of human prostate cancer. Nature genetics, 9(4), 401-406.

Walsh, P. C., DeWeese, T. L., & Eisenberger, M. A. (2007). Localized prostate cancer. *New England Journal of Medicine*, *357*(26), 2696-2705.

Wang, Q., Li, W., Zhang, Y., Yuan, X., Xu, K., Yu, J., … & Brown, M. (2009). Androgen receptor regulates a distinct transcription program in androgen-independent prostate cancer. Cell, 138(2), 245-256.

Wang, Y.; Ozawa, A.; Zaman, S.; Prasad, N.B.; Chandrasekharappa, S.C.; Agarwal, S.K.; Marx, S.J. The tumor suppressor protein menin inhibits akt activation by regulating its cellular localization. Cancer Res. 2011, 71, 371–382.

Wang, X. K., He, J. H., Xu, J. H., Ye, S., Wang, F., Zhang, H., … & Fu, L. W. (2014). Afatinib enhances the efficacy of conventional chemotherapeutic agents by eradicating cancer stem–like cells. Cancer research, 74(16), 4431-4445.

Wang, Z. F., Hong, X. Y., Zhu, L. Y., Zhang, L., Qiu, H., Zhang, Y. Y., … & Jin, G. H. (2020). Abnormal expression of menin predicts the pathogenesis and poor prognosis of adult gliomas. Cancer gene therapy, 27(7), 539-547.

Wang, J., Yang, D. H., Yang, Y., Wang, J. Q., Cai, C. Y., Lei, Z. N., … & Chen, Z. S. (2020). Overexpression of ABCB1 transporter confers resistance to mTOR inhibitor WYE-354 in cancer cells. International journal of molecular sciences, 21(4), 1387.

Ween, M. P., Armstrong, M. A., Oehler, M. K., & Ricciardelli, C. (2015). The role of ABC transporters in ovarian cancer progression and chemoresistance. Critical reviews in oncology/hematology, 96(2), 220-256.

Wei, X. X., Hsieh, A. C., Kim, W., Friedlander, T., Lin, A. M., Louttit, M., & Ryan, C. J. (2017). A phase I study of abiraterone acetate combined with BEZ235, a dual PI3K/mTOR inhibitor, in metastatic castration resistant prostate cancer. The oncologist, 22(5), 503-e43.

Weichert, W., Röske, A., Gekeler, V., Beckers, T., Stephan, C., Jung, K., … & Kristiansen, G. (2008). Histone deacetylases 1, 2 and 3 are highly expressed in prostate cancer and HDAC2 expression is associated with shorter PSA relapse time after radical prostatectomy. British journal of cancer, 98(3), 604-610.

Welti, J., Sharp, A., Brooks, N., Yuan, W., McNair, C., Chand, S. N., … & de Bono, J. S. (2021). Targeting the p300/CBP axis in lethal prostate cancer. Cancer Discovery, 11(5), 1118-1137.

Wen, Y., Hu, M. C., Makino, K., Spohn, B., Bartholomeusz, G., Yan, D. H., & Hung, M. C. (2000). HER-2/neu promotes androgen-independent survival and growth of prostate cancer cells through the Akt 127athways. Cancer research, 60(24), 6841-6845.

Widschwendter, M., Siegmund, K. D., Müller, H. M., Fiegl, H., Marth, C., Müller-Holzner, E., … & Laird, P. W. (2004). Association of breast cancer DNA methylation profiles with hormone receptor status and response to tamoxifen. Cancer research, 64(11), 3807-3813.

Willems, L., Tamburini, J., Chapuis, N., Lacombe, C., Mayeux, P., & Bouscary, D. (2012). PI3K and mTOR signaling pathways in cancer: new data on targeted therapies. Current oncology reports, 14, 129-138.

Wiltshire, C., Singh, B. L., Stockley, J., Fleming, J., Doyle, B., Barnetson, R., … & Leung, H. Y. (2010). Docetaxel-resistant prostate cancer cells remain sensitive to S-trityl-L-cysteine–mediated Eg5 inhibition. Molecular cancer therapeutics, 9(6), 1730-1739.

Wise, H. M., Hermida, M. A., & Leslie, N. R. (2017). Prostate cancer, PI3K, PTEN and prognosis. Clinical science, 131(3), 197-210.

Won, K. A., Xiong, Y., Beach, D., & Gilman, M. Z. (1992). Growth-regulated expression of D-type 128athwa genes in human diploid fibroblasts. *Proceedings of the National Academy of Sciences*, *89*(20), 9910-9914.

Woodson, K., Hayes, R., Wideroff, L., Villaruz, L., & Tangrea, J. (2003). Hypermethylation of GSTP1, CD44, and E-cadherin genes in prostate cancer among US Blacks and Whites. The Prostate, 55(3), 199-205.

Wu, J. D., Haugk, K., Woodke, L., Nelson, P., Coleman, I., & Plymate, S. R. (2006). Interaction of IGF signaling and the androgen receptor in prostate cancer progression. Journal of cellular biochemistry, 99(2), 392-401.

Wu, T., Zhang, X., Huang, X., Yang, Y., & Hua, X. (2010). Regulation of 128athwa B2 expression and cell cycle G2/m transition by menin. *Journal of Biological Chemistry*, *285*(24), 18291-18300.

Wu, S., Yang, Z., Ye, R., An, D., Li, C., Wang, Y., … & Cai, Z. (2016). Novel variants in MLL confer to 128athway cancer recurrence identified by whole-exome sequencing. *Oncotarget*, *7*(3), 2629.

Wu, G., Yuan, M., Shen, S., Ma, X., Fang, J., Zhu, L., … & Gao, P. (2017). Menin enhances c-Myc-mediated transcription to 128athways cancer progression. Nature communications, 8(1), 15278.

Wu, Y., Diao, P., Li, Z., Zhang, W., Wang, D., Wang, Y., & Cheng, J. (2018). Overexpression of WD repeat domain 5 associates with aggressive clinicopathological features and unfavorable prognosis in head neck squamous cell carcinoma. *Journal of Oral Pathology & Medicine*, *47*(5), 502-510.

Wu, J., Chai, H., Li, F., Ren, Q., & Gu, Y. (2020). SETD1A augments sorafenib primary resistance via activating YAP in hepatocellular carcinoma. *Life Sciences*, *260*, 118406.

Wu, J., Chai, H., Shan, H., Pan, C., Xu, X., Dong, W., … & Gu, Y. (2021). Histone methyltransferase SETD1A induces epithelial-mesenchymal transition to 128athways invasion and metastasis through epigenetic reprogramming of snail in gastric cancer. *Frontiers in Cell and Developmental Biology*, *9*, 657888.

Wu, C. P., Hsieh, Y. J., Tseng, H. Y., Huang, Y. H., Li, Y. Q., Hung, T. H., … & Wu, Y. S. (2022). The WD repeat-containing protein 5 (WDR5) antagonist WDR5-0103

restores the efficacy of cytotoxic drugs in multidrug-resistant cancer cells overexpressing ABCB1 or ABCG2. Biomedicine & Pharmacotherapy, 154, 113663.

Xie, J., Wang, X., & Proud, C. G. (2016). mTOR inhibitors in cancer therapy. F1000Research, 5.

Xie, H., Zhao, J., Wan, J., Zhao, J., Wang, Q., Yang, X., … & Yu, X. (2021). Long non-coding RNA AC245100. 4 promotes prostate cancer tumorigenesis via the microRNA-145-5p/RBBP5 axis Corrigendum in/10.3892/or. 2023.8499. *Oncology Reports*, *45*(2), 619-629.

Xu, B., Li, S. H., Zheng, R., Gao, S. B., Ding, L. H., Yin, Z. Y., … & Jin, G. H. (2013). Menin promotes hepatocellular carcinogenesis and epigenetically up-regulates Yap1 transcription. *Proceedings of the National Academy of Sciences*, *110*(43), 17480-17485.

Xue, Q., Nagy, J. A., Manseau, E. J., Phung, T. L., Dvorak, H. F., & Benjamin, L. E. (2009). Rapamycin inhibition of the Akt/mTOR pathways blocks select stages of VEGF-A164–driven angiogenesis, in part by blocking S6Kinase. Arteriosclerosis, thrombosis, and vascular biology, 29(8), 1172-1178.

Yabuki, N., Sakata, K., Yamasaki, T., Terashima, H., Mio, T., Miyazaki, Y., … & Kitada, K. (2007). Gene amplification and expression in lung cancer cells with acquired paclitaxel resistance. Cancer genetics and Cytogenetics, 173(1), 1-9.

Yan, L. H., Wei, W. Y., Cao, W. L., Zhang, X. S., Xie, Y. B., & Xiao, Q. (2014). Overexpression of E2F1 in human gastric carcinoma is involved in anti-cancer drug resistance. *BMC cancer*, *14*, 1-10.

Yan, L. H., Wang, X. T., Yang, J., Kong, F. B., Lian, C., Wei, W. Y., … & Xiao, Q. (2014). Reversal of multidrug resistance in gastric cancer cells by E2F-1 downregulation in vitro and in vivo. *Journal of cellular biochemistry*, *115*(1), 34-41.

Yang, Z., Wu, D., Bui, T., & Ho, R. J. (2008). A novel human multidrug resistance gene MDR1 variant G571A (G191R) modulates cancer drug resistance and efflux transport. Journal of Pharmacology and Experimental Therapeutics, 327(2), 474-481.

Yang, Y. J., Song, T. Y., Park, J., Lee, J., Lim, J., Jang, H., … & Cho, E. J. (2013). Menin mediates epigenetic regulation via histone H3 lysine 9 methylation. Cell Death & Disease, 4(4), e583-e583.

Yang, L., Jin, M., & Jeong, K. W. (2021). Histone H3K4 methyltransferases as targets for drug-resistant cancers. *Biology*, *10*(7), 581.

Yang, Z., Jia, Y., Wang, S., Zhang, Y., Fan, W., Wang, X., … & Yang, H. (2023). Retinoblastoma-Binding Protein 5 Regulates H3K4 Methylation Modification to Inhibit the Proliferation of Melanoma Cells by Inactivating the Wnt/β-Catenin and Epithelial-Mesenchymal Transition Pathways. *Journal of Oncology*, *2023*(1), 5093941.

Ye, J., Zha, J., Shi, Y., Li, Y., Yuan, D., Chen, Q., … & Xu, B. (2019). Co-inhibition of HDAC and MLL-menin interaction targets MLL-rearranged acute myeloid leukemia cells via disruption of DNA damage checkpoint and DNA repair. *Clinical epigenetics*, *11*, 1-14.

Yin, X. H., Wang, Z. Q., Guo, Q. H., Wu, H., & Shi, M. (2017). Overexpressed LEDGF is a novel biomarker of poor prognosis in patients with cervical cancer. Eur J Gynaecol Oncol, 38(2), 245-250.

Yin, Y., Xu, L., Chang, Y., Zeng, T., Chen, X., Wang, A., … & Huang, J. (2019). N-Myc promotes therapeutic resistance development of neuroendocrine prostate cancer by differentially regulating miR-421/ATM 130athways. *Molecular cancer*, *18*, 1-13.

You, D., J.R. Richardson, and L.M. Aleksunes, Epigenetic Regulation of Multidrug Resistance Protein 1 and Breast Cancer Resistance Protein Transporters by Histone Deacetylase Inhibition. Drug Metab Dispos, 2020. 48(6): p. 459-480.

Yokoyama A, Somervaille TC, Smith KS, Rozenblatt-Rosen O, Meyerson M, Cleary ML. The menin tumor suppressor protein is an essential oncogenic cofactor for MLL-associated leukemogenesis. Cell. 2005;123:207–218.

Yokoyama, A., & Cleary, M. L. (2008). Menin critically links MLL proteins with LEDGF on cancer-associated target genes. Cancer cell, 14(1), 36-46.

Yu, B. D., Hess, J. L., Horning, S. E., Brown, G. A., & Korsmeyer, S. J. (1995). Altered Hox expression and segmental identity in Mll-mutant mice. Nature, 378(6556), 505-508.

Yu, H. G., Ai, Y. W., Yu, L. L., Zhou, X. D., Liu, J., Li, J. H., … & Yu, J. P. (2008). Phosphoinositide 3-kinase/Akt 130athways plays an important role in chemoresistance of gastric cancer cells against etoposide and doxorubicin induced cell death. International journal of cancer, 122(2), 433-443.

Yuan, R., Kay, A., Berg, W. J., & Lebwohl, D. (2009). Targeting tumorigenesis: development and use of mTOR inhibitors in cancer therapy. Journal of hematology & oncology, 2(1), 45.

Zahan, T., Das, P. K., Akter, S. F., Habib, R., Rahman, M. H., Karim, M. R., & Islam, F. (2020). Therapy resistance in cancers: phenotypic, metabolic, epigenetic and tumour microenvironmental perspectives. Anti-Cancer Agents in Medicinal Chemistry (Formerly Current Medicinal Chemistry-Anti-Cancer Agents), 20(18), 2190-2206.

Zappe, K., & Cichna-Markl, M. (2020). Aberrant DNA methylation of ABC transporters in cancer. Cells, 9(10), 2281.

Zaytseva, Y. Y., Valentino, J. D., Gulhati, P., & Evers, B. M. (2012). mTOR inhibitors in cancer therapy. Cancer letters, 319(1), 1-7.

Zhang, L., Altuwaijri, S., Deng, F., Chen, L., Lal, P., Bhanot, U. K., … & Gerald, W. L. (2009). NF-κB regulates androgen receptor expression and prostate cancer growth. The American journal of pathology, 175(2), 489-499.

Zhang, D., An, X., Li, Q., Man, X., Chu, M., Li, H., … & Li, Z. (2020). Thioguanine induces apoptosis in triple-negative breast cancer by regulating PI3K–AKT 131athways. *Frontiers in Oncology*, *10*, 524922.

Zhou, Q., Chen, X., He, H., Peng, S., Zhang, Y., Zhang, J., … & Huang, J. (2021). WD repeat domain 5 promotes chemoresistance and Programmed Death-Ligand 1 expression in prostate cancer. *Theranostics*, *11*(10), 4809.

Zhu, Y., Liu, C., Nadiminty, N., Lou, W., Tummala, R., Evans, C. P., & Gao, A. C. (2013). Inhibition of ABCB1 expression overcomes acquired 131athways131 resistance in prostate cancer. Molecular cancer therapeutics, 12(9), 1829-1836.

Zhu, Y., & Luo, J. (2020). Regulation of androgen receptor variants in prostate cancer. Asian Journal of Urology, 7(3), 251-257.

Zhu, Q., Fang, L., Heuberger, J., Kranz, A., Schipper, J., Scheckenbach, K., … & Birchmeier, W. (2019). The Wnt-driven Mll1 epigenome regulates salivary gland and head and neck cancer. *Cell Reports*, *26*(2), 415-428.

Zhu, L. Y., Yuan, J. B., Zhang, L., He, C. X., Lin, X., Xu, B., & Jin, G. H. (2022). Loss of mll induces epigenetic dysregulation of rasgrf1 to attenuate kras-driven lung tumorigenesis. *Cancer Research*, *82*(22), 4153-4163.

Zeng, K., Wu, Y., Wang, C., Wang, S., Sun, H., Zou, R., … & Zhao, Y. (2019). ASH2L Acts As a Co-Activator of ERα to Participate in the Promotion of Endometrial Cancer Progression.

Zindy, P. J., L'Helgoualc'h, A., Bonnier, D., Le Béchec, A., Bourd-Boitin, K., Zhang, C. X., … & Théret, N. (2006). Upregulation of the tumor suppressor gene menin in hepatocellular carcinomas and its 132athways132nce in fibrogenesis. *Hepatology*, *44*(5), 1296-1307.

Zou, Z., Tao, T., Li, H., & Zhu, X. (2020). mTOR signaling 132athways and mTOR inhibitors in cancer: progress and challenges. Cell & bioscience, 10(1), 31.

WEB REFERENCES

Biorender, accessed June 26, 2024
https://www.biorender.com/

cBioPortal, accessed June 30, 2024
https://www.cbioportal.org/

ChIP Atlas: Peak Browser, accessed June 26, 2024
https://chip-atlas.org/peak_browser

Cancer Treatment Response gene signature data base, accessed June 1, 2024
http://ctrdb.cloudna.cn/browse

DESeq2, accessed June 20, 2024
https://bioconductor.org/packages/release/bioc/html/DESeq2.html

Ensembl, accessed June 20, 2024
https://m.ensembl.org/info/data/biomart/index.html

FastQC software, accessed June 20, 2024
http:/www.bioinformatics.Babraham.ac.uk/projects/fastqc/

FeatureCounts, accessed June 20, 2024
http://bioinf.wehi.edu.au/featureCounts/).

HiSAT2, accessed June 20, 2024
http://daehwankimlab.github.io/hisat2/

SRPlot, accessed June 15, 2024
https://www.bioinformatics.com.cn/en

TCGA Wanderer, accessed June 12, 2024
http://maplab.imppc.org/wanderer/